ArevaEPRDCPEm Resource

From: WILLIFORD Dennis (AREVA) [Dennis.Williford@areva.com]
Sent: Thursday, August 25, 2011 3:38 PM
To: Tesfaye, Getachew
Cc: BENNETT Kathy (AREVA); CRIBB Arnie (EXTERNAL AREVA); DELANO Karen (AREVA); HALLINGER Pat (EXTERNAL AREVA); HATHCOCK Phillip (AREVA); ROMINE Judy (AREVA); RYAN Tom (AREVA); WELLS Russell (AREVA); HARRINGTON James (AREVA); WILLIAMSON Rick (AREVA)
Subject: DRAFT Response to U.S. EPR Design Certification Application RAI No. 467, FSAR Ch. 3, Question 03.06.03-28
Attachments: RAI 467 Q.3-6-3-28 Resp. Master US EPR DC Draft.pdf

Getachew,

Attached is a draft response for RAI No. 467, FSAR Ch. 3, Question 03.06.03-28 as shown below in advance of the September 15, 2011 final date. To assist in the NRC review, a complete version of U.S. EPR FSAR Tier 2, Section 3.6.3 is included as a part of this draft response.

Let me know if the staff has questions or if this can be sent as a final response.

Thanks,

Dennis Williford, P.E.
U.S. EPR Design Certification Licensing Manager
AREVA NP Inc.
7207 IBM Drive, Mail Code CLT 2B
Charlotte, NC 28262
Phone: 704-805-2223
Email: Dennis.Williford@areva.com

From: WILLIFORD Dennis (RS/NB)
Sent: Friday, August 05, 2011 10:37 AM
To: Tesfaye, Getachew
Cc: BENNETT Kathy (RS/NB); DELANO Karen (RS/NB); ROMINE Judy (RS/NB); RYAN Tom (RS/NB); WELLS Russell (RS/NB)
Subject: Response to U.S. EPR Design Certification Application RAI No. 467, FSAR Ch. 3, Supplement 9

Getachew,

AREVA NP Inc. (AREVA NP) provided a schedule for the 14 questions of RAI No. 467 on February 24, 2011. AREVA NP submitted Supplement 1 on April 1, 2011 to provide technically correct and complete responses to 4 of the remaining 14 questions. AREVA NP submitted Supplement 2 on April 15, 2011, Supplement 3 on May 27, 2011, and Supplement 4 on June 22, 2011, to provide a revised schedule for 9 of the 10 remaining questions. AREVA NP submitted RAI 467 Supplement 5 on July 7, 2011, which provided a technically correct and complete response to 1 of the remaining 10 questions. AREVA NP submitted RAI 467 Supplement 6 on July 27, 2011, which provided a revised schedule for the remaining 9 questions. AREVA NP submitted RAI 467 Supplement 7 on July 29, 2011, which provided a technically correct and complete final responses to 3 of the remaining 9 questions. AREVA NP submitted RAI 467 Supplement 8 on August 3, 2011, which provided a technically correct and complete final response to 1 of the 6 remaining questions. The attached file, "RAI 467 Supplement 9 Response US EPR DC.pdf" provides technically correct and complete FINAL responses to 2 of the remaining 5 questions, as committed.

The following table indicates the respective pages in the response document, "RAI 467 Supplement 9 Response US EPR DC.pdf" that contain AREVA NP's final response to the subject questions.

Question #	Start Page	End Page
RAI 467 — 03.09.02-157	2	4
RAI 467 — 03.09.02-165	5	5

The schedule for technically correct and complete final responses to the remaining 3 questions is unchanged as provided below.

Question #	Response Date
RAI 467 — 03.06.03-28	September 15, 2011
RAI 467 — 03.09.02-160	September 9, 2011
RAI 467 — 03.09.02-161	September 9, 2011

Sincerely,

Dennis Williford, P.E.
U.S. EPR Design Certification Licensing Manager
AREVA NP Inc.
7207 IBM Drive, Mail Code CLT 2B
Charlotte, NC 28262
Phone: 704-805-2223
Email: Dennis.Williford@areva.com

From: WILLIFORD Dennis (RS/NB)
Sent: Wednesday, August 03, 2011 12:38 PM
To: 'Tesfaye, Getachew'
Cc: BENNETT Kathy (RS/NB); DELANO Karen (RS/NB); ROMINE Judy (RS/NB); RYAN Tom (RS/NB); WELLS Russell (RS/NB)
Subject: Response to U.S. EPR Design Certification Application RAI No. 467, FSAR Ch. 3, Supplement 8

Getachew,

AREVA NP Inc. letter NRC:11:084 dated August 2, 2011 provides a technically correct and complete final response to 1 of the 6 remaining questions in RAI 467. AREVA NP considers some of the material contained in the response to be proprietary information. As required by 10 CFR 2.390(b), an affidavit is provided to support the withholding of the proprietary information from public disclosure. Proprietary and non-proprietary versions of the enclosure to this letter are provided separately.

The following table indicates the respective pages in the enclosed response that contain AREVA NP's final response to the subject question.

Question #	Start Page	End Page
RAI 467 — 03.09.02-163	2	5

The schedule for a technically correct and complete final response to Question 03.06.03-28 has been revised as shown below in bold. The schedule for technically correct and complete final responses to the remaining questions is unchanged as provided below.

Question #	Response Date
RAI 467 — 03.06.03-28	**September 15, 2011**
RAI 467 — 03.09.02-157	September 9, 2011
RAI 467 — 03.09.02-160	September 9, 2011
RAI 467 — 03.09.02-161	September 9, 2011

RAI 467 — 03.09.02-165	September 9, 2011

Sincerely,

Dennis Williford, P.E.
U.S. EPR Design Certification Licensing Manager
AREVA NP Inc.
7207 IBM Drive, Mail Code CLT 2B
Charlotte, NC 28262
Phone: 704-805-2223
Email: Dennis.Williford@areva.com

From: WELLS Russell (RS/NB)
Sent: Friday, July 29, 2011 2:45 PM
To: Tesfaye, Getachew
Cc: WILLIFORD Dennis (RS/NB); ROMINE Judy (RS/NB); BENNETT Kathy (RS/NB); DELANO Karen (RS/NB); RYAN Tom (RS/NB)
Subject: Response to U.S. EPR Design Certification Application RAI No. 467, FSAR Ch. 3, Supplement 7

Getachew,

AREVA NP Inc. (AREVA NP) provided a schedule for the 14 questions of RAI No. 467 on February 24, 2011. AREVA NP submitted Supplement 1 on April 1, 2011 to provide technically correct and complete responses to 4 of the remaining 14 questions. AREVA NP submitted Supplement 2 on April 15, 2011, Supplement 3 on May 27, 2011, and Supplement 4 on June 22, 2011, to provide a revised schedule for 9 of the 10 remaining questions. AREVA NP submitted RAI 467 Supplement 5 on July 7, 2011, which provided a technically correct and complete response to 1 of the remaining 10 questions. AREVA NP submitted RAI 467 Supplement 6 on July 27, 2011, which provided a revised schedule for the remaining 9 questions. The attached file, "RAI 467 Supplement 7 Response US EPR DC.pdf" provides technically correct and complete FINAL responses to 3 of the remaining 9 questions, as committed.

The following table indicates the respective pages in the response document, "RAI 467 Supplement 7 Response US EPR DC.pdf" that contain AREVA NP's response to the subject questions.

Question #	Start Page	End Page
RAI 467 — 03.09.02-155	2	3
RAI 467 — 03.09.02-156	4	4
RAI 467 — 03.09.02-162	5	6

The schedule for technically correct and complete FINAL responses to the remaining 6 questions is unchanged as provided below.

Question #	Response Date
RAI 467 — 03.06.03-28	August 15, 2011
RAI 467 — 03.09.02-157	September 9, 2011
RAI 467 — 03.09.02-160	September 9, 2011
RAI 467 — 03.09.02-161	September 9, 2011
RAI 467 — 03.09.02-163	September 9, 2011
RAI 467 — 03.09.02-165	September 9, 2011

Sincerely,

Russ Wells for
Dennis Williford, P.E.
U.S. EPR Design Certification Licensing Manager
AREVA NP Inc.
7207 IBM Drive, Mail Code CLT 2B
Charlotte, NC 28262
Phone: 704-805-2223
Email: Dennis.Williford@areva.com

From: WELLS Russell (RS/NB)
Sent: Wednesday, July 27, 2011 10:23 AM
To: 'Tesfaye, Getachew'
Cc: WILLIFORD Dennis (RS/NB); ROMINE Judy (RS/NB); BENNETT Kathy (RS/NB); DELANO Karen (RS/NB); RYAN Tom (RS/NB)
Subject: Response to U.S. EPR Design Certification Application RAI No. 467, FSAR Ch. 3, Supplement 6

Getachew,

AREVA NP Inc. (AREVA NP) provided a schedule for the 14 questions of RAI No. 467 on February 24, 2011. AREVA NP submitted Supplement 1 on April 1, 2011 to provide technically correct and complete responses to 4 of the remaining 14 questions. AREVA NP submitted Supplement 2 on April 15, 2011, Supplement 3 on May 27, 2011, and Supplement 4 on June 22, 2011, to provide a revised schedule for 9 of the 10 remaining questions. AREVA NP submitted RAI 467 Supplement 5 on July 7, 2011, which provided a technically correct and complete response to 1 of the remaining 10 questions.

The schedule for technically correct and complete responses to the remaining 9 questions has been changed as provided below.

Question #	Response Date
RAI 467 — 03.06.03-28	August 15, 2011
RAI 467 — 03.09.02-155	**September 9, 2011**
RAI 467 — 03.09.02-156	**September 9, 2011**
RAI 467 — 03.09.02-157	**September 9, 2011**
RAI 467 — 03.09.02-160	**September 9, 2011**
RAI 467 — 03.09.02-161	**September 9, 2011**
RAI 467 — 03.09.02-162	**September 9, 2011**
RAI 467 — 03.09.02-163	**September 9, 2011**
RAI 467 — 03.09.02-165	**September 9, 2011**

Sincerely,

Russ Wells for
Dennis Williford, P.E.
U.S. EPR Design Certification Licensing Manager
AREVA NP Inc.
7207 IBM Drive, Mail Code CLT 2B
Charlotte, NC 28262
Phone: 704-805-2223
Email: Dennis.Williford@areva.com

From: WILLIFORD Dennis (RS/NB)
Sent: Thursday, July 07, 2011 11:35 AM
To: Tesfaye, Getachew
Cc: BENNETT Kathy (RS/NB); DELANO Karen (RS/NB); ROMINE Judy (RS/NB); RYAN Tom (RS/NB); WELLS Russell (RS/NB)
Subject: Response to U.S. EPR Design Certification Application RAI No. 467, FSAR Ch. 3, Supplement 5

Getachew,

AREVA NP Inc. (AREVA NP) provided a schedule for the 14 questions of RAI No. 467 on February 24, 2011. AREVA NP submitted Supplement 1 on April 1, 2011 to provide technically correct and complete responses to 4 of the remaining 14 questions. AREVA NP submitted Supplement 2 on April 15, 2011, Supplement 3 on May 27, 2011, and Supplement 4 on June 22, 2011, to provide a revised schedule for 9 of the 10 remaining questions.

The attached file, "RAI 467 Supplement 5 Response US EPR DC.pdf" provides a technically correct and complete response to 1 of the remaining 10 questions.

The following table indicates the respective pages in the response document, "RAI 467 Supplement 5 Response US EPR DC.pdf," that contain AREVA NP's response to the subject questions.

Question #	Start Page	End Page
RAI 467 — 03.09.02-167	2	2

The schedule for technically correct and complete responses to the remaining 9 questions is unchanged as provided below.

Question #	Response Date
RAI 467 — 03.06.03-28	August 15, 2011
RAI 467 — 03.09.02-155	July 27, 2011
RAI 467 — 03.09.02-156	July 27, 2011
RAI 467 — 03.09.02-157	July 27, 2011
RAI 467 — 03.09.02-160	July 27, 2011
RAI 467 — 03.09.02-161	July 27, 2011
RAI 467 — 03.09.02-162	July 27, 2011
RAI 467 — 03.09.02-163	July 27, 2011
RAI 467 — 03.09.02-165	July 27, 2011

Sincerely,

Dennis Williford, P.E.
U.S. EPR Design Certification Licensing Manager
AREVA NP Inc.
7207 IBM Drive, Mail Code CLT 2B
Charlotte, NC 28262
Phone: 704-805-2223
Email: Dennis.Williford@areva.com

From: WILLIFORD Dennis (RS/NB)
Sent: Wednesday, June 22, 2011 12:57 PM
To: 'Tesfaye, Getachew'
Cc: BENNETT Kathy (RS/NB); DELANO Karen (RS/NB); ROMINE Judy (RS/NB); RYAN Tom (RS/NB); WELLS Russell

(RS/NB)
Subject: Response to U.S. EPR Design Certification Application RAI No. 467, FSAR Ch. 3, Supplement 4

Getachew,

AREVA NP Inc. (AREVA NP) provided a schedule for the 14 questions of RAI No. 467 on February 24, 2011. AREVA NP submitted Supplement 1 on April 1, 2011 to provide technically correct and complete responses to 4 of the remaining 14 questions. AREVA NP submitted Supplement 2 on April 15, 2011 and Supplement 3 on May 27, 2011, to provide a revised schedule for 9 of the 10 remaining questions

The schedule for 9 of the 10 questions, shown in bold below, has been changed. The schedule for the remaining question is unchanged. The schedule for technically correct and complete responses to the remaining questions is provided below.

Question #	Response Date
RAI 467 — 03.06.03-28	August 15, 2011
RAI 467 — 03.09.02-155	**July 27, 2011**
RAI 467 — 03.09.02-156	**July 27, 2011**
RAI 467 — 03.09.02-157	**July 27, 2011**
RAI 467 — 03.09.02-160	**July 27, 2011**
RAI 467 — 03.09.02-161	**July 27, 2011**
RAI 467 — 03.09.02-162	**July 27, 2011**
RAI 467 — 03.09.02-163	**July 27, 2011**
RAI 467 — 03.09.02-165	**July 27, 2011**
RAI 467 — 03.09.02-167	**July 27, 2011**

Sincerely,

Dennis Williford, P.E.
U.S. EPR Design Certification Licensing Manager
AREVA NP Inc.
7207 IBM Drive, Mail Code CLT 2B
Charlotte, NC 28262
Phone: 704-805-2223
Email: Dennis.Williford@areva.com

From: WILLIFORD Dennis (RS/NB)
Sent: Friday, May 27, 2011 11:11 AM
To: Tesfaye, Getachew
Cc: BENNETT Kathy (RS/NB); DELANO Karen (RS/NB); ROMINE Judy (RS/NB); RYAN Tom (RS/NB); WELLS Russell (RS/NB); CORNELL Veronica (External RS/NB)
Subject: Response to U.S. EPR Design Certification Application RAI No. 467, FSAR Ch. 3, Supplement 3

Getachew,

AREVA NP Inc. (AREVA NP) provided a schedule for the 14 questions of RAI No. 467 on February 24, 2011. AREVA NP submitted Supplement 1 on April 1, 2011 to provide technically correct and complete responses to 4 of the remaining 14 questions. AREVA NP submitted Supplement 2 on April 15, 2011 to provide a revised schedule for 9 of the 10 remaining questions

The schedule for 9 of the 10 questions, shown in bold below, has been changed. The schedule for the remaining question is unchanged. The schedule for technically correct and complete responses to the remaining questions is provided below.

Question #	Response Date
RAI 467 — 03.06.03-28	August 15, 2011
RAI 467 — 03.09.02-155	**June 27, 2011**
RAI 467 — 03.09.02-156	**June 27, 2011**
RAI 467 — 03.09.02-157	**June 27, 2011**
RAI 467 — 03.09.02-160	**June 27, 2011**
RAI 467 — 03.09.02-161	**June 27, 2011**
RAI 467 — 03.09.02-162	**June 27, 2011**
RAI 467 — 03.09.02-163	**June 27, 2011**
RAI 467 — 03.09.02-165	**June 27, 2011**
RAI 467 — 03.09.02-167	**June 27, 2011**

Sincerely,

Dennis Williford, P.E.
U.S. EPR Design Certification Licensing Manager
AREVA NP Inc.
7207 IBM Drive, Mail Code CLT 2B
Charlotte, NC 28262
Phone: 704-805-2223
Email: Dennis.Williford@areva.com

From: WELLS Russell (RS/NB)
Sent: Friday, April 15, 2011 4:15 PM
To: Tesfaye, Getachew
Cc: BENNETT Kathy (RS/NB); DELANO Karen (RS/NB); ROMINE Judy (RS/NB); RYAN Tom (RS/NB)
Subject: Response to U.S. EPR Design Certification Application RAI No. 467, FSAR Ch. 3, Supplement 2

Getachew,

AREVA NP Inc. (AREVA NP) provided a schedule for the 14 questions of RAI No. 467 on February 24, 2011. AREVA NP submitted Supplement 1 on April 1, 2011 to provide technically correct and complete responses to 4 of the remaining 14 questions.

To allow additional time to interact with NRC staff, the schedule for technically correct and complete responses to 9 of the 10 has been changed and is provided below. The schedule for a technically correct and complete response to the remaining question is unchanged and is provided below:

Question #	Response Date
RAI 467 — 03.06.03-28	August 15, 2011
RAI 467 — 03.09.02-155	**May 27, 2011**
RAI 467 — 03.09.02-156	**May 27, 2011**
RAI 467 — 03.09.02-157	**May 27, 2011**
RAI 467 — 03.09.02-160	**May 27, 2011**
RAI 467 — 03.09.02-161	**May 27, 2011**
RAI 467 — 03.09.02-162	**May 27, 2011**
RAI 467 — 03.09.02-163	**May 27, 2011**
RAI 467 — 03.09.02-165	**May 27, 2011**
RAI 467 — 03.09.02-167	**May 27, 2011**

Sincerely,

Russ Wells
U.S. EPR Design Certification Licensing Manager
AREVA NP, Inc.
3315 Old Forest Road, P.O. Box 10935
Mail Stop OF-57
Lynchburg, VA 24506-0935
Phone: 434-832-3884 (work)
434-942-6375 (cell)
Fax: 434-382-3884
Russell.Wells@Areva.com

From: WELLS Russell (RS/NB)
Sent: Friday, April 01, 2011 1:24 PM
To: 'Tesfaye, Getachew'
Cc: BENNETT Kathy (RS/NB); DELANO Karen (RS/NB); ROMINE Judy (RS/NB); RYAN Tom (RS/NB)
Subject: Response to U.S. EPR Design Certification Application RAI No. 467, FSAR Ch. 3, Supplement 1

Getachew,

AREVA NP Inc. (AREVA NP) provided a schedule for the 14 questions of RAI No. 467 on February 24, 2011. The attached file, "RAI 467 Supplement 1 Response US EPR DC.pdf" provides technically correct and complete responses to 4 of the remaining 14 questions, as committed.

Appended to this file are affected pages of the U.S. EPR Final Safety Analysis Report in redline-strikeout format which support the response to RAI 467 Questions 03.09.02-158, 03.09.02-159, and 03.09.02-164.

The following table indicates the respective pages in the response document, "RAI 467 Supplement 1 Response US EPR DC.pdf," that contain AREVA NP's response to the subject questions.

Question #	Start Page	End Page
RAI 467 — 03.09.02-158	6	6
RAI 467 — 03.09.02-159	7	7
RAI 467 — 03.09.02-164	12	12
RAI 467 — 03.09.02-166	14	14

The schedule for technically correct and complete responses to the remaining questions is unchanged and is provided below:

Question #	Response Date
RAI 467 — 03.06.03-28	August 15, 2011
RAI 467 — 03.09.02-155	April 28, 2011
RAI 467 — 03.09.02-156	April 28, 2011
RAI 467 — 03.09.02-157	April 28, 2011
RAI 467 — 03.09.02-160	April 28, 2011
RAI 467 — 03.09.02-161	April 28, 2011
RAI 467 — 03.09.02-162	April 28, 2011
RAI 467 — 03.09.02-163	April 28, 2011
RAI 467 — 03.09.02-165	April 28, 2011
RAI 467 — 03.09.02-167	April 28, 2011

Sincerely,

Russ Wells
U.S. EPR Design Certification Licensing Manager
AREVA NP, Inc.
3315 Old Forest Road, P.O. Box 10935
Mail Stop OF-57
Lynchburg, VA 24506-0935
Phone: 434-832-3884 (work)
434-942-6375 (cell)
Fax: 434-382-3884
Russell.Wells@Areva.com

From: WELLS Russell (RS/NB)
Sent: Thursday, February 24, 2011 2:08 PM
To: 'Tesfaye, Getachew'
Cc: DELANO Karen (RS/NB); ROMINE Judy (RS/NB); BENNETT Kathy (RS/NB); BRYAN Martin (External RS/NB)
Subject: Response to U.S. EPR Design Certification Application RAI No. 467, FSAR Ch. 3

Getachew,

Attached please find AREVA NP Inc.'s response to the subject request for additional information (RAI). The attached file, "RAI 467 Response US EPR DC.pdf" provides a schedule for a technically correct and complete response to the 14 questions.

The following table indicates the respective pages in the response document, "RAI 467 Response US EPR DC.pdf" that contain AREVA NP's response to the subject questions.

Question #	Start Page	End Page
RAI 467 — 03.06.03-28	2	2
RAI 467 — 03.09.02-155	3	3
RAI 467 — 03.09.02-156	4	4
RAI 467 — 03.09.02-157	5	5
RAI 467 — 03.09.02-158	6	6
RAI 467 — 03.09.02-159	7	7
RAI 467 — 03.09.02-160	8	8
RAI 467 — 03.09.02-161	9	9
RAI 467 — 03.09.02-162	10	10
RAI 467 — 03.09.02-163	11	11
RAI 467 — 03.09.02-164	12	12
RAI 467 — 03.09.02-165	13	13
RAI 467 — 03.09.02-166	14	14
RAI 467 — 03.09.02-167	15	15

A complete answer is not provided for the 14 questions. The schedule for a technically correct and complete response to these questions is provided below.

Question #	Response Date

RAI 467 — 03.06.03-28	August 15, 2011
RAI 467 — 03.09.02-155	April 28, 2011
RAI 467 — 03.09.02-156	April 28, 2011
RAI 467 — 03.09.02-157	April 28, 2011
RAI 467 — 03.09.02-158	April 28, 2011
RAI 467 — 03.09.02-159	April 28, 2011
RAI 467 — 03.09.02-160	April 28, 2011
RAI 467 — 03.09.02-161	April 28, 2011
RAI 467 — 03.09.02-162	April 28, 2011
RAI 467 — 03.09.02-163	April 28, 2011
RAI 467 — 03.09.02-164	April 28, 2011
RAI 467 — 03.09.02-165	April 28, 2011
RAI 467 — 03.09.02-166	April 28, 2011
RAI 467 — 03.09.02-167	April 28, 2011

Sincerely,

Russ Wells
U.S. EPR Design Certification Licensing Manager
AREVA NP, Inc.
3315 Old Forest Road, P.O. Box 10935
Mail Stop OF-57
Lynchburg, VA 24506-0935
Phone: 434-832-3884 (work)
434-942-6375 (cell)
Fax: 434-382-3884
Russell.Wells@Areva.com

From: Tesfaye, Getachew [mailto:Getachew.Tesfaye@nrc.gov]
Sent: Wednesday, January 26, 2011 3:34 PM
To: ZZ-DL-A-USEPR-DL
Cc: Reichelt, Eric; Terao, David; Wong, Yuken; Dixon-Herrity, Jennifer; Miernicki, Michael; Colaccino, Joseph; ArevaEPRDCPEm Resource
Subject: U.S. EPR Design Certification Application RAI No. 467 (5333, 5344), FSAR Ch. 3

Attached please find the subject requests for additional information (RAI). A draft of the RAI was provided to you on January 6, 2011, and discussed with your staff on January 20 and 24, 2011. No change is made to the draft RAI as a result of those discussions. The schedule we have established for review of your application assumes technically correct and complete responses within 30 days of receipt of RAIs. For any RAIs that cannot be answered within 30 days, it is expected that a date for receipt of this information will be provided to the staff within the 30 day period so that the staff can assess how this information will impact the published schedule.

Thanks,
Getachew Tesfaye
Sr. Project Manager
NRO/DNRL/NARP
(301) 415-3361

Hearing Identifier: AREVA_EPR_DC_RAIs
Email Number: 3353

Mail Envelope Properties (2FBE1051AEB2E748A0F98DF9EEE5A5D486D043)

Subject: DRAFT Response to U.S. EPR Design Certification Application RAI No. 467, FSAR Ch. 3, Question 03.06.03-28
Sent Date: 8/25/2011 3:38:18 PM
Received Date: 8/25/2011 3:38:32 PM
From: WILLIFORD Dennis (AREVA)

Created By: Dennis.Williford@areva.com

Recipients:
"BENNETT Kathy (AREVA)" <Kathy.Bennett@areva.com>
Tracking Status: None
"CRIBB Arnie (EXTERNAL AREVA)" <arnie.cribb.ext@areva.com>
Tracking Status: None
"DELANO Karen (AREVA)" <Karen.Delano@areva.com>
Tracking Status: None
"HALLINGER Pat (EXTERNAL AREVA)" <Pat.Hallinger.ext@areva.com>
Tracking Status: None
"HATHCOCK Phillip (AREVA)" <Phillip.Hathcock@areva.com>
Tracking Status: None
"ROMINE Judy (AREVA)" <Judy.Romine@areva.com>
Tracking Status: None
"RYAN Tom (AREVA)" <Tom.Ryan@areva.com>
Tracking Status: None
"WELLS Russell (AREVA)" <Russell.Wells@areva.com>
Tracking Status: None
"HARRINGTON James (AREVA)" <James.Harrington@areva.com>
Tracking Status: None
"WILLIAMSON Rick (AREVA)" <Rick.Williamson@areva.com>
Tracking Status: None
"Tesfaye, Getachew" <Getachew.Tesfaye@nrc.gov>
Tracking Status: None

Post Office: auscharmx02.adom.ad.corp

Files	**Size**	**Date & Time**
MESSAGE	22186	8/25/2011 3:38:32 PM
RAI 467 Q.3-6-3-28 Resp. Master US EPR DC Draft.pdf	1428158	

Options
Priority: Standard
Return Notification: No
Reply Requested: No
Sensitivity: Normal
Expiration Date:
Recipients Received:

Response to

Request for Additional Information No. 467(5333, 5344)
Question 03.06.03-28

1/26/2011

U.S. EPR Standard Design Certification
AREVA NP Inc.
Docket No. 52-020
SRP Section: 03.06.03 - Leak-Before-Break Evaluation Procedures
SRP Section: 03.09.02 - Dynamic Testing and Analysis of Systems Structures and Components
Application Section: FSAR Chapter 3

QUESTIONS for Component Integrity, Performance, and Testing Branch 1 (AP1000/EPR Projects) (CIB1)
QUESTIONS for Engineering Mechanics Branch 2 (ESBWR/ABWR Projects) (EMB2)

Question 03.06.03-28:

Follow-up to RAI 265, Question 03.06.03-26

The Allowable Load Limit (ALL) Diagrams are presented in FSAR Tier 2, Section 3.6.3, Figure 3.6.3-12 through Figure 3.6.3-23 for the Main Steam Line (MSL), Main Coolant Line (MCL), and the Surge Line (SL) cases. As a result of the confirmatory calculations performed by the staff and the resulting RAI 265 Question 03.06.03-26, AREVA proposed (i.e., in its Supplemental 5 response to RAI 265 dated September 30, 2010) revising FSAR Tier 2, Figures 3.6.3-18, 3.6.3-19 and 3.6.3-20. Based on a telephone conference call with the applicant on April 7, 2010, the staff understood that AREVA would also revise the remaining ALL diagrams for MCL, MSL, and SL per the same procedure used for the SL. As stated in the telecon dated December 15, 2010, AREVA is requested to provide the NRC staff with revised versions of FSAR Tier 2, Figures 3.6.3-12,-13,-14,-15,-16,-17,-21,-22, and -23.

Response to Question 03.06.03-28:

As noted in the question, the revised ALL diagrams for the SL were provided to the NRC in the Response to RAI 265, Supplement 5, Question 03.06.03-26. U.S. EPR FSAR Tier 2, Section 3.6.3 will be revised to include the revised ALL diagrams for the MCL. Corresponding changes will be made to the text and tables. The ALL diagrams for the MSL do not need to be revised for the following reasons:

- The MSL contains no dissimilar metal welds; therefore, no equivalent material properties calculations are needed.
- The reference strain in the Ramberg-Osgood (R-O) was correctly defined as the ratio of reference stress to the elastic modulus. The Response to RAI 265, Supplement 5, Question 03.06.03-26 corrected a typing error of the reference strain values for the MSL piping in U.S. EPR FSAR Tier 2, Table 3.6.3-7 (the reference strain values varied by an order of magnitude). In the calculations for the MSL, since the reference strain was calculated explicitly as the ratio of reference stress to the elastic modulus, the correct value was used. Therefore, the correction to the reference strain values in U.S. EPR FSAR Tier 2, Table 3.6.3-7 did not affect the ALL diagrams for the MSL in U.S. EPR FSAR Tier 2, Section 3.6.3.
- The leakage calculations for the MSL line were determined using SQUIRT with single phase steam, and the fatigue crack morphology was used demonstrating that the recommended number of turns was used. The NRC also performed independent confirmatory analysis and had similar leakage results to those performed by AREVA NP.

FSAR Impact:

U.S. EPR FSAR Tier 2, Section 3.6.3 will be revised as described in the response and indicated on the enclosed markup. Note that some of these changes were made in U.S. EPR FSAR Revision 3 and boxed and flagged where the changes were made.

.

U.S. EPR Final Safety Analysis Report Markups

3.6.3 Leak-Before-Break Evaluation Procedures

This section describes the analyses used to eliminate from the design basis the dynamic effects of certain pipe ruptures for high-energy piping systems and demonstrate that the probability of pipe rupture is extremely low under conditions consistent with the design basis for the piping.

GDC 4 requires structures, systems, and components important to safety to be designed to accommodate the effects from loss-of-coolant accidents. However, dynamic effects associated with postulated pipe ruptures may be excluded from the design basis when analyses reviewed and approved by the NRC demonstrate that the probability of fluid system piping rupture is extremely low under conditions consistent with the design basis for the piping. Accordingly, this section addresses the piping systems that are qualified to be considered for the leak-before-break (LBB) application, the potential for piping failure mechanisms, the fracture mechanics analyses of postulated pipe cracks, and the leak detection system capability, which collectively demonstrate that the probability of pipe rupture is extremely low. This section also provides a description of the applicable piping and the analysis techniques used to eliminate from the structural design basis for the identified piping systems the dynamic effects of double-ended guillotine and equivalent longitudinal breaks.

A COL applicant that references the U.S. EPR design certification will confirm that the design LBB analysis remains bounding for each piping system and provide a summary of the results of the actual as-built, plant-specific LBB analysis, including material properties of piping and welds, stress analyses, leakage detection capability, and degradation mechanisms. The results of the bounding analyses are provided in the form of LBB allowable range of loadings or "LBB allowable load window."

3.6.3.1 Application of Leak-Before-Break to the U.S. EPR

The application of LBB is limited to the following high energy piping systems:

- Main coolant loop (MCL) piping, (hot legs, crossover legs, and cold legs).
- Pressurizer surge line (SL).
- Main steam line (MSL) piping inside the containment (i.e., from the steam generators to the first anchor point location at the Containment Building penetration).

3.6.3.2 Methods and Criteria

The methods and criteria to evaluate LBB are consistent with the guidance in NUREG-1061, Volume 3 (Reference 1), and the Standard Review Plan (SRP) 3.6.3 (Reference 2) and are described in the following sections. The following steps are used to perform the LBB analyses:

- Evaluate potential failure mechanisms (Section 3.6.3.3).
- Perform bounding analyses (Sections 3.6.3.4 and 3.6.3.5).

The results of the analyses are provided in Section 3.6.3.6. A description of the leakage detection capability is provided in Section 3.6.3.6.1.

3.6.3.3 Potential Piping Failure Mechanisms

3.6.3.3.1 Water Hammer

Water hammer is a generic term that includes various unanticipated high-frequency hydrodynamic events, such as steam hammer and water slugging.

3.6.3.3.1.1 Main Coolant Loop Piping and Surge Line Piping

Operating experience with existing plants has demonstrated that water hammer is not an issue with the MCL or SL piping for pressurized water reactors (PWR), as addressed in NUREG-0582 (Reference 3), NUREG-0927, Revision 1 (Reference 4), and NRC Information Notices 91-50 and Supplement 1. Water/steam events, as described in these documents, resulted in only support damage. There were no events in the MCL or SL piping systems that resulted in loss of pressure boundary integrity. NUREG-0927 evaluated 67 events, five of which were in the primary system and were caused by relief valve discharge. Relief valve actuation and the associated transients following valve opening have been considered in the U.S EPR design.

The MCL and SL pipes and supports are designed to ASME Class 1 requirements and are designed for Level A, B, C, and D service conditions. These portions of the reactor coolant system (RCS) are also designed to preclude void formation during normal operation. Because safety valve discharge loads associated with the pressurizer have been identified and included in the component design basis, MCL and SL piping have a very low level of susceptibility to failure from water hammer.

3.6.3.3.1.2 Main Steam Line

The U.S. EPR main steam supply system, including MSL pipe support system components, is designed to accommodate dynamic loads resulting from inadvertent closure of the main steam isolation valve (MSIV). To reduce the effects of steam and water hammer, the numbers of elbows and miters in the MSL piping layout are minimized. Valves in the main steam supply system are designed to withstand loads developed from the various operating and design basis events and transients described in Section 3.9.1. Steam-propelled water slug transients are prevented by design features in the system design and layout.

Based on the low severity of the water hammer events described in NUREG/CR-2781 (Reference 5) and the design considerations of the main steam supply system, the LBB

portion of the MSL piping has a very low level of susceptibility to failure from water hammer.

3.6.3.3.2 Creep

Creep and creep fatigue are not a concern for ferritic steel piping when operated below 700°F and for austenitic steel piping below 800°F. Because operating temperatures of the U.S. EPR piping systems are below these limits, creep and creep fatigue are not a concern.

3.6.3.3.3 Corrosion and Erosion/Corrosion

The MCL and SL piping are fabricated from austenitic stainless steel materials that are resistant to corrosion. Because water chemistry for the main coolant system is closely controlled and monitored, these pipes have a very low level of susceptibility to failure from these failure mechanisms.

Flow-accelerated corrosion (FAC) (also referred to as flow-assisted corrosion, flow-induced corrosion or erosion-corrosion), has been observed in the secondary side of PWR water-steam systems. Operating conditions such as steam quality, intended operating temperatures, various secondary chemistry regimes, and materials of construction are evaluated in order to minimize the potential for FAC in the main steam piping. Programs in operating plants that manage aging effects due to FAC consider operating experience (e.g., NRC Bulletin 87-01, Information Notice 91-18) and the guidelines for an effective FAC program presented in EPRI Report 1011838 (Reference 6). Additional details regarding FAC in the main steam supply system are provided in Section 10.3.6.3

3.6.3.3.4 Stress Corrosion Cracking

This section demonstrates that the piping and weld materials for the LBB piping are not susceptible to stress corrosion cracking (SCC) and that primary water stress corrosion cracking (PWSCC), intergranular stress corrosion cracking (IGSCC), and transgranular stress corrosion cracking (TGSCC) are also unlikely to occur in these piping systems.

3.6.3.3.4.1 Main Coolant Loop and Surge Line Piping

The following conditions are required for SCC to occur: material susceptibility, a corrosive environment, and tensile stress. These conditions are addressed below.

Material Susceptibility

In some stainless steels and high nickel alloys, slow cooling through the 800°F–1500°F temperature range allows the precipitation of chromium carbides at grain boundaries, depleting the area adjacent to grain boundaries of chromium. This process is termed

"sensitization" and renders materials susceptible to SCC. To reduce the susceptibility to SCC, the MCL and SL piping conform to ASME Boiler and Pressure Vessel Code, Section III (Reference 7) requirements supplemented by the guidelines of RG 1.44 and ASME NQA-1-1994 (Reference 8). The stainless steel piping has a carbon content that does not exceed 0.03 wt% and welds are either "L" grade or limited by a maximum carbon content that does not exceed 0.03 wt%, which reduces the potential for sensitization. The welds between the stainless steel safe ends and the low alloy steel nozzles are Alloy 52, which has a higher resistance to SCC than Alloy 600/82/182.

Corrosive Environment

Reactor coolant chemistry controls prevent the occurrence of SCC. Dissolved oxygen, halides, and other impurities are monitored by plant surveillance testing. Controlling oxygen is a key to avoiding a corrosive environment. Dissolved oxygen concentrations are maintained at very low levels during normal plant operation by applying hydrogen injection to the coolant system. The design of non-metallic insulation for the RCS conforms to the guidelines in RG 1.36, which restricts the use of chlorides and fluorides in the thermal insulation to prevent SCC.

Tensile Stress

As the imposed tensile stress increases, the likelihood of initiation and propagation of SCC increases. Stresses close to the material yield strength are required in a light water reactor environment to initiate SCC. The MCL and SL piping conform to ASME Code, Section III requirements, which provide the code-specified margin to yield stress during normal operation. Weld residual stresses can exceed yield; however, because of the U.S. operational experience for controlling material susceptibility and the environment described above, the potential for SCC is minimized.

As noted in SRP 3.6.3, "Primary water stress corrosion cracking (PWSCC) is considered to be an active degradation mechanism in Alloy 600/82/182 materials in pressurized water reactor plants. Alloy 690/52/152 material is not currently considered susceptible to PWSCC for the purposes of LBB application." As noted above, Alloy 52 weld material is used for the U.S. EPR. To further demonstrate that PWSCC is not a concern for LBB candidate piping, the U.S EPR inservice inspection (ISI) program will consider the operating experience of the materials used in the U.S. EPR piping systems qualified for LBB. The U.S. EPR inspection program will be consistent with the inspection program adopted for operating PWRs that use Alloy 690, 52, and 152 in approved LBB applications. A COL applicant that references the U.S. EPR design certification will implement the ISI program as augmented with NRC approved ASME Code cases that are developed and approved for augmented inspections of Alloy 690/152/52 material to address PWSCC concerns.

Avoiding intergranular attack and IGSCC in austenitic stainless steels is accomplished by the following methods:

- Use of low carbon (less than 0.03 wt% carbon) unstabilized austenitic stainless steels.
- Measuring for correct ferrite content.
- Utilizing materials in the solution annealed plus rapidly cooled condition and the prohibition of subsequent heat treatments in the 800°F to 1500°F temperature range.
- Control of primary water chemistry to maintain an environment that does not promote intergranular attack.
- Control of welding processes and procedures to avoid heat affected zone sensitization, as addressed in RG 1.44.

Additional details regarding the above methods are presented in Section 5.2.3.

The prerequisite for TGSCC in 300-series austenitic stainless steels is an aggressive species, such as chloride, in association with oxygen. If high levels of dissolved oxygen are present in stagnant conditions, a higher susceptibility to SCC exists. When the stainless steel material is sensitized, IGSCC or mixed modes of cracking can occur and the material is more susceptible to SCC, as described by Gordon (Reference 9). Chloride and oxygen are typically associated as corrosive agents, although fluoride and sulfate can also be associated with SCC. Oxygen has a dominant role in the SCC susceptibility of austenitic stainless steels, with a small increase in oxygen resulting in a dramatic response in SCC. Very low levels of oxygen prevent TGSCC in these materials. TGSCC is unlikely at dissolved oxygen concentrations of less than 100 ppb and chloride levels of less than 150 ppb for various austenitic stainless steel alloys in both the annealed and sensitized heat treated condition when exposed to 480°F– 660°F water (Reference 9). The likelihood of both IGSCC and TGSCC for susceptible alloys exposed to dissolved oxygen of less than 100 ppb and chloride of less than 150 ppb at lower temperatures is significantly reduced. These limits are the historical basis for PWR RCS chemistry limits to prevent SCC.

Proper control of RCS water chemistry prevents the impurity intrusion that provides the necessary environment for TGSCC. The water chemistry limits verify that dissolved oxygen, sulfates, and halogens are minimized. Additionally, the MCL and SL piping are not subject to stagnant conditions during normal operation. Due to controls on RCS water chemistry and non-stagnant conditions in the main coolant loop and surge line piping, TGSCC is not expected in these piping systems.

3.6.3.3.4.2 Main Steam Line Piping

The U.S. EPR uses an all volatile chemistry treatment on the secondary system to increase cycle pH and provide a reducing environment. This produces the lowest possible general corrosion rate of the different materials present in the secondary system, thus minimizing flow-assisted corrosion and corrosion transport. Additionally, there has been no evidence of stress corrosion cracking in the carbon steel piping of the main steam lines of operating plants. The secondary side water chemistry program is addressed in Section 10.3.5.

3.6.3.3.5 Fatigue

3.6.3.3.5.1 Main Coolant Loop and Surge Line Piping

An evaluation of fatigue for Class 1 piping is provided in U.S. EPR Piping Analysis and Pipe Support Design (Reference 10). Additionally, Section 3.12 addresses the effects of the reactor coolant environment on fatigue. Normal and upset thermal and seismic loadings are evaluated as part of the piping stress analysis.

The potential for high cycle fatigue is primarily due to excessive pump vibrations. The reactor coolant pumps (RCP) have instrumentation that alarms in the Main Control Room, to identify excessive pump shaft vibrations and preclude damage. Additionally, the RCS is monitored to provide an accurate assessment of fatigue over the lifetime of the plant. SL thermal stratification is not a concern due to the layout of the SL geometry and the continuous bypass spray flow. This is addressed further in Section 3.6.3.3.7.

3.6.3.3.5.2 Main Steam Line Piping

As noted in Reference 10, Class 2 and 3 piping is evaluated for fatigue due to thermal cycles by following the requirements in the ASME Code, Section III, Subsection NC on fatigue criteria.

The applicable design basis transients identified in Section 3.9.1 are considered in establishing the allowable stress limits, in accordance with Subsection NC, Subparagraph 3611.2. The allowable stress for thermal expansion is reduced for cyclic conditions based on the number of equivalent full temperature cycles.

The MSL piping is not subjected to severe Level A or B thermal or pressure transients when compared against the RCS primary piping. The impact of gross bending on the fatigue life of the piping is considered in the Class 2 design. The range of expected equivalent full temperature cycles in the steam line is less than 7000 cycles. Additionally, there are no normal or upset temperature or pressure variations that would result in significant local or through-wall stresses. Accordingly, a low usage factor is expected if the MSL is evaluated as Class 1 piping.

3.6.3.3.6 Thermal Aging

Forged austenitic stainless steel is used for the MCL and SL piping. Austenitic stainless steel forgings have a low susceptibility to thermal aging. The welds in the MCL stainless steel piping are fabricated using the gas tungsten arc welding (GTAW) process and meet the requirements of the ASME Code, Section III and the guidance of RG 1.31, which minimizes the effects of thermal aging. Lower bound toughness properties used in flaw stability analysis conservatively considers reduction because of thermal aging in the stainless steel weld metal and the component nozzles.

The component in the RCS loop that is predicted to experience the greatest reduction in toughness due to thermal aging is the RCP casing, which is made of cast austenitic stainless steel, type CF-3. The accepted screening limit for aging considerations states that static cast low-molybdenum steels with <20 percent ferrite are not susceptible to thermal aging embrittlement at the RCP operating temperature to an extent that would be of concern. Delta ferrite (δ_c) is limited to <20 percent and silicon to <1.5 percent. Lower bound curves were developed using a predictive model. The material properties used in the LBB analysis are based on the results predicted for the saturated condition. Therefore, thermal aging is not a concern for the RCP case.

Ferrite limitations for CASS RCPB materials are described in Section 5.2.3.4.6.

The MSL piping is carbon steel and contains no cast materials. Therefore, thermal aging of the MSL piping is not a concern.

3.6.3.3.7 Thermal Stratification

Thermal stratification is a potential issue in horizontal pipe segments when fluid at a significantly different temperature than the fluid in the piping is introduced at low flow velocities. The U.S. EPR is designed to preclude those conditions (refer to Section 3.7 of Reference 10 and FSAR Section 3.12). Each of the piping systems is addressed below.

3.6.3.3.7.1 Main Coolant Loop Piping

The MCL piping is not susceptible to thermal stratification since it does not experience stagnant flow conditions.

3.6.3.3.7.2 Surge Line Piping

Section 3.7.2 of Reference 10 and FSAR Section 3.12 describe the design features that minimize the potential for thermal stratification in the SL. The SL geometry is also described in Section 5.4.10.

3.6.3.3.7.3 Main Steam Line Piping

Because the MSL operates in a saturated steam environment, thermal stratification is not a concern for the MSL piping.

3.6.3.3.8 Other Mechanisms

3.6.3.3.8.1 Failure from Indirect Causes

Pipe degradation or failure by indirect causes (e.g., fires, missiles, or component support failures) is precluded by design, fabrication, and inspection. Additionally, piping design considers separation of potential hazards in the vicinity of the safety-related piping. The structures, larger pipe, and components in the vicinity of pipe evaluated for LBB are safety-related and seismically designed, or are seismically supported if they are non-safety-related. Further information is provided below:

- Missiles: Missile prevention and protection are described in Section 3.5.
- Flooding: Flood protection and analysis are provided in Section 3.4.
- Fires: Fire prevention and protection are described in Section 9.5.1.
- System overpressurization: The reactor coolant system is protected from over-pressurization by ASME Code safety relief valves (refer to Section 5.2.2). Overpressure protection for the MSL is described in Section 10.1.
- Damages from moving equipment: Load drops are highly improbable due to the design of handling devices and administrative controls. Additionally heavy loads are not handled inside containment while at power. Chapter 15 describes accident analyses due to load drops.
- Seismic: The RCS and the MSL are designed to maintain their integrity during a safe shutdown earthquake (see Section 3.2).

3.6.3.3.8.2 Cleavage Type Failures

Cleavage type failures are not a concern for the system operating temperatures and materials present in the MCL, SL, and MSL. Material tests for these components show the materials to be highly ductile and resistant to cleavage type failures at operating temperatures.

3.6.3.3.9 Failure Prevention and Detection

3.6.3.3.9.1 Snubber Reliability

Snubber use and locations are determined during detailed design in accordance with Reference 10 and tested as described in Section 3.9.6.

3.6.3.3.9.2 Inservice Inspection

For ASME Code Class 1 and Class 2 systems for which LBB is demonstrated, the ASME Code, Section III (Reference 7) and ASME Code, Section XI (Reference 11) preservice and inservice inspection requirements provide for the integrity of each system. Pressure-retaining components are designed to permit preservice and inservice inspections. The design provides accessibility for inspection in accordance with ASME Code Section XI, Division 1, Subarticle IWA-1500 and the requirements of 10 CFR 50.55a(g)(3)(i). Welds in Class 2 high-energy piping are subject to augmented inservice inspection, in accordance with the requirements of Article IWC-2000 for Examination Category C–F welds.

3.6.3.4 Inputs for Leak-Before-Break Analysis

3.6.3.4.1 Geometry and Operating Condition

The dimensional information and operating conditions for each MCL piping assembly are summarized in Table 3.6.3-1—Main Coolant System Piping Dimensions and Operating Condition. The U.S. EPR design minimizes the number of butt welds in the RCS primary piping. The butt welds are a narrow-groove design. The locations and number of narrow-groove butt welds are illustrated for loop 4 of the MCL piping by the plan and elevation views in Figure 3.6.3-1—Plain View of U.S. EPR RCS Primary Piping and Figure 3.6.3-2—Elevation View of U.S. EPR RCS Primary Piping, respectively.

The dimensional information and operating conditions for each SL piping assembly are summarized in Table 3.6.3-2—Surge Line Piping Dimensions and Operating Condition. The locations and number of narrow-groove butt welds in the SL piping are shown in Table 3.6.3-3—Plan, Elevation, and Isometric View of the U.S. EPR Surge Line.

The dimensional information and operating conditions for each MSL piping assembly are shown in Table 3.6.3-3—Main Steam Line Dimensions and Operating Condition. The location and number of butt welds for the LBB portion of a typical MSL piping are depicted in Figure 3.6.3-4—Isometric View of the Main Steam Line.

For the LBB evaluation, the plant is assumed to be operating under normal full power conditions with a postulated flaw size that produces ten times the overall leak detection capability of a given piping system.

3.6.3.4.2 Materials

3.6.3.4.2.1 Main Coolant Loop and Surge Line Piping Materials

The MCL and SL piping consist of SA-336 F304 or SA-182 F304 austenitic stainless steel. The MCL and SL piping is solution annealed and rapidly cooled, and has carbon

content that does not exceed 0.03 wt%. The RCP casings are the only cast stainless product form within the MCL, and are made of SA-351 CF-3 with additional restrictions described in Section 3.6.3.4.3.3 The stainless steel pipe welds are fabricated with dual-certified ER308/308L using the narrow-groove GTAW welding process. The safe end forging material is SA-182 F316 or SA-336 F316. The dissimilar metal weld joints between the safe ends and the respective component nozzles of the pressurizer surge nozzle, the steam generator (SG) nozzles, and RPV nozzles are fabricated using NiCrFe alloy filler metal Alloy 52/52M (ERNiCrFe-7/ ERNiCrFe-7A respectively). The pressurizer surge nozzle (forging) material and the steam generator inlet and outlet nozzle (forging) material are SA-508 Grade 3 Class 2 and the RPV inlet and outlet nozzle material is SA-508 Grade 3 Class 1.

3.6.3.4.2.2 Main Steam Line Piping Materials

The MSL piping is made of SA 106 Grade C carbon steel material.

3.6.3.4.3 Material Properties

3.6.3.4.3.1 Main Coolant Loop Piping Weld and Base Metal Properties

A test program based on Reference 1 was conducted on three ER308/308L narrow groove GTAW welds with different wire heats to provide for lower bound J-R fracture toughness and tensile data. The testing was conducted using compact tension specimens cut from the full thickness of the pipe welds, as wells as 1T size compact tension specimens. The lower bounding J-R curve, with projected reduction of toughness because of thermal aging, was derived from the test results for the welds. The J-R properties for low alloy steel nozzles and the J-R properties for cast austenitic stainless steel (CASS) pump casing nozzles that account for thermal aging are determined from applicable industry data.

The engineering stress-strain curves for the base metal and weld metal are obtained from the test program and converted to true-stress true-strain curves. The following Ramberg-Osgood equation is used to fit the stress-strain curve data:

$$\frac{\varepsilon}{\varepsilon_o} = \frac{\sigma}{\sigma_o} + \alpha\left(\frac{\sigma}{\sigma_o}\right)^n$$

where:

σ, ε = true-stress, true-strain

σ_o, ε_o = yield stress, yield strain

α, n = Ramberg-Osgood material parameters

The tensile properties and the Ramberg-Osgood parameters for the hot and cold leg piping are presented in Table 3.6.3-4—Tensile Properties of Materials at Various Locations of Main Coolant Loop Piping. The material parameters for the J-R equation (C and N) are determined using the $J_{Deformation}$ and Δa experimental data of the applicable compact tension specimens. The power law formula for the J-R data is obtained using a linear regression analysis and is given below:

$$J_D = C(\Delta a)^N$$

where:

J_D = $J_{Deformation}$ in units of lbs/in

Δa is in inches

C = the material constant

N = the exponent

The J-R curve for the base metal of the MCL piping material is determined from the test results, as well as from similar materials in the industry as summarized in NUREG/CR-6446 (Reference 12), NUREG/CR-4082, Vol. 8 (Reference 13), and NUREG/CR-4599 (Reference 14). The lower bound J-R curve power law parameters for the MCL base metal are determined for the LBB analysis. Thermal aging of wrought 304 and 316 is expected to be negligible, therefore it is not considered in this evaluation.

3.6.3.4.3.2 Dissimilar Metal Weld between Component Nozzle and MCL Piping

Alloy 52/52M is the dissimilar metal weld that is used between the MCL piping and both the primary component nozzles of the reactor vessel and the primary nozzles of the steam generators. The J-R curve for the Alloy 52 weld metal is determined using specimens that are fatigue pre-cracked on the fusion line. The J-R curve parameters, using ASTM Standard E1820 (Reference 15), were used in this assessment considering the case without a limit on crack extension. The J-R curve for Alloy 52 weld metal, developed at the fusion line, is lower than the J-R curve for the base metal and the stainless steel weld metal of the MCL piping. For the Alloy 52 weld metal, the J-R parameters considering the fusion line toughness are used in the LBB analysis. The equivalent material tensile properties for the dissimilar metal weld (DMW) at the fusion line location are determined using finite element based elastic-plastic fracture mechanics analysis and provided in Table 3.6.3-4. These material properties at the DMW fusion line region are determined considering the adjoining base metal materials which are F304LN and SA-508 Grade 3 Class 2. The material properties for SA-508 Grade 3 Class 2 are approximated by the material properties for SA-508 Class 3 which are obtained from NUREG/CR-6837, Volume 2 (Reference 25).

RAI 467
Q.03.06.03-28

3.6.3.4.3.3 Primary Component Nozzles of the MCL

The effects of thermal aging for the primary component nozzles of the reactor vessel and the steam generator nozzles, fabricated from SA-508 Grade 3 Class 1, and SA-508 Grade 3 Class 2, respectively, are considered in determining the lower bound J-R curves for the nozzles. The J-R curves for these materials are determined from published literature. Adjustments to the J-R curves for the reactor vessel nozzle materials are made to account for operating conditions and anticipated aging effects. The J-R curves for SA-508 Grade 3, Class 2 material are determined using the correlation between upper shelf energy and upper shelf J-R properties for SA-508 Grade 3 Class1 material. Based on the correlation, the SA-508 Grade 3 Class 1 curves are reduced by 30 percent to approximate the J-R curves for SA-508 Grade 3 Class 2 material.

3.6.3.4.3.4 RCP Casing Nozzles

The RCP casings (including the nozzles) are fabricated from static CASS. The RCP casings are fabricated using SA-351 CF-3 material specification with additional restrictions on silicon (1.5 percent maximum) and niobium (restricted to trace amounts). In addition, the ferrite number is restricted to <20 percent. The lower bound J-R curves for the saturated condition are determined based on a predictive model developed in NUREG/CR-6177 (Reference 16).

3.6.3.4.3.5 Surge Line Weld and Base Metal Properties

The SL weld and base metal properties are determined from the same test program described in Section 3.6.3.4.3. The testing was conducted using compact tension specimens cut from the full thickness of the SL pipe weld geometry. The lower bound SL weld and base metal J-R curves are developed using the same approach as provided in Section 3.6.3.4.3 for the MCL. Therefore, the thermal aging effects of the SL weld metal are considered. The tensile properties with associated Ramberg-Osgood parameters of the various SL piping materials are shown in Table 3.6.3-5—Tensile Properties for the Surge Line Piping.

3.6.3.4.3.6 Dissimilar Metal Weld between Pressurizer Surge Nozzle and Surge Line Piping

The Alloy 52 fusion line toughness J-R properties, determined in Section 3.6.3.4.3.2, are used in the analysis. The equivalent material tensile properties for the dissimilar metal weld (DMW) at the fusion line location are determined using finite element based elastic-plastic fracture mechanics analysis and provided in Table 3.6.3-5. These material properties at the DMW fusion line region are determined considering the adjoining base metal materials which are F304LN and SA-508 Grade 3 Class 2. The material properties for SA-508 Grade 3 Class 2 are approximated by the material

properties for SA-508 Class 3 which are obtained from NUREG/CR-6837, Volume 2 (Reference 25).

3.6.3.4.3.7 Pressurizer Surge Nozzle

The pressurizer surge nozzle is fabricated from SA-508 Grade 3 Class 2 material. The lower bound J-R properties, considering the effects of thermal aging, for SA-508 Grade 3 Class 2, addressed in Section 3.6.3.4.3.3 are also applicable to the pressurizer surge nozzle. In the region of the pressurizer nozzle it is the dissimilar metal weld location that is limiting for LBB application, as shown in Table 3.6.3-6—Surge Line Piping Locations Based on Key Geometry, Operating Conditions & Lower Bound Material Toughness.

3.6.3.4.3.8 Main Steam Line Weld and Base Metal Properties

The tensile and fracture material properties for ASME SA-106 Grade C carbon steel material and associate weld material used in this analysis are based on a piping material test program that examined six heats of weld metals. Three heats were manual weld metals (one E7015 SMAW and two E8015 SMAW), and the other three heats were automatic submerged weld metals (High Mn-Mo SAW). The properties used in the analysis are the lower bound properties obtained from the test program. The tensile properties are provided in terms of the yield stress, ultimate strength, flow stress, and Young's modulus and are shown in Table 3.6.3-7—Tensile Properties for the Main Steam Line Piping. The Ramberg-Osgood material model parameters are also summarized in Table 3.6.3-7. The fracture toughness properties are provided in terms of the J-R curve. The lower bound material J-R curves for the SA106, Grade C and the weld metals are determined and used in the flaw stability analysis of Section 3.6.3.5.4.1.

3.6.3.5 General Methodology

The load combination methods described in Section 3.6.3.5.1 are applicable to the LBB analyses. For the MCL and the SL piping, the leak rate calculations, performed considering fatigue crack morphology, are determined using AREVA NP computer code KRAKFLO (see Section 3.6.3.5.2). For the MSL LBB analysis, computer code SQUIRT Version 1.1 (see Section 3.6.3.5.3) is used. Since the MCL and SL piping materials are highly ductile austenitic stainless steels, both the limit load analysis and the flaw stability analysis methodology are considered appropriate. For the MCL and SL piping, the flaw stability analysis methodology is used. Since the MSL is made of ferritic steel, the flaw stability methodology is also used in that analysis.

3.6.3.5.1 Load Combination Methods

SRP 3.6.3 addresses two load combination methods: the absolute sum load combination method and the algebraic sum load combination method. The absolute

sum load combination method is provided in SRP 3.6.3. The algebraic sum load combination method is shown below:

$$M_{XMAX} = \left|M_{Xdw} + M_{Xth} + M_{Xpress}\right| + \left|M_{Xsse}\right| + \left|M_{Xsam}\right|$$

$$M_{YMAX} = \left|M_{Ydw} + M_{Yth} + M_{Ypress}\right| + \left|M_{Ysse}\right| + \left|M_{Ysam}\right|$$

$$M_{ZMAX} = \left|M_{Zdw} + M_{Zth} + M_{Zpress}\right| + \left|M_{Zsse}\right| + \left|M_{Zsam}\right|$$

where:

M_{idw} = the moment due to deadweight, for I = X, Y, and Z

M_{ith} = the moment due thermal expansion, for I = X, Y, and Z

M_{ipress}= the moment due to pressure, for I = X, Y, and Z

M_{isse} = the moment due seismic, for I = X, Y, and Z

M_{isam} = the moment due seismic anchor motion moment, for I = X, Y, and Z

and

$$M_{MAX} = 1.4\sqrt{M_{XMAX}^2 + M_{YMAX}^2 + M_{ZMAX}^2}$$

For the calculations of the minimum moment, only the algebraic sum load combination method is applicable. However, for the calculations of the maximum moment, the algebraic sum load combination method or the absolute sum load combination method may be used. The LBB flaw stability analyses summarized in Section 3.6.3.5.4 are performed using the absolute sum load combination method.

The premise of the LBB concept in piping is that a flaw will be detected via loss of fluid prior to the failure of the pipe. This requires two types of analyses: one in which the minimum load that leads to a detectable leak rate is calculated, and another which calculates the maximum allowable load in the flawed pipe. The minimum and maximum moment loads are defined below. The maximum allowable load must exceed the minimum load evaluated for leakage crack size, with applicable margins of safety on both flaw size and load.

Minimum Moment

The minimum moment corresponds to deadweight, steady state pressure and thermal expansion moment for normal operation. The minimum moment is obtained by

algebraically summing the individual components of moments due to deadweight, steady state pressure, and thermal expansion, and then determining its square root of the sum of the squares value. The minimum moment, including axial load due to operating pressure, is present during steady state conditions; if a leaking crack exists it tends to open the crack and allow flow through the crack. For a higher operating pressure and minimum moment at a constant leak rate (gallons per minute), the crack length necessary to produce the same leak rate is actually smaller, since higher stress enlarges the crack width.

Maximum Moment

The maximum moment to be evaluated combines the minimum moment with the moments due to seismic and seismic anchor motions. The SSE loadings include the seismic anchor motion loads. As previously noted, the maximum moment is determined using the absolute sum load combination method.

Loadings on Main Coolant Loop, Surge Line, and Main Steam Line

A bounding analysis in the form of LBB allowable load window approach is used in this analysis. Once the allowable load window for a given piping system is generated, the loads for the piping system can then be plotted on the allowable load window. If the applied loading points lie within the allowable load window, LBB is justified for the pipe with appropriate safety margins already included in the window.

3.6.3.5.2 Leak Rate Determination Method for Main Coolant Loop and Surge Line

Leak rate calculations for MCL and SL piping are performed using AREVA NP computer code KRAKFLO, which is similar to the NRC code LKRATE. The leak flow calculations used in KRAKFLO are benchmarked against the Battelle Columbus Laboratories data as presented in EPRI Report NP-3395 (Reference 17). KRAKFLO is based on the LEAK-01 program documented in Reference 17 but has improved ability to determine pressure drops for initially subcooled, non-flashing liquid. KRAKFLO's crack geometry methodology is based on NUREG/CR-3464 (Reference 18); and its flow rate calculation is based on NUREG/CR-1319 (Reference 19). This code has been benchmarked and is in agreement with experimental data.

Leakage crack sizes associated with a leak rate of 5 gpm are determined in the analysis. This leak rate provides a factor of ten to the leak detection system (LDS) capability. The leakage rate calculations are performed for straight pipe with both axial and circumferential through-wall cracks. For the axial through-wall crack orientations, pressure-only loading is considered, while external bending and pressure loadings are considered for the circumferential through-wall cracks.

Main Coolant Loop

The leakage rate calculations are determined at the following locations (Location 1 through Location 9) in the MCL piping:

1. RV Outlet Nozzle Region at Hot Leg.
2. Hot Leg Pipe.
3. SG Inlet Nozzle Region at Hot Leg.
4. SG Outlet Nozzle Region.
5. Crossover Leg.
6. RCP Inlet Nozzle Region.
7. RCP Outlet Nozzle Region.
8. Cold Leg Pipe.
9. RV Inlet Nozzle Region.

RAI 467 Q.03.06.03-28

Surge Line

For the SL piping, the leakage rate calculations are determined at the following locations:

- Pressurizer surge nozzle end of the SL.
- Pressurizer SL
- Hot leg nozzle end of the SL.

The leak rate analysis considers fatigue (air) crack morphology with applicable number of turns and roughness values reported in NUREG/CR-6004 (Reference 29) and shown in Table 3.6.3-26. The leakage crack lengths versus minimum moment at each of the above nine locations for the MCL are shown in Table 3.6.3-8—Minimum Moment versus Circumferential Crack Leakage Crack Sizes for 5 gpm at Various Main Coolant Loop Piping Locations and are illustrated in Figure 3.6.3-5—Minimum Moment versus Circumferential Leakage Crack Sizes for 5 gpm at Various Main Coolant Loop Locations. For the through-wall axial cracks, the leakage crack sizes are shown in Table 3.6.3-9—Axial Through-Wall Leakage Crack Sizes for 5 gpm at Various Main Coolant Loop Piping Locations. For SL piping, the leakage crack lengths versus moment at each of the above three locations are shown in Table 3.6.3-10—Minimum Moment versus Circumferential Leakage Crack Sizes for 5 gpm at Two Surge Line Piping Locations and are illustrated in Table 3.6.3-6—Surge Line Piping Locations Based on Key Geometry, Operating Conditions & Lower Bound Material Toughness.

RAI 467 Q.03.06.03-28

RAI 467 Q.03.06.03-28

For the through-wall axial cracks, the leakage crack sizes are shown in Table 3.6.3-11—Axial Through-Wall Leakage Crack Sizes for 5 gpm at Three Surge Line Piping Locations.

RAI 467
Q.03.06.03-28

3.6.3.5.3 Leak Rate Determination Method for Main Steam Line

The leak rate calculations for the MSL piping are performed using SQUIRT Code Version 1.1. The SQUIRT Code is described in NUREG/CR-5128 (Reference 20) and the SQUIRT User's Manual (Reference 21) and has been benchmarked to the experimental steam data developed in Japan, as described in NUREG/CR-6861 (Reference 22). The SQUIRT code has been updated with technical enhancements as part of the NRC large break LOCA program. The SQUIRT Code is used to calculate the leakage rate through the cracked pipe for single phase steam conditions.

Leakage crack sizes associated with a leak rate of one gpm are determined in the analysis. This leak rate provides a factor of ten to the LDS capability. The leakage rate calculations are performed for straight pipe with both axial and circumferential through-wall cracks. Similar to MCL, for the axial through-wall crack orientation, pressure-only loading is considered while external bending and pressure loading is considered for the circumferential through-wall crack. The results of the pressure-only case, as depicted in Figure 3.6.3-7—Pressure Only Leakage Rate versus Crack Length for Both Axial and Circumferential Crack Morphologies in Main Steam Line, show that for a given crack size the axial through-wall cracks produced a higher leakage rate. As a result, the circumferential leakage crack sizes are conservatively used when analyzing axial leakage cracks. The results of the leak rate calculations provided in Table 3.6.3-12—Minimum Moment versus Circumferential Leakage Crack Leakage Sizes for 1 gpm in the Main Steam Line Piping. The results are also shown in Figure 3.6.3-8—Minimum Moment versus Circumferential Crack Leakage Crack Sizes for 1 gpm in Main Steam Line Piping, in terms of the minimum moment diagrams for a leakage rate of one gpm. The external axial load is set equal to zero in the leak rate calculations. This is considered conservative, since the crack size required to produce a given leakage rate will actually be smaller in the presence of external axial tensile loads. The leakage crack sizes calculated from the circumferential through-wall crack in straight pipe are also used for analyzing circumferential through-wall extrados crack in an elbow.

RAI 467
Q.03.06.03-28

RAI 467
Q.03.06.03-28

3.6.3.5.4 Flaw Stability Analysis Method

The method employed for the flaw stability analysis is the tearing instability analysis method, using a J versus T diagram. The inputs for the flaw stability analysis include the applied J and the material J-R curves. The applied J ($J_{applied}$) depends on the geometry, material, and the applied loads. The material properties are described in terms of the J-R fracture resistance curves which are obtained from tests in accordance with Reference 15 as well as industry data of comparable materials.

To estimate the $J_{applied}$, a J-integral solution is needed. The J-integral solution is a function of geometry, material, and crack size and orientation. Each J-integral solution is usually tabulated in terms of influence coefficients that are calculated based on finite element analyses. The stability analysis covers the following crack geometries:

- Circumferential through-wall crack in a straight pipe.
- Axial through-wall crack in straight pipe.
- Circumferential through-wall extrados crack in an elbow.

A J-integral solution is used for each of the above crack orientations. The following sections address the J-integral solution for each of the crack geometries. For the circumferential through-wall cracks in a straight pipe, the EPRI/GE method reported in EPRI NP-5596 (Reference 23) is used to calculate the J-integral. For the MCL and SL piping, the alpha term in the $J_{Plastic}$ part of the equation given in Section 3.6.3.5.4.1 is modified based on the recommendation provided in Analysis of Experiments on Stainless Steel Flux Welds (Reference 24). This modification of the alpha term is provided as the last set of J-integral equations for SL piping in Section 3.6.3.5.4.1. For a circumferential through-wall extrados crack in an elbow, the criteria of NUREG/CR-6837 (Reference 25) are used to evaluate the J-integral.

3.6.3.5.4.1 Circumferential Through-Wall Crack in Straight Pipe Solution

Main Steam Line Piping

RAI 467
Q.03.06.03-28

The J-integral solution for a circumferentially through-wall cracked cylinder for a combined tension and bending loading condition is used for this analysis. A schematic of this cracked pipe geometry is illustrated in Figure 3.6.3-9—Schematics of Analyzed Crack Geometries Considered for Straight Pipe Section. The solution procedure is summarized as follows:

$$J = J_{Bending-Elastic} + J_{Axial-Elastic} + J_{Plastic}$$

where:

$$J_{Bending-Elastic} = \frac{M^2}{E}\pi a\left(\frac{R}{I}\right)^2 F_B^2\left(\frac{a_e}{b},\frac{R}{T}\right)$$

$$J_{Axial-Elastic} = \frac{P^2}{E}\frac{aF_T^2\left(\frac{a_e}{b},\frac{R}{t}\right)}{4\pi R^2 t^2}$$

RAI 467
Q.03.06.03-28

$$J_{Plastic} = \alpha\sigma_o\varepsilon_o c\frac{a}{b}h_1\left(\frac{a}{b}, n, \lambda, \frac{R}{t}\right)\left[\frac{P}{P_o'}\right]^{n+1}$$

The P_o' in the $J_{Plastic}$ equation is the reference load for the combined tension and bending loads given as:

$$P_o' = \frac{1}{2}\left[\frac{-\lambda P_o^{\,2} R}{M_o} + \sqrt{\left(\frac{\lambda P_o^{\,2} R}{M_o}\right)^2 + 4P_o^{\,2}}\right]$$

where:

Limit Load

$$P_o = 2\sigma_o Rt\left(\pi - \gamma - 2\arcsin\left(\frac{1}{2}\sin\gamma\right)\right)$$

Limit Moment

$$M_o = 4\sigma_o R^2 t\left(\cos\left(\frac{\gamma}{2}\right) - \frac{1}{2}\sin\gamma\right)$$

Un-Cracked Ligament

$$2c = 2R(\pi - \gamma)$$

Non-Dimensional Parameter

$$\lambda = \frac{M}{PR}$$

Plastic Zone Correction

$$a_e = a + \frac{1}{1+\left(\frac{P}{P_o}\right)^2}\frac{1}{6\pi}\left[\frac{n-1}{n+1}\right]\frac{EJ_{Elastic}}{\sigma_o^2}$$

where:

R = the pipe mean radius

t = the pipe thickness

I = area moment of inertia of the pipe section

a = the flaw size or one-half the leakage crack size

b = one-half the pipe circumference

c = uncracked ligament (b – a)

E = Young's modulus

M = the bending moment

P = the tensile load

σ_o and ε_o= the reference stress and reference strain in the Ramberg-Osgood material model

γ = the crack half-angle

F_B and F_T = the tabulated elastic solution coefficients for bending and axial loading (functions of geometry only – a/b and R/t) as provided in Reference 23

h_1 = the tabulated fully plastic solution parameter, function of (material strain hardening exponent, n and geometry, a/b and R/t)

RAI 467
Q.03.06.03-28

For the MSL piping, the elastic solution coefficients (F_B and F_T) from the EPRI reports are linearly interpolated where applicable to generate the solution for the specific R/t geometry that is being evaluated.

Main Coolant Loop and Surge Line Piping

A J-integral solution for a circumferentially through-wall cracked cylinder subjected to bending loads is used in the analysis for the SL piping. This EPRI/GE solution is provided in Reference 23. The alpha term in the solution is corrected based on Reference 24. This particular J-integral solution is chosen since the SL geometry has an R_m/t ratio of approximately five (with Ramberg-Osgood material constant n=7) and the h-function for $R_m/t = 5$ is available for through-wall cracks in bending. For the SL piping, the J-integral solution for combined tension and bending provided above (main coolant loop and main steam line piping) is not used, since the coefficients for this solution are only developed for R_m/t of 10 or greater.

In order to use the J-integral solution for bending loads only, the axial forces due to end cap pressure or external loads are converted into an equivalent moment. The equivalent bending is then combined with the applied moment to obtain the total moment to which the pipe is subjected. The general approach of calculating an equivalent moment is outlined below.

The moment M_{eq} is considered to be equivalent to axial load P when the Mode I stress intensity factor, K_I due to bending moment M_{eq} is the same as K_I due to axial tensile load P.

From the Ductile Fracture Handbook (Reference 26):

$$K_1 = \sigma_b(\pi R\gamma)^{0.5} \bullet F_b = \sigma_t(\pi R\gamma)^{0.5} \bullet F_t$$

where:

$$\sigma_b = \frac{M_{eq}}{\pi R_m{}^2 t}$$

$$\sigma_t = \frac{P}{2\pi R_m t}$$

$$F_b = 1 + A\left[4.5967(\gamma/\pi)^{1.5} + 2.6422(\gamma/\pi)^{4.24}\right]$$

$$F_t = 1 + A\left[5.3303(\gamma/\pi)^{1.5} + 18.773(\gamma/\pi)^{4.24}\right]$$

$$A = \left[0.125(R_m/t) - 0.25\right]^{0.25}$$

therefore:

$$M_{eq} = 0.5 R_m (F_t/F_b) \bullet P$$

In the above equations, R_m is the pipe mean radius, t is the pipe thickness, M_{eq} is the equivalent bending moment, P is the axial tensile load, and γ is the crack half-angle. The F_t and F_b formulas listed above are used for calculating M_{eq} only.

The J-integral solution from Reference 23 for bending load is summarized as follows:

$$J = J_{elastic} + J_{plastic}$$

where:

$$J_{elastic} = \frac{M^2}{E}\pi a\left(\frac{R_m}{I}\right)^2 F^2$$

$$J_{plastic} = \alpha\sigma_o\varepsilon_o c\frac{a}{b}h_1\left[\frac{M}{M_o}\right]^{n+1}$$

where:

Limit Moment

$$M_o = 4\sigma_o R_m^2 t\left(\cos(\frac{\gamma}{2}) - \frac{1}{2}\sin\gamma\right)$$

Un-Cracked Ligament

$2c = 2R(\pi - \gamma)$

Plastic Zone Correction

$$a_e = a + \frac{1}{1+\left(\frac{M}{M_0}\right)^2}\frac{1}{6\pi}\left[\frac{n-1}{n+1}\right]\frac{EJ_{elastic}}{\sigma_o^2}$$

α Correction

$$\alpha = \left[\alpha_o(\frac{\sigma_o}{\sigma_y})^{[(n-1)n]}\right]^{(\frac{1}{n+1})}$$

where:

R_m = the pipe mean radius

t = the pipe thickness

I = the pipe section moment of inertia

a = the flaw size or one-half the leakage crack size

b = the half-circumference

c = the uncracked ligament

E = Young's modulus

M = the total bending moment (applied moment + equivalent moment)

σ_o and ε_o = the reference stress and reference strain in the Ramberg-Osgood material model

α_o and n = the Ramberg-Osgood material constants

γ = the crack half-angle.

The solution coefficient F (a function of the material strain hardening exponent, n and geometry, a/b and R_m/t) is the tabulated elastic solution parameter for remote bending for a circumferential crack in a straight pipe and is from Reference 23. The solution coefficient h_1 (a function of the material strain hardening exponent, n and geometry, a/b and R_m/t) is the tabulated fully plastic solution parameter for remote bending for a circumferential crack in a straight pipe per Reference 23.

The solution coefficients h_1 and F (for bending only) are provided for only limited a/b R_m/t, and n values in Reference 23. Therefore, a polynomial curve approximately fitting these limited data points is developed and used to interpolate for the specific a/b or R_m/t geometry that is being evaluated.

3.6.3.5.4.2 Axial Through-Wall Crack in Straight Pipe

The Ductile Fracture Handbook (Reference 26) solution for an axial through wall crack in a straight pipe under internal pressure only was used to evaluate crack stability for the range of leakage crack sizes evaluated in this analysis.

The J-integral solution is provided in Reference 26 as:

$$J = \frac{8C\sigma_f^2}{\pi E} \ln\left(\sec\left(\frac{M\pi\sigma}{2\sigma_f}\right)\right)$$

where:

$$M = [1 + 1.12987\ \lambda^2 - 0.026905\ \lambda^4 + 5.3549 \times 10^{-4}\ \lambda^6]^{0.5}$$

$$\lambda = \frac{C}{\sqrt{Rt}}$$

$$\sigma = \frac{pR}{t}$$

where:

p = the internal pressure

σ = the hoop stress

R and t = the pipe mean radius and wall thickness, respectively

C = the crack half length

σ_f = the reference flow stress.

3.6.3.5.4.3 Circumferential Through-Wall Extrados Crack in an Elbow

Main Coolant Loop and Main Steam Line Piping

The J-integral solution in Reference 25 is used to address the stability of circumferential through-wall extrados crack in an elbow. Reference 25 provides J solutions for crack sizes with crack half angles of 45° and 90°. Thus, the reference does not provide a solution for interpolating a J solution for an arbitrary crack size. However, the J-integral solution in Reference 25 provides some bases to determine whether the straight pipe solution is sufficiently conservative to lower-bound the window of stable loads for cracked elbows. Thus, the goal of the evaluation of a circumferential through-wall crack in an elbow is to demonstrate whether the straight pipe solution conservatively estimates the stable load limit in the cracked elbow for the MCL piping. The J-integral solution for a through-wall circumferential crack in an elbow is given by:

$$J = J^e + J^P$$

where:

$$J^e = J_T^e + J_B^e = \frac{\left[F_T \sigma_T \sqrt{\pi a}\right]^2}{E} + \frac{\left[F_B \sigma_B \sqrt{\pi a}\right]^2}{E}$$

For Circumferential Cracks:

$$\sigma_T = \frac{p(\pi R_i^2)}{\pi(R_o^2 - R_i^2)}$$

and

$$\sigma_B = \frac{M(R_m)}{\frac{\pi}{4}(R_o^4 - R_i^4)}$$

Plastic Component

$$J^{p} = \alpha\sigma_{o}\varepsilon_{o}a\left(1-\frac{\theta}{\pi}\right)h_{1}\left(\frac{P}{P_{o}}\right)^{n+1}$$

$$P_{o}' = \frac{1}{2}\left[\frac{-\lambda P_{o}^{2}R_{m}}{M_{o}} + \sqrt{\left(\frac{\lambda P_{o}^{2}R_{m}}{M_{o}}\right)^{2} + 4P_{o}^{2}}\right]$$

$$\lambda = \frac{M}{PR_{m}}$$

$$P = \sigma_{T}\pi(R_{o}^{2} - R_{i}^{2})$$

$$M_{o} = 4\sigma_{o}R_{m}^{2}t\left[\cos\left(\frac{\theta}{2}\right) - 0.5\sin\theta\right]$$

$$P_{o} = 2\sigma_{o}R_{m}t\left[\pi - \theta - 2\sin^{-1}(0.5\sin\theta)\right]$$

where:

R_i and R_o = the inner and outer radii of the pipe

R_m = the mean radius

t = pipe wall thickness

a and θ = flaw size (half leakage crack size) and half angle

σ_T and σ_B = the axial and bending stresses

E = Young's modulus

P = the end cap pressure load

p = the operating pressure

M = the external applied moment

P_0 = the limit axial load

M_0 = the limit moment

The F_T, F_B, and h solution coefficients for the through-wall circumferential crack in an elbow are determined for the applicable R/t pipe geometry.

Surge Line Piping

The J-integral solution for the SL is similar to that of the MCL and the MSL. However, the equivalent bending moment approach is followed to consider the axial loads P, thus slightly modifying the evaluation of the J-integral.

The J-integral solution from Reference 25 for bending is:

$$J_{applied} = J_{elastic} + J_{plastic}$$

where:

$$J_{elastic} = \frac{M^2}{E}\pi a(\frac{R_m}{I})^2 F^2$$

$$J_{plastic} = \alpha\sigma_o\varepsilon_o a(1-\frac{\gamma}{\pi})h_1\left[\frac{M}{M_o}\right]^{n+1}$$

where:

Limit Moment

$$M_o = 4\sigma_o R_m^2 t\left(\cos(\frac{\gamma}{2}) - \frac{1}{2}\sin\gamma\right)$$

In the above equations, the solutions coefficient F (a function of the material strain hardening exponent n and geometry Rm/t and γ) is the tabulated elastic solution parameter for remote bending for a circumferential crack in an elastic elbow from Reference 25. The solution coefficient h_1 (a function of the material strain hardening exponent n and geometry Rm/t and γ) is the tabulated fully plastic solution parameter for remote bending for a circumferential crack in an elbow from Reference 25. All other terms of the equations are as previously defined for the J-integral solution in a straight pipe for the surge line piping reported in Section 3.6.3.5.4.1.

3.6.3.5.5 J-T Stability Analysis Procedure

The purpose of J-Tearing (J-T) stability analysis is to determine at what applied load the crack becomes unstable. After the J-integral solutions are identified, it is possible to evaluate $J_{applied}$ for a given crack geometry and loading condition. The next step is to compare the $J_{applied}$ to $J_{material}$. The material resistance to fracture ($J_{material}$) is defined by the J-R curve in the form of a power law equation fit as:

$$J_{material} = C\Delta a^N$$

If the applied J ($J_{applied}$) is equal to the material J ($J_{material}$), any crack growth may be stable as long as the applied tearing modulus ($T_{applied}$) is less than the material tearing modulus ($T_{material}$). To achieve the condition of instability, the applied tearing modulus must be greater than or equal to the material tearing modulus. To evaluate the tearing modulus at the instability point ($T_{material} = T_{applied}$ when $J_{material} = J_{applied}$), $J_{applied}$ may be differentiated with respect to the crack length, a, and the slope of the $J_{applied}$, (dJ/da) can be obtained, using the following equation:

$$\frac{dJ}{da} = \frac{J(a+\varsigma) - J(a-\varsigma)}{2\varsigma}$$

where ζ is a small increment in crack size. The tearing modulus, T, for $J_{applied}$ can then be determined as follows:

$$T = \left(\frac{E}{\sigma_f^2}\right)\frac{dJ}{da}$$

where E is Young's modulus and σ_f is the flow stress. The tearing modulus, T, is dimensionless. For a given tearing modulus (T), the material J-integral ($J_{material}$) is determined according to the following equation:

$$J_{material} = \left(\frac{T\sigma_f^2}{NE}C^{\frac{-1}{N}}\right)^{\frac{N}{N-1}}$$

where C and N are the coefficient and exponent in the J-R fracture resistance power law curve, respectively. For a stable crack growth, the material's tearing modulus must be greater than or equal to the tearing modulus obtained from the applied load ($T_{material} \geq T_{applied}$) where $J_{applied} \leq J_{material}$. The instability point may be found by plotting $J_{applied}$ against $T_{applied}$ and $J_{material}$ versus $T_{material}$ on a single graph called a J-T diagram, as shown in Figure 3.6.3-10—Schematic of J-Tearing Instability Diagram. The intersection of the two curves depicts the instability point (the point where $J_{applied} = J_{material}$ when $T_{applied} = T_{material}$) and the corresponding J value is $J_{instability}$.

To solve for the instability point, the material J-integral ($J_{material}$) is set equal to the applied J-integral ($J_{applied}$) in the J-T diagram. The applied load that achieves this equality is determined through an iterative process. This load represents the maximum allowable load.

For the SL piping that uses the J-integral solution due to bending moment only, the applied load that achieves the equality is the total moment (i.e., the applied bending moment and the equivalent moment due to end cap pressure loading). This total

moment minus the equivalent moment is the maximum allowable load that may be applied. Since the J-integral solution used for the MCL and MSL piping is the tension and bending solution, the maximum load that can be applied is the maximum allowable bending moment for a given total tension loading.

3.6.3.5.6 Determination of Maximum Allowable Piping Moment

Leakage crack sizes (twice the flaw size) with corresponding minimum moments that produced the desired leak rate were determined in the leak rate analysis. Since flaw stability has to be demonstrated considering a safety factor of two on the leakage crack size per SRP 3.6.3, these leakage crack sizes are assumed as the flaw sizes in the J-T stability analysis described in Section 3.6.3.5.5. For a given flaw size, the maximum allowable moment associated with a given minimum moment loading is subsequently determined. The maximum moment calculations were determined using the solutions provided in Section 3.6.3.5.4. Since the absolute load combination method is considered for the analyses, a safety factor of one is appropriate per SRP 3.6.3. For each pipe size, LBB analysis requires identifying locations that have the least favorable combination of stress and material properties for base metal, weldments, nozzles, and safe ends. The lower bounding material properties associated with a given location, as described in Section 3.6.3.5.7, are used in the analysis to determine the lower bound maximum allowable piping moments.

3.6.3.5.7 Identification of Locations for Flaw Stability Analysis

LBB analysis normally considers the applied loadings for the piping system. Therefore, the least favorable combination of stress and material properties of the base metal (piping), weldments, nozzles, and safe ends can be identified. Since the applied loadings are not available, the "LBB allowable load windows" approach is used in this analysis. Using this approach, the identification of the locations is based on consideration of the pipe geometry, operating condition, and consideration of the lower bound material toughness at the given location.

3.6.3.5.7.1 Locations in Main Coolant Loop Piping

Based on the above approach, the locations in the MCL, shown in Table 3.6.3-1 are revised to the locations with associated lower bounding materials shown in Table 3.6.3-13—Main Coolant Loop Piping Locations based on Key Geometry, Operating Conditions and Lower Bound Material Toughness. The geometry and operating conditions helped establish the number of locations for leakage calculations. The lower bounding material properties associated with the location is subsequently used in the flaw stability analysis.

3.6.3.5.7.2 Locations in the Surge Line Piping

Using a similar approach as above, the locations in Table 3.6.3-2 are identified with the associated lower bounding materials as shown in Table 3.6.3-6.

3.6.3.5.7.3 Locations in the Main Steam Line Piping

Since the pipe geometry and operating condition throughout the LBB portion of the MSL piping are the same, as reflected in Table 3.6.3-3, the flaw stability analysis is performed considering both the base and the weld metal properties.

3.6.3.5.8 Development of Allowable Load Limit Diagrams

The lower bound maximum moment curve developed by the approach provided in Section 3.6.3.5.3 is plotted against the minimum moment loadings addressed in Section 3.6.3.5.1. This is referred to as an Allowable Load Limit (ALL) diagram, which is illustrated in Figure 3.6.3-11—Typical Allowable Load Limit (ALL) Diagram Considering Various Axial Loadings. In this plot, the minimum moment is plotted against the maximum moment. The presence of the 45 degree minimum moment line is due to the fact that the maximum moment cannot be lower than the minimum moment. The region between the maximum and the minimum curve is the "ALL LBB Zone," as depicted in Figure 3.6.3-11. It is also referred to as the "LBB Window." Maximum moment curves can also be developed for various assumed axial loadings as illustrated in Figure 3.6.3-11.

3.6.3.6 Results

The results for each of the three LBB piping systems addressed in Section 3.6.3.5.4, and for each of the cracked pipe geometries, are shown in this section. The results in the form of ALL diagrams are provided only for the limiting cracked pipe geometry, which is the geometry for the circumferential through-wall crack in a straight pipe. For the MCL and SL piping, the results for the circumferential through-wall crack in a straight pipe are given in Sections 3.6.3.6.1.1 and 3.6.3.6.2.1, respectively. For the circumferential through-wall extrados crack in an elbow, the results are presented in Sections 3.6.3.6.1.2 and 3.6.3.6.2.2 for the MCL and SL piping, respectively. The results for the MCL and SL piping, involving the axial through-wall crack in straight pipe geometry, are described in Sections 3.6.3.6.1.3 and 3.6.3.6.2.3, respectively. Similarly, the results for the MSL piping for each of the cracked pipe geometries are addressed in Section 3.6.3.6.3.

3.6.3.6.1 Main Coolant Loop Piping

3.6.3.6.1.1 Circumferential Through-Wall Crack in a Straight Pipe (ALL Diagrams)

The results of the flaw stability analysis are shown in terms of ALL diagrams for circumferential through-wall cracks in a straight pipe. The results for the reactor

vessel outlet nozzle at the Alloy 52 weld fusion line region are depicted in Figure 3.6.3-12—ALL for Reactor Vessel Outlet Nozzle Region at Hot Leg (Location 1). Similarly, the results for other components are shown in the figures as listed below:

RAI 467
Q.03.06.03-28

- Figure 3.6.3-13—ALL for Hot Leg Pipe (Location 2).
- Figure 3.6.3-14—ALL for Steam Generator Inlet Nozzle at Hot Leg (Location 3).
- Figure 3.6.3-15—ALL for Steam Generator Outlet Nozzle (Location 4).
- Figure 3.6.3-16—ALL for Crossover & Cold Leg Pipe (Locations 5 & 8).
- Figure 3.6.3-17—ALL for RCP Inlet Nozzle (Location 6).
- Figure 3.6.3-24—ALL for RCP Outlet Nozzle (Location 7)
- Figure 3.6.3-25—ALL for RV Inlet Nozzle (Location 9)

These regions are identified in Table 3.6.3-13. The Alloy 52 weld locations (see Figure 3.6.3-12, Figure 3.6.3-14, Figure 3.6.3-15, and Figure 3.6.3-25 ~~through Figure 3.6.3-14~~) that use the fusion line toughness values were evaluated using the equivalent material tensile properties. The locations in Figure 3.6.3-17 and Figure 3.6.3-24 were evaluated using the lower bound toughness properties for the CASS RCP casing so that the cold leg pipe and RPV inlet nozzles are conservatively evaluated. The locations in Figure 3.6.3-13 and Figure 3.6.3-16 were evaluated considering the tensile and toughness properties of the base metal of the piping.

RAI 467
Q.03.06.03-28

The explanations for the interpretation of the ALL diagrams are provided in Figure 3.6.3-12 through Figure 3.6.3-17, Figure 3.6.3-24 and Figure 3.6.3-25. As long as the maximum applicable moment (normal operating plus SSE loading) load for the applicable location is within the "ALL LBB Zone," LBB is justified for that location. The maximum moment loads are derived considering various coincident axial loading conditions (1000 kilo lbs (kips), 1500 kilo lbs (kips), 2000 kilo lbs (kips), 2500 kips, and 3000 kips). The maximum axial loading (i.e., external applied loading plus 100 percent normal operating pressure end-cap load) that is applicable for the location is used as the maximum moment curve for the location. The "ALL LBB Zone" region is reduced as the axial loading is increased from 1000 kips to 3000 kips. The corresponding tabulated values for the ALL diagrams in Figure 3.6.3-12 through Figure 3.6.3-17, Figure 3.6.3-24 and Figure 3.6.3-25 are provided in the following tables:

RAI 467
Q.03.06.03-28

- ~~Figure 3.6.3-14—ALL for Steam Generator Inlet Nozzle at Hot Leg (Location 3).~~Table 3.6.3-14—ALL for RV Outlet Nozzle Region at the Hot Leg (Location 1)
- ~~Figure 3.6.3-15—ALL for Steam Generator Outlet Nozzle (Location 4).~~Table 3.6.3-15—ALL for Hot Leg Pipe (Location 2)

- Table 3.6.3-16—ALL for SG Inlet Nozzle at Hot Leg (Location 3).
- Table 3.6.3-17—ALL for SG Outlet Nozzle (Location 4).
- Table 3.6.3-18—ALL for Crossover & Cold Leg Pipe (Locations 5 & 8).
- Table 3.6.3-19—ALL for RCP Inlet Nozzle (Location 6).
- Table 3.6.3-27—ALL for RCP Outlet Nozzle (Location 7)
- Table 3.6.3-28—ALL for RV Inlet Nozzle (Location 9)

RAI 467 Q.03.06.03-28

3.6.3.6.1.2 Circumferential Through-Wall Extrados Crack in an Elbow

A sample problem was evaluated to demonstrate that this cracked geometry is bounded by the results of the circumferential through-wall crack in the adjoining straight pipe at a given location. That analysis showed that the maximum allowable moment in the steam generator inlet elbow with a flaw size of 12.4 in is 54,067 in-kips. This evaluation accounts for the wall thinning at the extrados of the elbow where the wall thickness is 2.91 in. The adjoining straight pipe at the steam generator inlet has a wall thickness of <3.66 in. Even with consideration of the greater wall thickness, the maximum allowable moment for a circumferential crack of the same size in a straight pipe is only 52,133 in-kips considering the base metal properties. This corresponds to a 3.7 percent increase in allowable moment obtained for the circumferential extrados crack in the elbow compared to the circumferential crack in the straight pipe. The ALL diagram results provided in Section 3.6.3.6.1.1 are also applicable for the circumferential extrados crack in an elbow.

RAI 467 Q.03.06.03-28

3.6.3.6.1.3 Axial Through-Wall Crack in a Straight Pipe

The axial through-wall cracks in a straight pipe were evaluated at each of the regions identified for the circumferential through-wall crack in a straight pipe. The critical crack sizes for each of the regions are shown in Table 3.6.3-20—Critical Axial Crack Size at Main Coolant Loop Piping Locations. The minimum critical crack size was greater than 33 in. The appropriate lower bound material properties for each of the regions are also considered for the axial through-wall cracks. The minimum safety margin (ratio of critical crack size to leakage crack size) was determined to be 4.89 and occurs in the RPV outlet nozzle region. This is greater than the required safety factor of two for LBB analysis. Therefore, the LBB required safety margins are met for this cracked pipe geometry.

RAI 467 Q.03.06.03-28

RAI 467 Q.03.06.03-28

3.6.3.6.2 Surge Line Piping

3.6.3.6.2.1 Circumferential Through-Wall Crack in a Straight Pipe (ALL Diagrams)

The results of the flaw stability analysis are shown in terms of ALL diagrams for circumferential through-wall cracks in a straight pipe. The results for the pressurizer

surge nozzle at the Alloy 52 weld fusion line region are depicted in Figure 3.6.3-18—ALL for Pressurizer Surge Nozzle at Alloy 52 Weld. Similarly, the results for the SL piping and hot leg nozzle are illustrated in Figure 3.6.3-19—ALL for Surge Line Piping and Figure 3.6.3-20—ALL for Hot Leg Nozzle, respectively. These three regions are identified in Table 3.6.3-6.

As long as the maximum applicable moment (normal operating plus SSE loading) load for the applicable location is within the "ALL LBB Zone," LBB is considered to be justified for that location. The maximum moment loads are derived considering various coincident axial loading conditions due to normal operating pressure, as well as external loads whose magnitudes are noted on the curves. The maximum axial loading (external applied) that is applicable for the location is used as the maximum moment curve for the location. The "ALL LBB Zone" region is reduced as the axial loading is increased. The corresponding tabulated values for the ALL diagrams in Figure 3.6.3-18 through Figure 3.6.3-20 are provided in Table 3.6.3-21—ALL for Pressurizer Surge Nozzle at Alloy 52 Weld, Table 3.6.3-22—ALL for Surge Line Piping, and Table 3.6.3-23—ALL for Hot Leg Nozzle.

3.6.3.6.2.2 Circumferential Through-Wall Extrados Crack in an Elbow

A sample problem was evaluated to demonstrate that this cracked geometry is bounded by the results of the circumferential through-wall crack in the adjoining straight pipe at a given location. The results from that analysis showed that the maximum allowable moment in the SL piping elbow with a flaw size of 5.6 in is 5421 in-kips. This evaluation accounts for the wall thinning at the extrados of the elbow where the wall thickness is 1.4 in. The adjoining straight pipe at the SL piping has a wall thickness <1.55 in. The maximum allowable moment for a circumferential crack of the same size in a straight pipe is also about 5421 in-kips considering the base metal properties.

3.6.3.6.2.3 Axial Through-Wall Crack in a Straight Pipe

The axial through-wall cracks in a straight pipe are evaluated at each of the regions identified in Table 3.6.3-11. The critical crack sizes for each of the three regions are shown in Table 3.6.3-24—Critical Axial Crack Size at Surge Line Piping Locations. The appropriate lower bound material properties for each of the three regions are considered for the axial through-wall cracks. The minimum safety margin (ratio of critical crack size to leakage crack size) is determined to be 4.2 and occurs in the SL piping region. This is greater than the safety factor of two required for LBB analysis. Therefore, the LBB required safety margins are met for this cracked pipe geometry.

3.6.3.6.3 Main Steam Line Piping

3.6.3.6.3.1 Circumferential Through-Wall Crack in a Straight Pipe (ALL Diagrams)

The results of the flaw stability analysis are shown in terms of ALL diagrams for circumferential through-wall cracks in a straight pipe. The results considering the flaws in the base metal as well as the weld metal are shown in Figure 3.6.3-21—Comparison of Base and Weld Metal ALL in Main Steam Line Piping. These results demonstrate that the base metal is the most limiting material for the MSL piping. The results of the flaw stability analysis, considering the limiting base metal properties and all the required safety margins for LBB, are shown in Figure 3.6.3-22—ALL for Main Steam Line Piping with Safety Factor of 2 on Flaw Size (Base Metal).

The explanations for the interpretation of the ALL diagram are provided in Figure 3.6.3-22. As long as the maximum applicable moment (normal operating plus SSE loading) load for the applicable location is within the "ALL LBB Zone," LBB is justified for that location. The maximum moment loads are derived considering various coincident axial loading conditions (100 kips, 200 kips, 300 kips, 451 kips, and 600 kips). The maximum axial loading (external applied) that is applicable for the location, is used as the maximum moment curve for the location. These maximum moment curves already include the end cap load due to pressure at 100 percent power operating condition. The "ALL LBB Zone" region is reduced as the axial loading is increased from 100 kips to 600 kips. The corresponding tabulated values for the ALL diagrams in Figure 3.6.3-22 are provided in Table 3.6.3-25—ALL for the Main Steam Line Piping with Safety Factor of 2 on Flaw Size (Base Metal).

3.6.3.6.3.2 Circumferential Through-Wall Extrados Crack in an Elbow

A sample problem is evaluated to demonstrate that this cracked geometry is bounded by the results of the circumferential through-wall crack in the adjoining straight pipe at a given location. As previously noted in Section 3.6.3.5.4.3, the J-solutions for this cracked geometry are only available for crack half-angles of 45° and 90°. The results of the evaluation of the circumferential crack at the extrados of the elbow are illustrated in Figure 3.6.3-22 which also depicts the results of the circumferential through-wall crack in a straight pipe. As shown in this figure, the results for the circumferential crack at the extrados of the elbow are comparable to the results of the circumferential through-wall crack in a straight pipe.

3.6.3.6.3.3 Axial Through-Wall Crack in a Straight Pipe

The hoop stresses due to operating pressure are the main crack driving force on the axial through-wall crack in a straight pipe, while the effect of external loads are not considered significant for this crack orientation. Therefore, no allowable load limit diagram is generated for the axial through-wall crack in a straight pipe. Instead the critical crack size in the lower bounding base metal material is determined and

compared against the leakage crack size corresponding to a leak rate of one gpm. The critical crack size is 43.6 in, whereas the leakage crack size is only 15.75 in. This provides a safety factor of 2.8 on crack size, which is greater than the required safety factor of two. Therefore, the LBB required safety margins are met for this cracked geometry.

3.6.3.7 Leak Detection

As noted in Sections 3.6.3.5.2 and 3.6.3.5.3, in order to provide a factor of ten to the actual plant leakage detection system capabilities, leak rates of 5.0 gpm for the MCL and SL and 1.0 gpm for MSL were used for determining the leakage flaw sizes.

Section 5.2.5 describes the leak detection systems for the primary coolant inside containment. SRP 3.6.3 states "The specifications for plant-specific leakage detection systems inside the containment are equivalent to those in Regulatory Guide 1.45."

As noted in Section 5.2.5, the RCPB leakage detections systems for the U.S. EPR conform to the sensitivity and response times recommended in RG 1.45, Revision 1. Additionally, at least two of the RCPB leakage detections systems are capable of detecting a leakage rate of 0.5 gpm for the MCL and SL.

The primary method used to detect leakage from the MSL is the local humidity detection system, which has the capability of detecting a leakage of 0.1 gpm within four hours. RG 1.45, Revision 1 specifies a time frame of one hour for leakage detection. However, as noted in NUREG-1793 (Reference 28) leakage detection for LBB purposes does not require the same degree of timeliness. The local humidity detection system measures the moisture penetrating a sensor tube. A secondary method of detecting a leakage of 0.1 gpm within four hours for the MSL is the containment sump level, as described in Section 5.2.5. Containment air cooler condensate flow and containment atmosphere pressure, temperature, and humidity also provide an indication of possible leakage.

3.6.3.8 References

1. NUREG-1061, "Evaluation of Potential for Pipe Breaks, Report of the U.S. Nuclear Regulatory Commission Piping Review Committee," Volume 3, U.S. Nuclear Regulatory Commission, November 1984.

2. NUREG-0800, Revision 3, "Standard Review Plan for the Review of Safety Analysis Reports for Nuclear Power Plants," U.S. Nuclear Regulatory Commission, March 2007.

3. NUREG-0582, "Water Hammer in Nuclear Power Plants," U.S. Nuclear Regulatory Commission, July 1979.

4. NUREG-0927, Revision 1, "Evaluation of Water-Hammer Occurrence in Nuclear Power Plants: Technical Findings Relevant to Unresolved Safety Issue A-1," U.S. Nuclear Regulatory Commission, March 1984.

5. NUREG/CR-2781, "Evaluation of Water Hammer Events in Light Water Reactor Plants," U.S. Nuclear Regulatory Commission, July 1982.

6. EPRI Report 1011838, "Recommendations for an Effective Flow- Accelerated Corrosion Program (NSAC-202L-R3)," Electric Power Research Institute, May 2, 2006.

7. ASME Boiler and Pressure Vessel Code, Section III, "Rules for Construction of Nuclear Power Plant Components," The American Society of Mechanical Engineers, 2004.

8. ASME NQA-1-1994, "Quality Assurance Program for Nuclear Facilities," The American Society of Mechanical Engineers, 1994.

9. Barry M. Gordon, "The Effect of Chloride and Oxygen on the Stress Corrosion Cracking of Stainless Steels: Review of Literature," Materials Performance, Vol. 19, No. 4, April 1980, pp 29-38.

10. ANP-10264NP-A, Revision 0, "U.S. EPR Piping Analysis and Pipe Support Design Topical Report," AREVA NP Inc., November 2008.

11. ASME Boiler and Pressure Vessel Code, Section XI, "Rules for Inservice Inspection of Nuclear Power Plant Components," The American Society of Mechanical Engineers, 2004.

12. NUREG/CR-6446, "Fracture Toughness Evaluation of TP304 Stainless Steel Pipes," U.S. Nuclear Regulatory Commission, February 1997.

13. NUREG/CR-4082, Volume 8, "Degraded Piping Program - Phase II," Semiannual Report," U.S. Nuclear Regulatory Commission, March 1989.

14. NUREG/CR-4599, "Short Cracks in Piping and Piping Welds," First Semiannual Report, U.S. Nuclear Regulatory Commission, March 1991.

15. ASTM Standard E1820-01, "Standard Test Method for Measurement of Fracture Toughness," American Society for Testing and Materials International, 2001.

16. NUREG/CR-6177, "Assessment of Thermal Embrittlement of Cast Stainless Steels," U.S. Nuclear Regulatory Commission, May 1994.

17. EPRI NP-3395, "Calculation of Leak Rates Through Cracks in Pipes and Tubes," Electric Power Research Institute, 1983.

18. NUREG/CR-3464, "The Application of Fracture Proof Design Methods Using Tearing Instability Theory to Nuclear Piping Postulating Circumferential Through Wall Cracks," Nuclear Regulatory Commission, September 1983.

19. NUREG/CR-1319, "Cold Leg Integrity Evaluation," U.S. Nuclear Regulatory Commission, February 1980.

20. NUREG/CR-5128, Revision 1, "Evaluation and Refinement of Leak-Rate Estimation Models," U.S. Nuclear Regulatory Commission, June 1994.

21. SQUIRT: Seepage Quantification of Upsets in Reactor Tubes, User's Manual, Windows Version 1.1, Battelle, March 24, 2003.

22. NUREG/CR-6861, "Barrier Integrity Research Program," U.S. Nuclear Regulatory Commission, December 2004.

23. EPRI NP-5596, "Elastic-Plastic Fracture Analysis of Through-Wall and Surface Flaws in Cylinders," Electric Power Research Institute, January 1988.

24. NUREG/CR-4878, "Analysis of Experiments on Stainless Steel Flux Welds," Nuclear Regulatory Commission, April 1987

25. NUREG/CR-6837, Volume 2, "The Battelle Integrity of Nuclear Piping (BINP) Program Final Report Summary and Implications of Results," Appendices, U.S. Nuclear Regulatory Commission, June 2005.

26. EPRI NP-6301-D, Volumes 1–3, "Ductile Fracture Handbook," Electric Power Research Institute, June 1989.

27. NRC letter dated November 9, 1998, D.G. McDonald to M.L. Bowling, "Application of Leak-Before-Break Status to Portions of the Safety Injection and Shutdown Cooling System for the Millstone Nuclear Power Station, Unit No 2 (TAC NO MA2367)."

28. NUREG-1793, "Final Safety Evaluation Report Related to Certification of the AP1000 Standard Design," U.S. Nuclear Regulatory Commission, September 2004.

29. NUREG/CR-6004, "Probabilistic Pipe Fracture Evaluations for Leak-Rate-Detection Applications," Nuclear Regulatory Commission, April 1995.

Table 3.6.3-1—Main Coolant System Piping Dimensions and Operating Condition

Location	Description of Pipe Geometry	Temperature (°F)	Pressure (psia)	ID[1] (in)	Pipe Wall[2] Thickness (in)
1	RV Outlet at Hot Leg	625	2250	30.71	2.99
2	Hot Leg Pipe	625	2250	30.71	2.99
3	SG Inlet at Hot Leg	625	2250	30.71	3.82
4	SG Outlet	563	2250	30.71	3.82
5	Crossover Leg	563	2250	30.71	2.99
6	RCP Inlet	563	2250	30.71	3.54
7	RCP Outlet	563	2250	30.71	2.99
8	Cold Leg Pipe	563	2250	30.71	2.99
9	RPV Inlet	563	2250	30.71	2.99

Notes:

1. ID of the pipe. At the weld prep location the ID of pipe is 30.87 in.

2. For detailed J-T analysis the weld prep thickness is conservatively used. For leak rate analysis, the pipe wall thickness given in the table is used.

RAI 467
Q.03.06.03-28

Table 3.6.3-2—Surge Line Piping Dimensions and Operating Condition

Location	Description of Pipe Geometry	Temperature (°F)	Pressure (psia)	ID[1] (in)	Pipe Wall[2] Thickness (in)
1	Pressurizer Surge Nozzle	653	2250	13.61	2.055
2	Surge Line Piping near Pressurizer	653	2250	12.81	1.595
3	Hot Leg Nozzle	624	2250	12.91	1.545

Notes:

1. ID of the pipe. At the weld prep location, the ID of the pipe is 12.91 in.
2. For consistency, the pipe wall thickness is used in both the leak rate and flaw stability analysis.

RAI 467
Q.03.06.03-28

Table 3.6.3-3—Main Steam Line Dimensions and Operating Condition

Location	Description of Pipe Geometry	Temperature (°F)	Pressure (psia)	ID (in)	Pipe Wall[1] Thickness (in)
1	Main Steam Line Piping	556	1111	27.5	1.86

Note:

1. Pipe wall thickness is used for both the J-T analysis and the leak rate analysis.

Table 3.6.3-4—Tensile Properties of Materials at Various Locations of Main Coolant Loop Piping

Locations	Temp., °F	E (ksi)	σ_o (= σ_y, ksi)	ε_o	a	n	σ_u (ksi)
1*	625	25252	21.545	0.000853	5.570	4.090	61.356
2	625	25000	19.200	0.000768	5.850	3.878	59.200
3*	625	25396	22.885	0.000901	5.420	4.210	62.588
4*	563	25879	23.523	0.000909	4.930	4.290	62.588
5	563	25500	19.790	0.000776	5.280	3.997	59.200
6	563	25500	19.790	0.000776	5.280	3.997	59.200
7	563	25500	19.790	0.000776	5.280	3.997	59.200
8	563	25500	19.790	0.000776	5.280	3.997	59.200
9*	563	25741	22.167	0.000861	5.060	4.180	61.356

Note:

1. *Note: Dissimilar metal weld (DMW) at fusion line determined using elastic-plastic fracture mechanics (EPFM) and finite element method.

RAI 467
Q.03.06.03-28

Table 3.6.3-5—Tensile Properties for the Surge Line Piping

Tensile Properties (ksi)			
	SL Piping near Pressurizer	Pressurizer Nozzle DMW[1]	Hot Leg Nozzle
Yield Stress ($\sigma_{y)}$	18.0	22.9	18.21
Ultimate Strength ($\sigma_{ult)}$	59.2	62.6	59.2
Flow Stress ($\sigma_{f)}$	38.6	42.8	38.7
Young's Modulus (E)	25,000	25,400	25,180
Ramberg-Osgood Parameters ($\frac{\varepsilon}{\varepsilon_o} = \frac{\sigma}{\sigma_o} + \alpha\left(\frac{\sigma}{\sigma_o}\right)^n$)			
	SL Piping near Pressurizer	Pressurizer Nozzle	Hot Leg Nozzle
α	5.90	5.38	6.13
n	3.50	4.28	3.50
Reference Stress ($\sigma_{o)}$	18.0 ksi	22.9 ksi	18.21 ksi
Reference Strain (ε)	0.00072	0.000901	0.000723

Note:

1. Dissimilar metal weld (DMW) at fusion line determined using elastic-plastic fracture mechanics (EPFM) and finite element method.

Table 3.6.3-6—Surge Line Piping Locations Based on Key Geometry, Operating Conditions & Lower Bound Material Toughness

LBB Piping Location	Description of Pipe Geometry	Temperature (°F)	Thickness (in)	R_m/t	Lower Bounding Material
1	Pressurizer Surge Nozzle	653	2.005	3.81	Alloy 52
2	Surge Line Piping near Pressurizer	653	1.595	4.52	SS Base Metal
3	Hot leg Nozzle	624	1.545	4.68	SS Base Metal

Table 3.6.3-7—Tensile Properties for the Main Steam Line Piping

Tensile Properties (ksi)		
	Base Metal	Weld Metal
Yield Stress ($\sigma_{y)}$	39.0	76.0
Ultimate Strength ($\sigma_{ult)}$	81.0	89.5
Flow Stress ($\sigma_{f)}$	60.0	82.75
Young's Modulus (E)	26,750	26,750
Ramberg-Osgood Parameters ($\frac{\varepsilon}{\varepsilon_o} = \frac{\sigma}{\sigma_o} + \alpha\left(\frac{\sigma}{\sigma_o}\right)^n$)		
	Base Metal	Weld Metal
α	1.12	0.897
n	9.54	14.8
Reference Stress ($\sigma_{o)}$	39.0 ksi	76.0 ksi
Reference Strain (ε)	0.00146	0.00284

Table 3.6.3-8—Minimum Moment versus Circumferential Crack Leakage ~~Crack~~ Sizes for 5 gpm at Various Main Coolant Loop Piping Locations

Min Moment In-kips	Circumferential Leakage Flaw Size at 5.0 GPM, inch						
	1	2	3	4	5, 7, 8	6	9
0	11.322	10.314	14.683	12.824	9.592	11.549	9.985
10000	8.630	8.378	11.153	9.547	7.328	8.759	7.466
20000	6.764	6.442	9.035	7.709	5.688	6.948	5.889
30000	5.140	4.616	7.372	6.361	4.191	5.400	4.617
40000	3.662	3.214	5.927	5.205	2.975	4.074	3.344
50000	2.625	2.265	4.672	4.187	2.115	3.179	2.433
60000	1.912	1.645	3.653	3.358	1.536	2.283	1.784
70000	1.455	1.234	2.861	2.635	1.149	1.746	1.403
80000	1.095	0.954	2.262	2.097	0.884	1.361	1.021
90000	0.861	0.757	1.865	1.683	0.698	1.083	0.801
100000	0.691	0.614	1.468	1.366	0.563	0.879	0.641
110000	0.568	0.507	1.207	1.124	0.462	0.725	0.522
120000	0.472	0.427	1.028	0.956	0.386	0.606	0.434
130000	0.398	0.363	0.849	0.787	0.328	0.515	0.365
140000	0.340	0.318	0.723	0.670	0.282	0.442	0.310
150000	0.294	0.273	0.623	0.576	0.244	0.383	0.268
160000	0.258	0.251	0.542	0.500	0.214	0.335	0.234

Table 3.6.3-9—Axial Through-Wall Leakage Crack Sizes for 5 gpm at Various Main Coolant Loop Piping Locations

MCL Locations	Description	Leakage Crack Size (in)
1	RV Outlet at Hot Leg	7.189
2	Hot Leg Pipe	7.311
3	SG Inlet at Hot Leg	8.529
4	SG Outlet	7.395
5	Crossover Leg	6.342
6	RCP Inlet	7.124
7	RCP Outlet	6.342
8	Cold Leg Pipe	6.342
9	RV Inlet	6.254

RAI 467
Q.03.06.03-28

Table 3.6.3-10—Minimum Moment versus Circumferential Leakage Crack Sizes for 5 gpm at Two Surge Line Piping Locations

With Axial Load of:		1,000 kips	1,500 kips	2,000 kips	2,500 kips	3,000 kips
Flaw Size (in)	Min Moment (in-kips)	Max Moment (in-kips)	Max Moment (in-kips)	Max Moment (in-kips)	Max Moment (in-kips)	Max Moment (in-kips)
11.322	0	37,974	33,471	28,969	24,552	19,965
8.630	10,000	48,654	44,249	39,843	35,449	31,032
6.764	20,000	56,679	52,327	47,975	43,622	39,271
5.140	30,000	64,380	60,068	55,757	51,445	47,134
3.662	40,000	72,497	68,219	63,942	59,663	55,386
2.625	50,000	79,479	75,224	70,968	66,712	62,456
1.912	60,000	85,560	81,319	77,077	72,836	68,594
1.455	70,000	90,534	86,301	82,068	77,836	73,603
1.095	80,000	95,564	91,337	87,111	82,885	78,659
0.861	90,000	99,763	95,541	91,319	87,096	82,874
0.691	100,000	103,596	99,377	95,157	90,937	86,718
0.568	110,000	107,024	102,806	98,588	94,370	90,152
0.472	120,000	110,284	106,067	101,851	97,634	93,417
0.398	130,000	113,313	109,098	104,882	100,666	96,450
0.340	140,000	116,140	111,924	107,709	103,494	99,279
0.294	150,000	118,776	114,561	110,346	106,132	101,917
0.258	160,000	121,169	116,955	112,741	108,526	104,312

Table 3.6.3-11—Axial Through-Wall Leakage Crack Sizes for 5 gpm at Three Surge Line Piping Locations

SL Location	Leakage Crack Size (in)
Pressurizer Surge Nozzle at Alloy 52 weld	7.635
Surge Line Piping	6.665
Hot Leg Nozzle	6.526

RAI 467
Q.03.06.03-28

Table 3.6.3-12—Minimum Moment versus Circumferential Leakage Crack ~~Leakage~~ Sizes for 1 gpm in the Main Steam Line Piping

Leakage Size (in)	Minimum Moment (in-kips)
13.85	2400
12.05	4820
10.73	7270
9.75	9620
8.93	12,100
8.25	14,700
7.70	17,200
7.20	19,800
6.76	22,500
6.33	25,600
5.94	28,800

Table 3.6.3-13—Main Coolant Loop Piping Locations based on Key Geometry, Operating Conditions and Lower Bound Material Toughness

LBB Piping Location	Description of Pipe Geometry	Temperature (°F)	Pipe Wall Thickness[1], t (in)	Rm/t	Lower Bounding Material
1	RV Outlet at Hot Leg	625	2.913	5.80	Alloy 52
2	Hot Leg Pipe	625	2.835	5.94	Base Metal
3	SG Inlet at Hot Leg	625	3.661	4.72	Alloy 52
4	SG Outlet	563	3.661	4.72	Alloy 52
5	Crossover Leg	563	2.835	5.94	Base Metal
6	RCP Inlet	563	3.386	5.06	CASS
7	RCP Outlet	563	2.913	5.80	CASS
8	Cold Leg Pipe	563	2.913	5.80	Base Metal
9	RPV Inlet	563	2.913	5.80	Alloy 52

Note:

1. Corresponds to the minimum thickness at the weld prep location. However, for consistency with leak rate analysis, the thickness from Table 3.6.3-1 are used.

RAI 467
Q.03.06.03-28

Table 3.6.3-14—ALL for RV Outlet Nozzle Region at the Hot Leg (Location 1)

With Axial Load of:		1,000 kips	1,500 kips	2,000 kips	2,500 kips	3,000 kips
Flaw Size (in)	Min Moment (in-kips)	Max Moment (in-kips)	Max Moment (in-kips)	Max Moment (in-kips)	Max Moment (in-kips)	Max Moment (in-kips)
11.322	0	37,974	33,471	28,969	24,552	19,965
8.630	10,000	48,654	44,249	39,843	35,449	31,032
6.764	20,000	56,679	52,327	47,975	43,622	39,271
5.140	30,000	64,380	60,068	55,757	51,445	47,134
3.662	40,000	72,497	68,219	63,942	59,663	55,386
2.625	50,000	79,479	75,224	70,968	66,712	62,456
1.912	60,000	85,560	81,319	77,077	72,836	68,594
1.455	70,000	90,534	86,301	82,068	77,836	73,603
1.095	80,000	95,564	91,337	87,111	82,885	78,659
0.861	90,000	99,763	95,541	91,319	87,096	82,874
0.691	100,000	103,596	99,377	95,157	90,937	86,718
0.568	110,000	107,024	102,806	98,588	94,370	90,152
0.472	120,000	110,284	106,067	101,851	97,634	93,417
0.398	130,000	113,313	109,098	104,882	100,666	96,450
0.340	140,000	116,140	111,924	107,709	103,494	99,279
0.294	150,000	118,776	114,561	110,346	106,132	101,917
0.258	160,000	121,169	116,955	112,741	108,526	104,312

RAI 467
Q.03.06.03-28

Table 3.6.3-15—ALL for Hot Leg Pipe (Location 2)

With Axial Load of:		1,000 kips	1,500 kips	2,000 kips	2,500 kips	3,000 kips
Flaw Size (in)	Min Moment (in-kips)	Max Moment (in-kips)	Max Moment (in-kips)	Max Moment (in-kips)	Max Moment (in-kips)	Max Moment (in-kips)
10.314	0	51,970	47,519	43,069	38,632	34,168
8.378	10,000	60,759	56,371	51,984	47,529	43,209
6.442	20,000	70,317	65,983	61,648	57,313	52,978
4.616	30,000	80,643	76,351	72,059	67,767	63,475
3.214	40,000	90,395	86,133	81,870	77,608	73,345
2.265	50,000	98,991	94,747	90,503	86,259	82,015
1.645	60,000	106,485	102,252	98,019	93,786	89,553
1.234	70,000	113,105	108,878	104,652	100,426	96,200
0.954	80,000	119,029	114,807	110,585	106,362	102,140
0.757	90,000	121,754	118,551	114,863	110,702	106,088
0.614	100,000	122,516	119,346	115,690	111,561	106,976
0.507	110,000	123,085	119,940	116,307	112,202	107,639
0.427	120,000	123,509	120,383	116,768	112,680	108,135
0.363	130,000	123,848	120,737	117,137	113,063	108,531
0.318	140,000	124,086	120,985	117,396	113,331	108,809
0.273	150,000	124,324	121,234	117,654	113,600	109,087
0.251	160,000	124,441	121,355	117,781	113,731	109,222

RAI 467
Q.03.06.03-28

Table 3.6.3-16—ALL for SG Inlet Nozzle at Hot Leg (Location 3)

With Axial Load of:		1,000 kips	1,500 kips	2,000 kips	2,500 kips	3,000 kips
Flaw Size (in)	Min Moment (in-kips)	Max Moment (in-kips)	Max Moment (in-kips)	Max Moment (in-kips)	Max Moment (in-kips)	Max Moment (in-kips)
14.683	0	45,852	41,087	36,324	31,675	26,796
11.153	10,000	63,088	58,493	53,898	49,337	44,707
9.035	20,000	74,262	69,742	65,222	60,701	56,182
7.372	30,000	83,615	79,145	74,674	70,202	65,732
5.927	40,000	92,372	87,939	83,505	79,072	74,639
4.672	50,000	100,755	96,352	91,948	87,544	83,141
3.653	60,000	108,471	104,090	99,709	95,328	90,948
2.861	70,000	115,441	111,077	106,713	102,349	97,985
2.262	80,000	121,680	117,328	112,977	108,625	104,273
1.865	90,000	126,566	122,222	117,878	113,535	109,191
1.468	100,000	132,421	128,085	123,749	119,413	115,077
1.207	110,000	137,100	132,769	128,437	124,106	119,774
1.028	120,000	140,892	136,563	132,235	127,907	123,578
0.849	130,000	145,383	141,058	136,732	132,407	128,081
0.723	140,000	149,148	144,825	140,501	136,178	131,854
0.623	150,000	152,642	148,320	143,998	139,676	135,354
0.542	160,000	155,924	151,603	147,282	142,961	138,640

RAI 467
Q.03.06.03-28

Table 3.6.3-17—ALL for SG Outlet Nozzle (Location 4)

With Axial Load of:		1,000 kips	1,500 kips	2,000 kips	2,500 kips	3,000 kips
Flaw Size (in)	Min Moment (in-kips)	Max Moment (in-kips)	Max Moment (in-kips)	Max Moment (in-kips)	Max Moment (in-kips)	Max Moment (in-kips)
12.824	0	56,353	51,686	47,019	42,485	37,685
9.547	10,000	73,420	68,884	64,347	59,849	55,274
7.709	20,000	83,753	79,273	74,793	70,312	65,832
6.361	30,000	91,860	87,416	82,972	78,527	74,084
5.205	40,000	99,371	94,956	90,540	86,124	81,709
4.187	50,000	106,671	102,278	97,886	93,493	89,101
3.358	60,000	113,384	109,009	104,635	100,261	95,886
2.635	70,000	120,176	115,817	111,458	107,099	102,740
2.097	80,000	126,173	121,825	117,477	113,128	108,780
1.683	90,000	131,693	127,353	123,013	118,673	114,333
1.366	100,000	136,774	132,440	128,106	123,772	119,438
1.124	110,000	141,434	137,104	132,774	128,444	124,114
0.956	120,000	145,275	140,948	136,621	132,294	127,966
0.787	130,000	149,841	145,517	141,192	136,868	132,543
0.670	140,000	153,627	149,304	144,981	140,659	136,336
0.576	150,000	157,190	152,869	148,548	144,226	139,905
0.500	160,000	160,540	156,220	151,899	147,579	143,259

RAI 467
Q.03.06.03-28

Table 3.6.3-18—ALL for Crossover & Cold Leg Pipe (Locations 5 & 8)

With Axial Load of:		1,000 kips	1,500 kips	2,000 kips	2,500 kips	3,000 kips
Flaw Size (in)	Min Moment (in-kips)	Max Moment (in-kips)	Max Moment (in-kips)	Max Moment (in-kips)	Max Moment (in-kips)	Max Moment (in-kips)
9.592	0	56,384	51,959	47,535	43,126	38,685
7.328	10,000	67,088	62,731	58,374	53,951	49,659
5.688	20,000	75,660	71,344	67,028	62,711	58,395
4.191	30,000	84,645	80,362	76,079	71,796	67,514
2.975	40,000	93,589	89,332	85,074	80,816	76,559
2.115	50,000	101,800	97,558	93,317	89,076	84,834
1.536	60,000	109,177	104,946	100,715	96,484	92,253
1.149	70,000	115,773	111,548	107,323	103,098	98,873
0.884	80,000	121,736	117,515	113,294	109,073	104,852
0.698	90,000	123,105	119,937	116,286	112,165	107,592
0.563	100,000	123,827	120,691	117,070	112,979	108,435
0.462	110,000	124,367	121,254	117,656	113,587	109,064
0.386	120,000	124,772	121,677	118,096	114,044	109,537
0.328	130,000	125,081	121,999	118,431	114,392	109,897
0.282	140,000	125,325	122,254	118,697	114,668	110,183
0.244	150,000	125,527	122,465	118,917	114,896	110,418
0.214	160,000	125,687	122,631	119,090	115,075	110,604

RAI 467
Q.03.06.03-28

Table 3.6.3-19—ALL for RCP Inlet Nozzle (Location 6)

With Axial Load of:		1,000 kips	1,500 kips	2,000 kips	2,500 kips	3,000 kips
Flaw Size (in)	Min Moment (in-kips)	Max Moment (in-kips)	Max Moment (in-kips)	Max Moment (in-kips)	Max Moment (in-kips)	Max Moment (in-kips)
11.549	0	46,509	41,933	37,357	32,873	28,206
8.759	10,000	58,946	54,470	49,995	45,525	41,043
6.948	20,000	67,733	63,309	58,886	54,462	50,038
5.400	30,000	75,995	71,610	67,225	62,840	58,456
4.074	40,000	84,053	79,698	75,344	70,990	66,635
3.179	50,000	90,422	86,087	81,752	77,417	73,082
2.283	60,000	98,210	93,893	89,577	85,260	80,943
1.746	70,000	104,147	99,840	95,534	91,228	86,922
1.361	80,000	109,488	105,189	100,890	96,591	92,292
1.083	90,000	114,311	110,016	105,722	101,428	97,133
0.879	100,000	118,692	114,401	110,109	105,818	101,527
0.725	110,000	122,739	118,450	114,162	109,873	105,584
0.606	120,000	126,527	122,239	117,952	113,665	109,378
0.515	130,000	129,990	125,704	121,418	117,132	112,846
0.442	140,000	133,273	128,988	124,703	120,418	116,133
0.383	150,000	136,382	132,097	127,813	123,528	119,244
0.335	160,000	139,317	135,033	130,749	126,465	122,182

RAI 467
Q.03.06.03-28

Table 3.6.3-20—Critical Axial Crack Size at Main Coolant Loop Piping Locations

Location	Component	Leakage Flaw Size at 5.0 GPM, inch	Critical Flaw Sizes, inch	Safety Margin
1	RV Outlet Nozzle at Hot Leg	7.189	35.19	4.89
2	Hot Leg Pipe	7.311	37.68	5.15
3	SG Inlet Nozzle at Hot Leg	8.529	51.46	6.03
4	SG Outlet Nozzle	7.395	51.93	7.02
5	Crossover Leg	6.342	38.04	6.00
6	RCP Inlet Nozzle	7.124	42.84	6.01
7	RCP Outlet Nozzle	6.342	33.37	5.26
8	Cold Leg Pipe	6.342	38.04	6.00
9	RV Inlet Nozzle	6.254	35.52	5.68

RAI 467
Q.03.06.03-28

RAI 467
Q.03.06.03-28

Table 3.6.3-21—ALL for Pressurizer Surge Nozzle at Alloy 52 Weld
Sheet 1 of 2

With Axial Load of:			0 kips	1.5 kips	15 kips	30 kips	40 kips	50 kips	60 kips	70 kips
Set No.	Flaw Size (in)	Min Moment (in-kips)	Max Moment (in-kips)	Max Moment (in-kips)	Max Moment (in-kips)	Max Moment (in-kips)	Max Moment (in-kips)	Max Moment (in-kips)	Max Moment (in-kips)	Max Moment (in-kips)
1	12.318	0	2,076	2,068	1,993	1,910	1,855	1,800	1,745	1,690
2	11.094	500	2,934	2,927	2,855	2,779	2,728	2,676	2,625	2,573
3	10.142	1000	3,710	3,702	3,636	3,562	3,513	3,464	3,415	3,366
4	9.353	1500	4,435	4,428	4,363	4,292	4,245	4,197	4,150	4,103
5	8.634	2000	5,152	5,145	5,083	5,014	4,968	4,921	4,875	4,829
6	8.006	2500	5,819	5,813	5,752	5,684	5,639	5,594	5,549	5,504
7	7.377	3000	6,524	6,517	6,458	6,392	6,347	6,303	6,259	6,215
8	6.758	3500	7,251	7,244	7,185	7,120	7,077	7,034	6,990	6,947
9	6.152	4000	7,992	7,986	7,928	7,864	7,821	7,779	7,736	7,693
10	5.565	4500	8,737	8,731	8,674	8,611	8,569	8,527	8,485	8,442
11	5.008	5000	9,469	9,463	9,407	9,344	9,303	9,261	9,219	9,178
12	4.493	5500	10,168	10,162	10,106	10,044	10,003	9,962	9,920	9,879
13	4.021	6000	10,830	10,824	10,768	10,707	10,666	10,625	10,584	10,543
14	3.597	6500	11,445	11,439	11,384	11,323	11,282	11,241	11,201	11,160
15	3.219	7000	12,014	12,008	11,953	11,892	11,852	11,811	11,771	11,730
16	2.883	7500	12,540	12,534	12,479	12,419	12,378	12,338	12,298	12,257
17	2.587	8000	13,024	13,018	12,963	12,903	12,863	12,823	12,783	12,743
18	2.326	8500	13,471	13,465	13,411	13,351	13,311	13,271	13,231	13,191
19	2.098	9000	13,882	13,876	13,822	13,762	13,722	13,682	13,642	13,602

RAI 467
Q.03.06.03-28

Table 3.6.3-21—ALL for Pressurizer Surge Nozzle at Alloy 52 Weld
Sheet 2 of 2

With Axial Load of:			0 kips	1.5 kips	15 kips	30 kips	40 kips	50 kips	60 kips	70 kips
Set No.	Flaw Size (in)	Min Moment (in-kips)	Max Moment (in-kips)	Max Moment (in-kips)	Max Moment (in-kips)	Max Moment (in-kips)	Max Moment (in-kips)	Max Moment (in-kips)	Max Moment (in-kips)	Max Moment (in-kips)
20	1.897	9500	14,264	14,258	14,204	14,145	14,105	14,065	14,025	13,985
21	1.719	10000	14,622	14,616	14,562	14,503	14,463	14,423	14,383	14,344

Table 3.6.3-22—ALL for Surge Line Piping

With Axial Load of:			0 kips	1.5 kips	15 kips	30 kips	40 kips	50 kips	60 kips	70 kips
Set No.	Flaw Size (in)	Min Moment (in-kips)	Max Moment (in-kips)	Max Moment (in-kips)	Max Moment (in-kips)	Max Moment (in-kips)	Max Moment (in-kips)	Max Moment (in-kips)	Max Moment (in-kips)	Max Moment (in-kips)
1	9.459	0	2,547	2,539	2,468	2,388	2,335	2,281	2,227	2,172
2	8.536	500	3,386	3,378	3,311	3,236	3,186	3,135	3,084	3,033
3	7.639	1000	4,257	4,250	4,187	4,117	4,070	4,023	3,975	3,927
4	6.652	1500	5,228	5,222	5,167	5,106	5,065	5,025	4,984	4,944
5	5.616	2000	6,287	6,281	6,227	6,169	6,129	6,090	6,051	6,011
6	4.650	2500	7,358	7,352	7,300	7,243	7,204	7,166	7,127	7,089
7	3.826	3000	8,343	8,337	8,286	8,229	8,192	8,154	8,116	8,078
8	3.158	3500	9,144	9,140	9,104	9,062	9,034	9,006	8,977	8,941
9	2.628	4000	9,744	9,740	9,707	9,669	9,643	9,617	9,591	9,564
10	2.210	4500	10,214	10,211	10,180	10,145	10,122	10,097	10,073	10,048
11	1.878	5000	10,585	10,582	10,553	10,521	10,499	10,476	10,453	10,430
12	1.612	5500	10,880	10,877	10,850	10,820	10,799	10,778	10,756	10,734
13	1.397	6000	11,117	11,114	11,089	11,060	11,040	11,020	10,999	10,978
14	1.221	6500	11,309	11,307	11,283	11,255	11,236	11,216	11,197	11,176
15	1.077	7000	11,466	11,464	11,440	11,414	11,395	11,377	11,358	11,338
16	0.956	7500	11,597	11,595	11,572	11,546	11,529	11,511	11,492	11,473
17	0.854	8000	11,707	11,705	11,683	11,658	11,641	11,623	11,605	11,587

Table 3.6.3-23—ALL for Hot Leg Nozzle

With Axial Load of:			0 kips	1.5 kips	15 kips	30 kips	40 kips	50 kips	60 kips	70 kips
Set No.	Flaw Size(in)	Min Moment (in-kips)	Max Moment (in-kips)	Max Moment (in-kips)	Max Moment (in-kips)	Max Moment (in-kips)	Max Moment (in-kips)	Max Moment (in-kips)	Max Moment (in-kips)	Max Moment (in-kips)
1	8.776	0	3,060	3,052	2,984	2,907	2,855	2,803	2,751	2,698
2	7.897	500	3,883	3,876	3,812	3,740	3,691	3,642	3,593	3,544
3	7.039	1000	4,733	4,726	4,666	4,599	4,554	4,508	4,462	4,416
4	6.089	1500	5,657	5,651	5,597	5,538	5,498	5,458	5,418	5,378
5	5.102	2000	6,691	6,685	6,633	6,574	6,535	6,496	6,457	6,418
6	4.193	2500	7,719	7,713	7,661	7,604	7,566	7,528	7,489	7,451
7	3.429	3000	8,623	8,618	8,579	8,535	8,499	8,462	8,424	8,386
8	2.817	3500	9,302	9,298	9,263	9,223	9,196	9,168	9,140	9,112
9	2.336	4000	9,833	9,829	9,797	9,761	9,736	9,711	9,685	9,659
10	1.958	4500	10,247	10,244	10,214	10,181	10,158	10,134	10,110	10,086
11	1.660	5000	10,572	10,569	10,541	10,509	10,487	10,465	10,443	10,420
12	1.417	5500	10,834	10,831	10,805	10,775	10,755	10,734	10,712	10,691
13	1.228	6000	11,037	11,034	11,009	10,981	10,961	10,941	10,921	10,900
14	1.074	6500	11,201	11,199	11,175	11,147	11,128	11,109	11,089	11,069
15	0.945	7000	11,338	11,335	11,312	11,286	11,268	11,249	11,230	11,210
16	0.839	7500	11,450	11,447	11,425	11,399	11,381	11,363	11,345	11,326
17	0.749	8000	11,545	11,542	11,520	11,495	11,478	11,460	11,442	11,424

Table 3.6.3-24—Critical Axial Crack Size at Surge Line Piping Locations

LBB Piping Location	Description of Pipe Geometry	Leakage Crack Size (in)	Critical Crack Size (in)	Safety Margin
1	Pressurizer Surge Nozzle at Alloy 52 weld	7.635	33.65	4.41
2	Surge Line Piping	6.665	23.83	3.58
3	Hot Leg Nozzle	6.526	22.55	3.46

Table 3.6.3-25—ALL for the Main Steam Line Piping with Safety Factor of 2 on Flaw Size (Base Metal)

Minimum Moment (in-kips)	Maximum Allowable Moment with Moment Plus Axial Load					
	0 kip (in-kips)	100 kips (in-kips)	200 kips (in-kips)	300 kips (in-kips)	451 kips (in-kips)	600 kips (in-kips)
2402	25,153	24,495	23,892	23,214	22,047	20,720
4815	29,053	28,321	27,664	27,084	26,085	24,955
7270	32,379	31,626	30,859	30,241	29,339	28,320
9618	34,845	34,116	33,377	32,634	31,799	30,856
12,122	37,002	36,288	35,569	34,833	33,926	33,041
14,661	38,858	38,159	37,453	36,734	35,746	34,904
17,169	40,352	39,722	39,026	38,318	37,259	36,449
19,805	41,751	41,186	40,496	39,798	38,707	37,887
22,550	43,016	42,509	41,825	41,134	40,058	39,181
25,628	44,285	43,837	43,158	42,473	41,411	40,474
28,822	45,466	45,056	44,398	43,718	42,667	41,673

Table 3.6.3-26—Air Fatigue Crack Morphology Parameters

Material	Roughness μG, μinch	90-degree Turns per inch n, inch^{-1}
Carbon Steel	1325	51
Stainless Steel	1325	64

Table 3.6.3-27—ALL for RCP Outlet Nozzle (Location 7)

With Axial Load of:		1,000 kips	1,500 kips	2,000 kips	2,500 kips	3,000 kips
Flaw Size (in)	Min Moment (in-kips)	Max Moment (in-kips)	Max Moment (in-kips)	Max Moment (in-kips)	Max Moment (in-kips)	Max Moment (in-kips)
9.592	0	40,627	36,192	31,757	27,400	22,888
7.328	10,000	49,557	45,192	40,826	36,462	32,096
5.688	20,000	56,673	52,350	48,027	43,704	39,381
4.191	30,000	64,055	59,766	55,478	51,190	46,902
2.975	40,000	71,283	67,021	62,759	58,497	54,235
2.115	50,000	77,791	73,546	69,302	65,057	60,812
1.536	60,000	83,532	79,298	75,065	70,831	66,598
1.149	70,000	88,586	84,360	80,133	75,906	71,680
0.884	80,000	93,102	88,880	84,657	80,435	76,213
0.698	90,000	97,172	92,952	88,732	84,513	80,293
0.563	100,000	100,899	96,681	92,463	88,246	84,028
0.462	110,000	104,362	100,145	95,929	91,712	87,496
0.386	120,000	107,547	103,332	99,116	94,901	90,685
0.328	130,000	110,470	106,255	102,040	97,825	93,610
0.282	140,000	113,217	109,002	104,788	100,573	96,359
0.244	150,000	115,882	111,668	107,454	103,240	99,025
0.214	160,000	118,329	114,115	109,901	105,687	101,473

RAI 467
Q.03.06.03-28

Table 3.6.3-28—ALL for RV Inlet Nozzle (Location 9)

With Axial Load of:		1,000 kips	1,500 kips	2,000 kips	2,500 kips	3,000 kips
Flaw Size (in)	Min Moment (in-kips)	Max Moment (in-kips)	Max Moment (in-kips)	Max Moment (in-kips)	Max Moment (in-kips)	Max Moment (in-kips)
9.985	0	44,523	40,072	35,622	31,264	26,720
7.466	10,000	55,084	50,713	46,342	41,984	37,601
5.889	20,000	62,307	57,978	53,648	49,319	44,990
4.617	30,000	68,749	64,450	60,150	55,851	51,552
3.344	40,000	76,201	71,930	67,659	63,388	59,117
2.433	50,000	82,740	78,488	74,236	69,984	65,733
1.784	60,000	88,632	84,393	80,154	75,915	71,676
1.403	70,000	92,997	88,765	84,534	80,302	76,070
1.021	80,000	98,607	94,382	90,157	85,932	81,708
0.801	90,000	102,844	98,622	94,401	90,180	85,958
0.641	100,000	106,729	102,510	98,291	94,072	89,853
0.522	110,000	110,326	106,108	101,891	97,673	93,456
0.434	120,000	113,583	109,367	105,151	100,934	96,718
0.365	130,000	116,667	112,452	108,236	104,021	99,805
0.310	140,000	119,607	115,392	111,177	106,963	102,748
0.268	150,000	122,256	118,042	113,827	109,613	105,399
0.234	160,000	124,752	120,538	116,323	112,109	107,895

RAI 467
Q.03.06.03-28

Next File

Figure 3.6.3-1—Plain View of U.S. EPR RCS Primary Piping

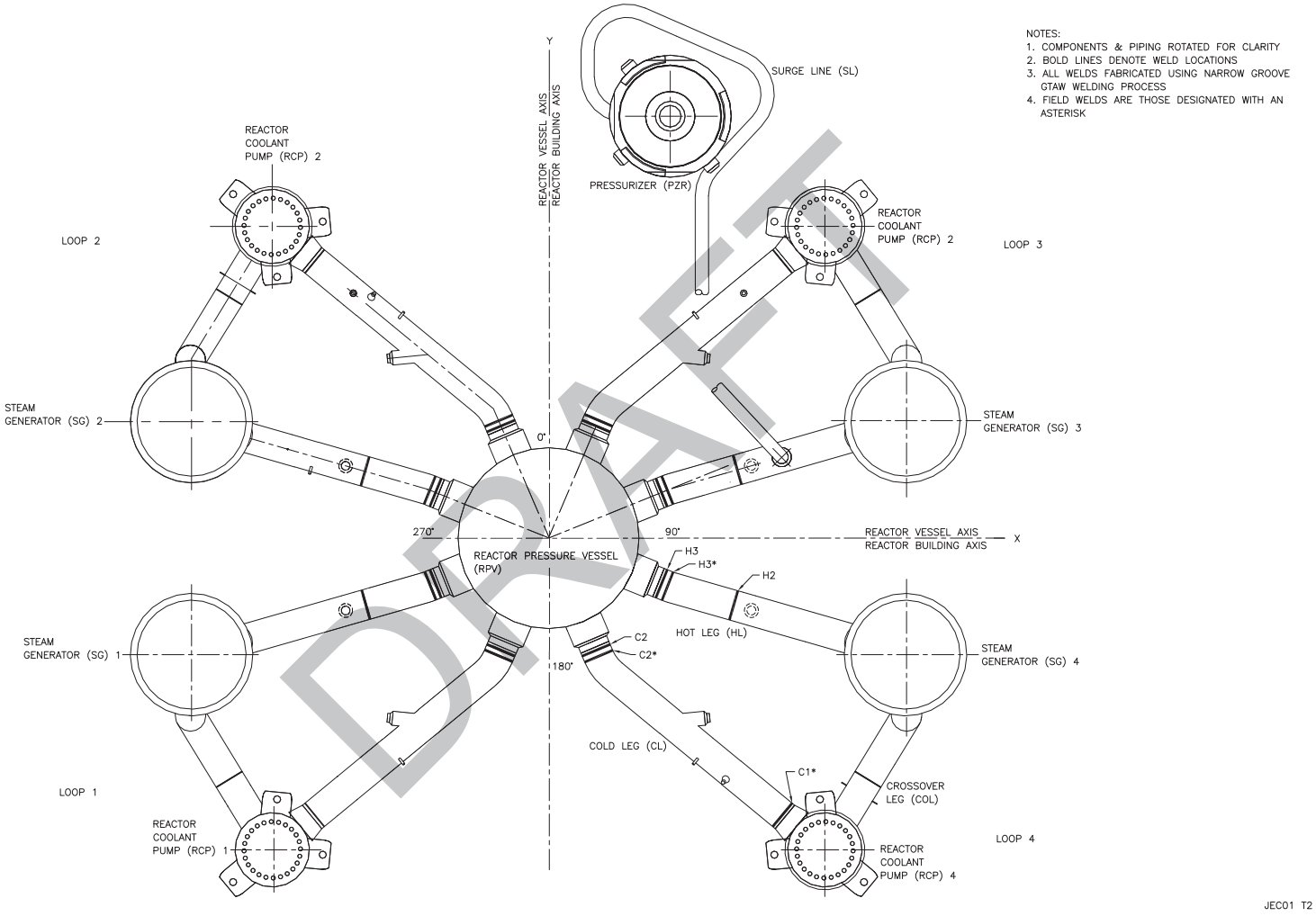

Figure 3.6.3-2—Elevation View of U.S. EPR RCS Primary Piping

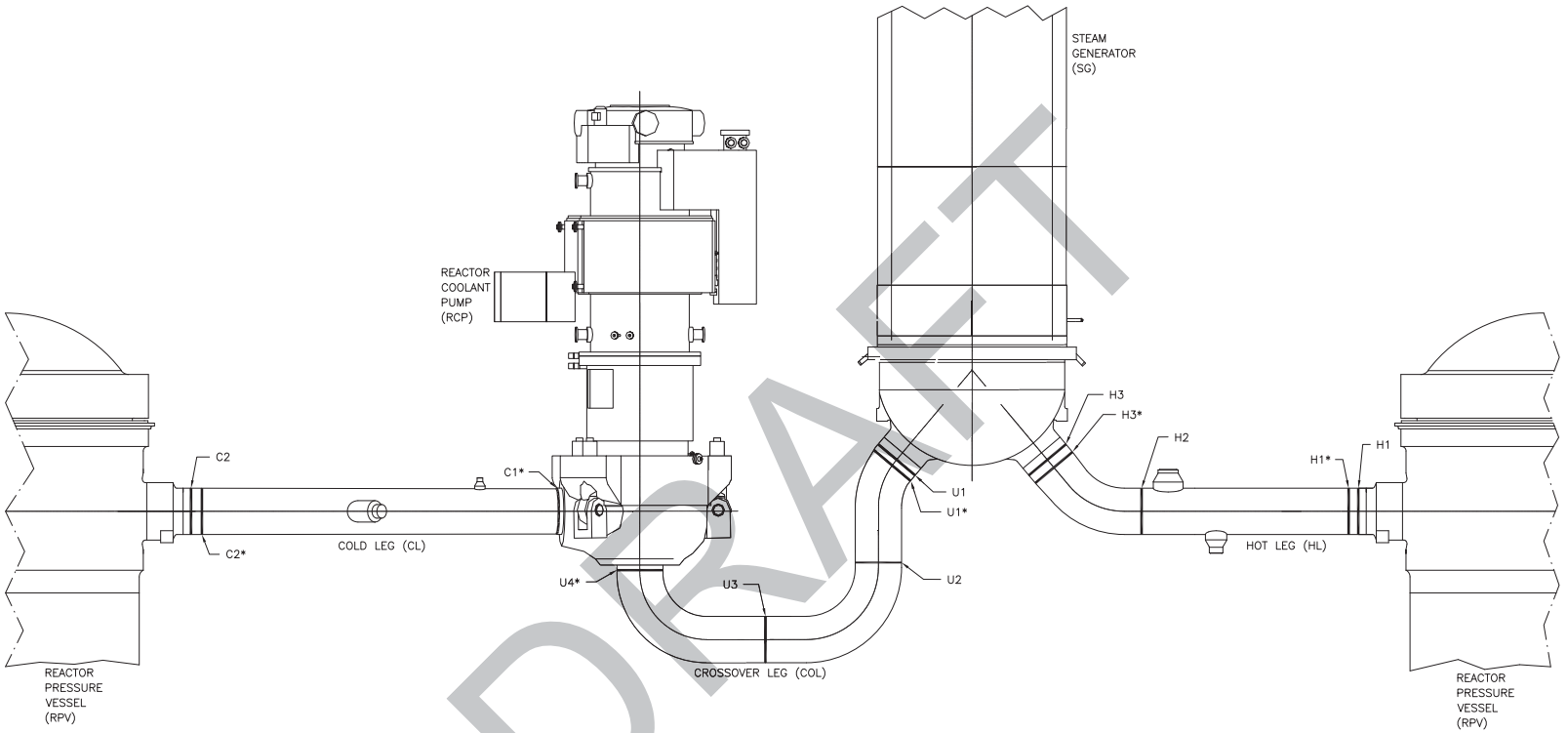

NOTES:
1. COMPONENTS & PIPING ROTATED FOR CLARITY
2. BOLD LINES DENOTE WELD LOCATIONS
3. ALL WELDS FABRICATED USING NARROW GROOVE GTAW WELDING PROCESS
4. FIELD WELDS ARE THOSE DESIGNATED WITH AN ASTERISK

JEC02 T2

Figure 3.6.3-3—Plan, Elevation, and Isometric View of the U.S. EPR Surge Line

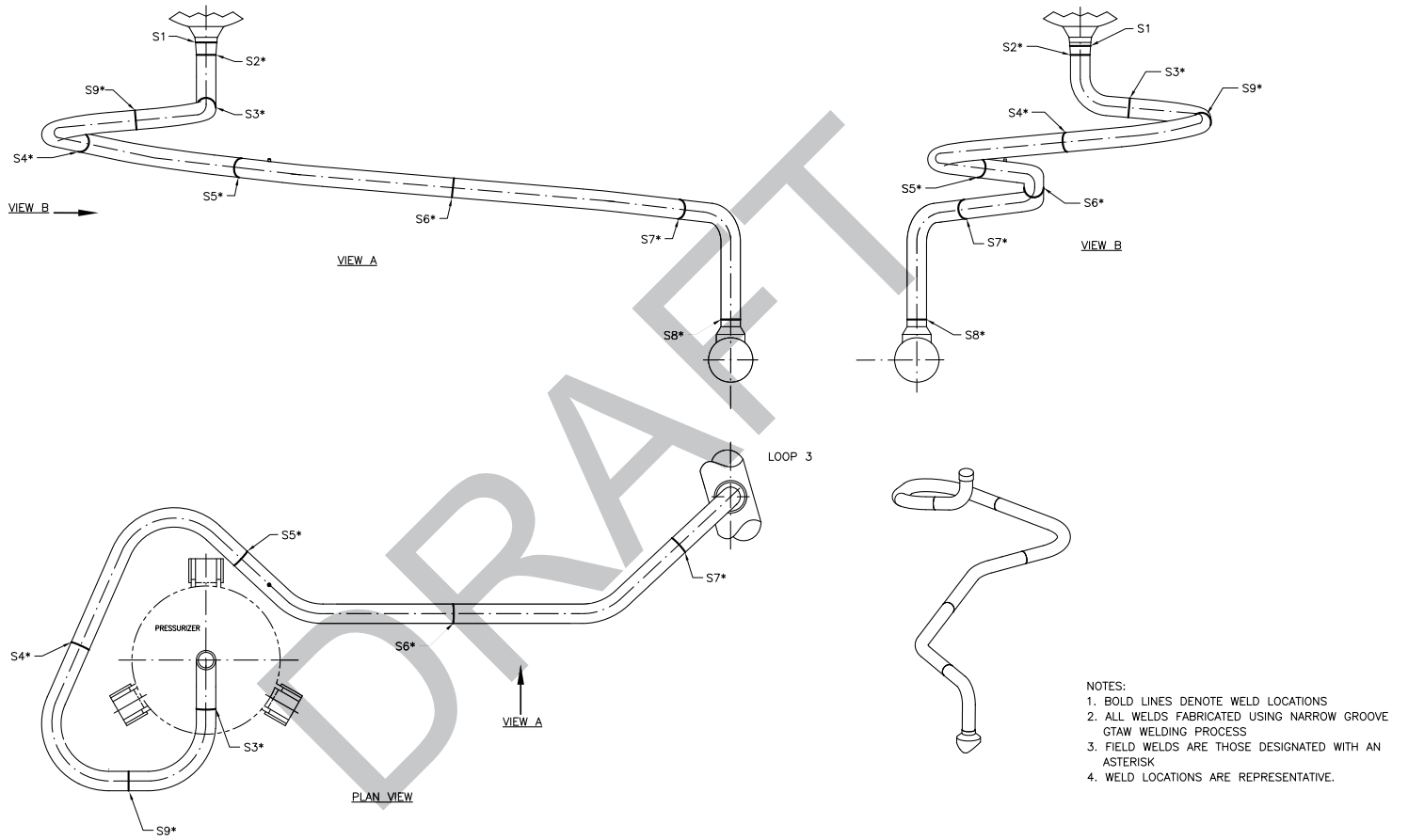

REV 002
JEC03 T2

Figure 3.6.3-4—Isometric View of the Main Steam Line

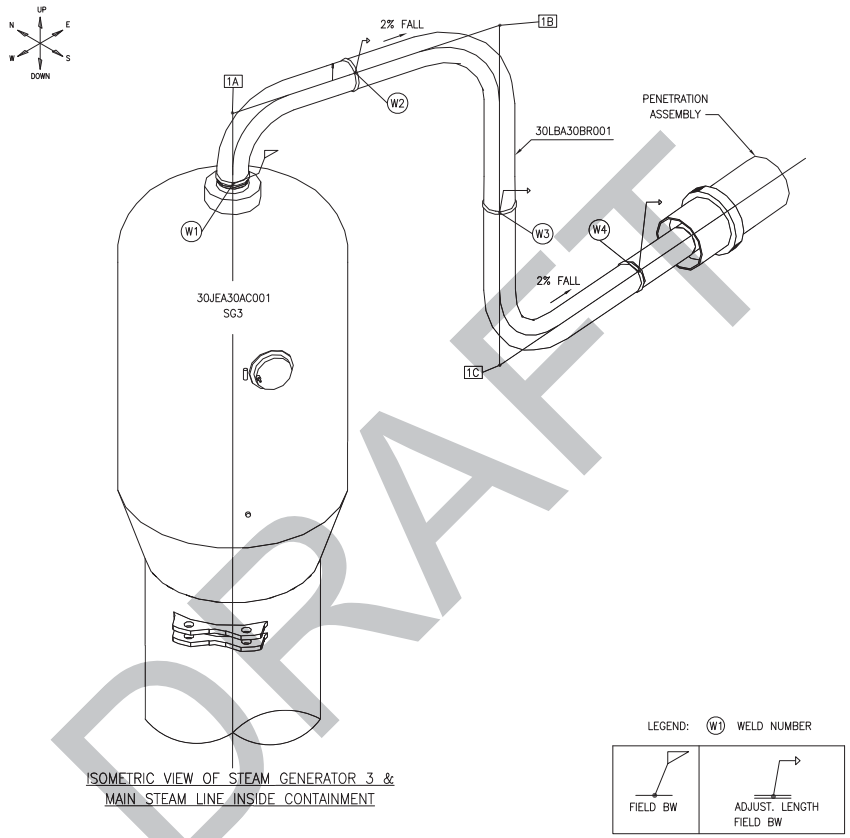

LBA001 T2

Next File

Figure 3.6.3-5—Minimum Moment versus Circumferential Leakage Crack Sizes for 5 gpm at Various Main Coolant Loop Locations

RAI 467
03.06.03-28

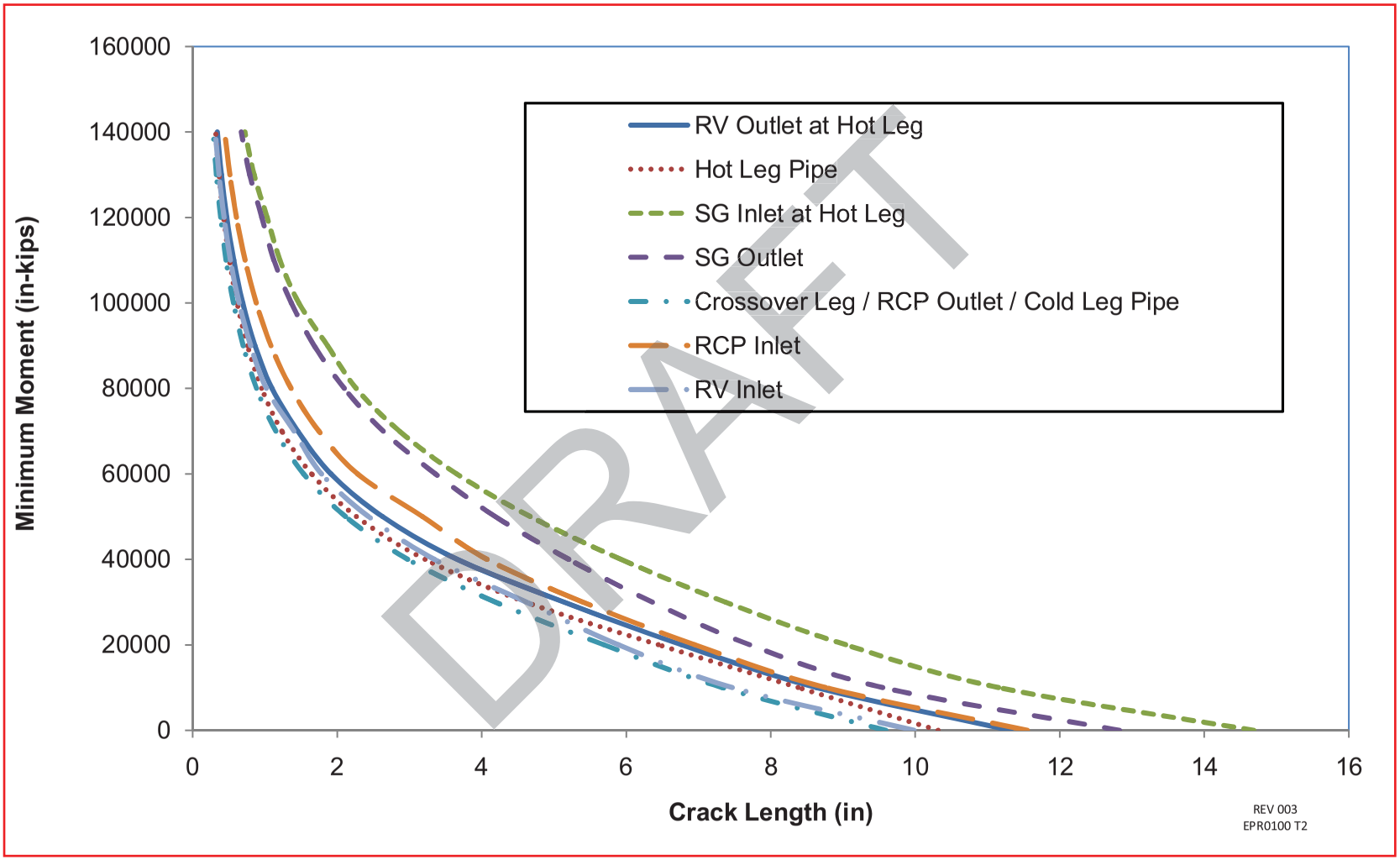

Figure 3.6.3-6—Minimum Moment versus Circumferential Leakage Crack Sizes for 5 gpm at Three Surge Line Locations

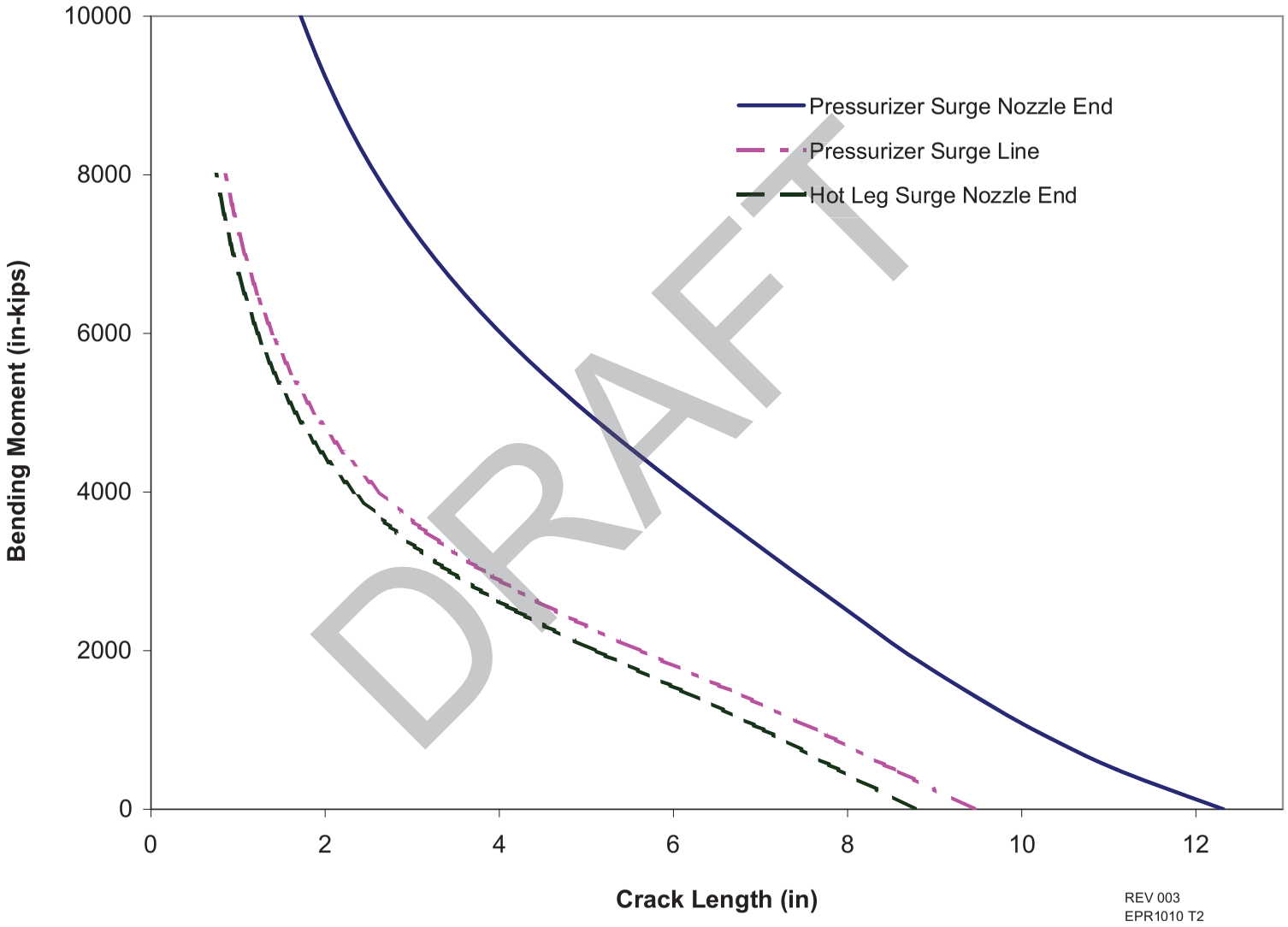

Figure 3.6.3-7—Pressure Only Leakage Rate versus Crack Length for Both Axial and Circumferential Crack Morphologies in Main Steam Line

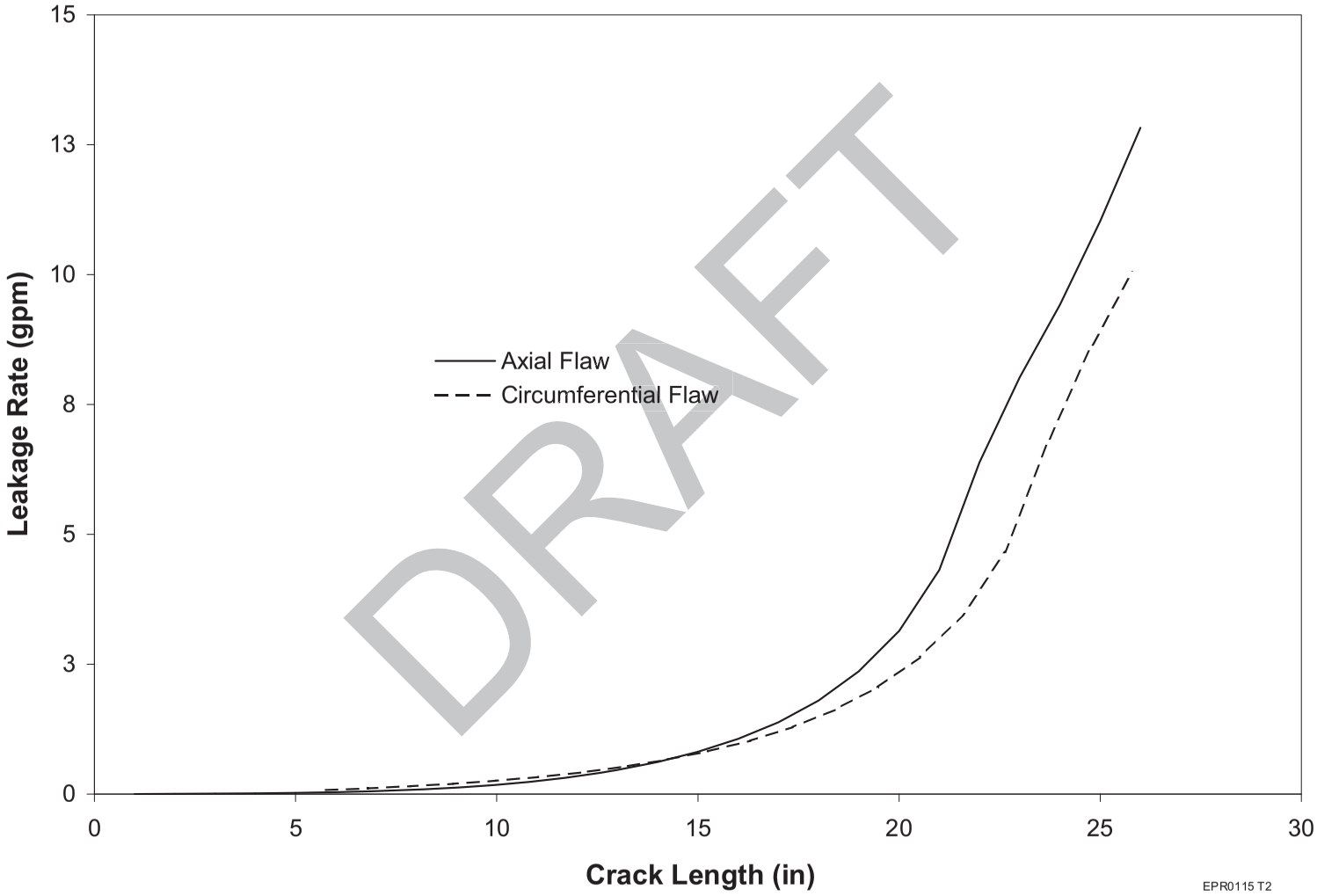

RAI 467
03.06.03-28

Figure 3.6.3-8—Minimum Moment versus Circumferential Crack Leakage ~~Crack~~ Sizes for 1 gpm in Main Steam Line Piping

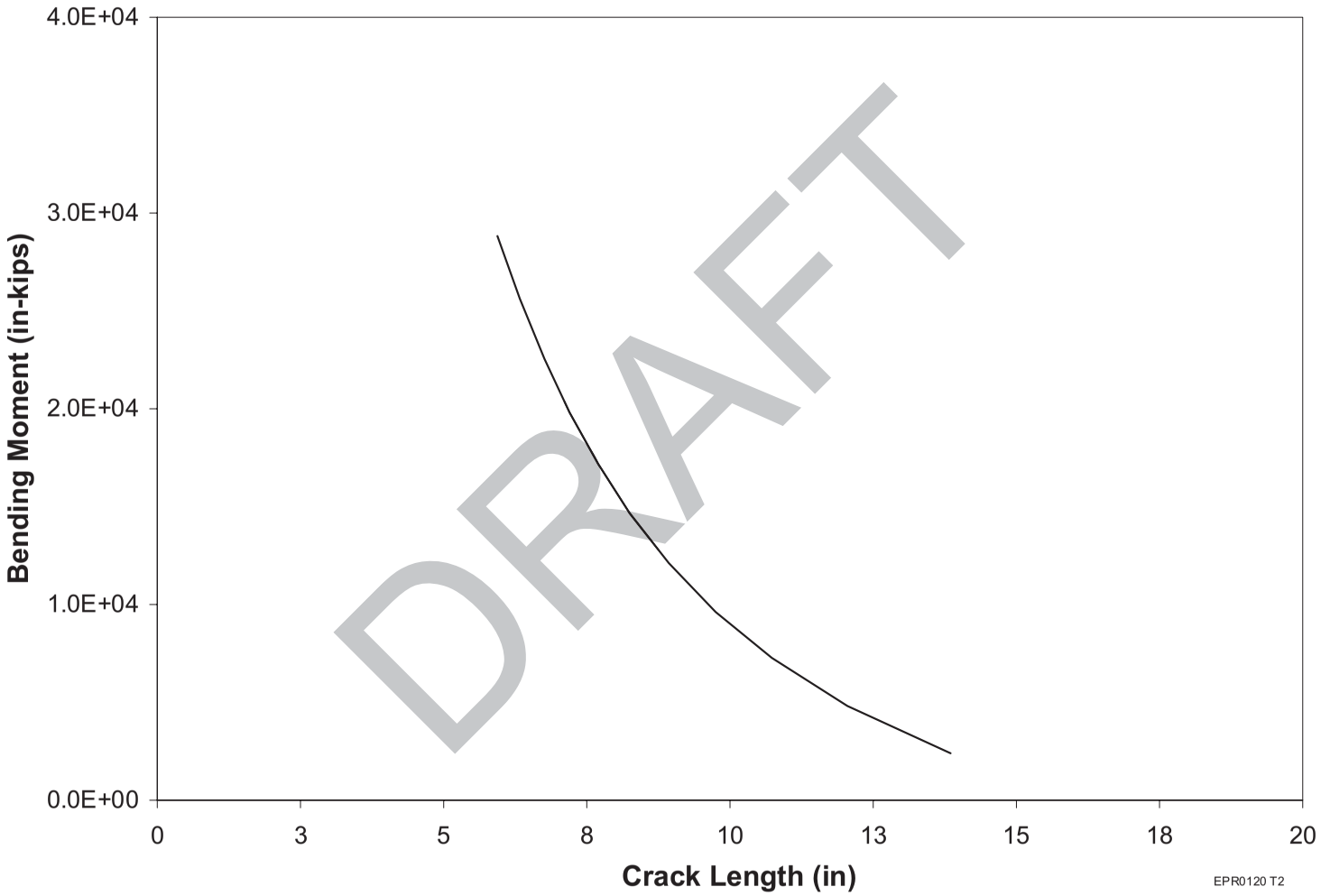

Figure 3.6.3-9—Schematics of Analyzed Crack Geometries Considered for Straight Pipe Section

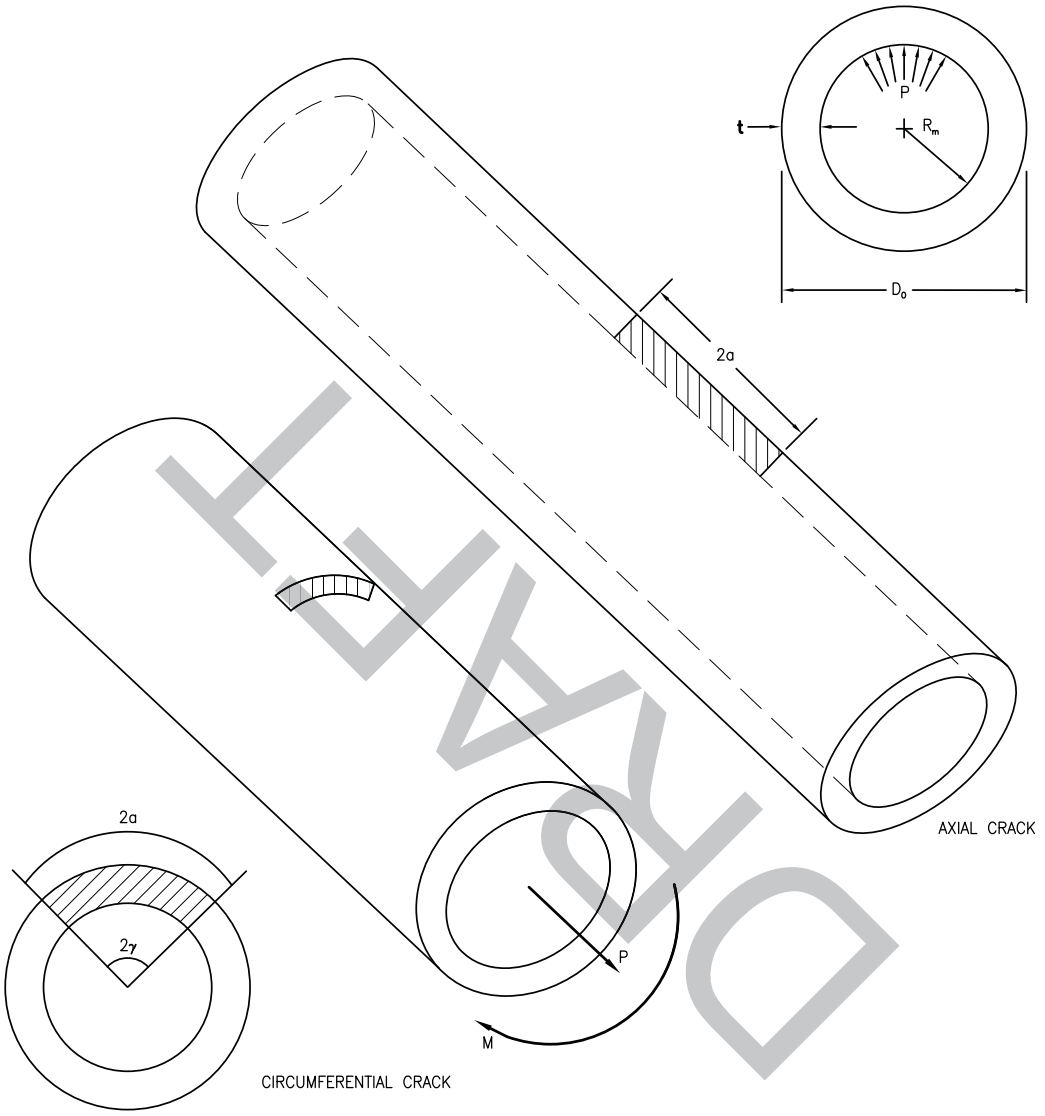

EPR0125 T2

Figure 3.6.3-10—Schematic of J-Tearing Instability Diagram

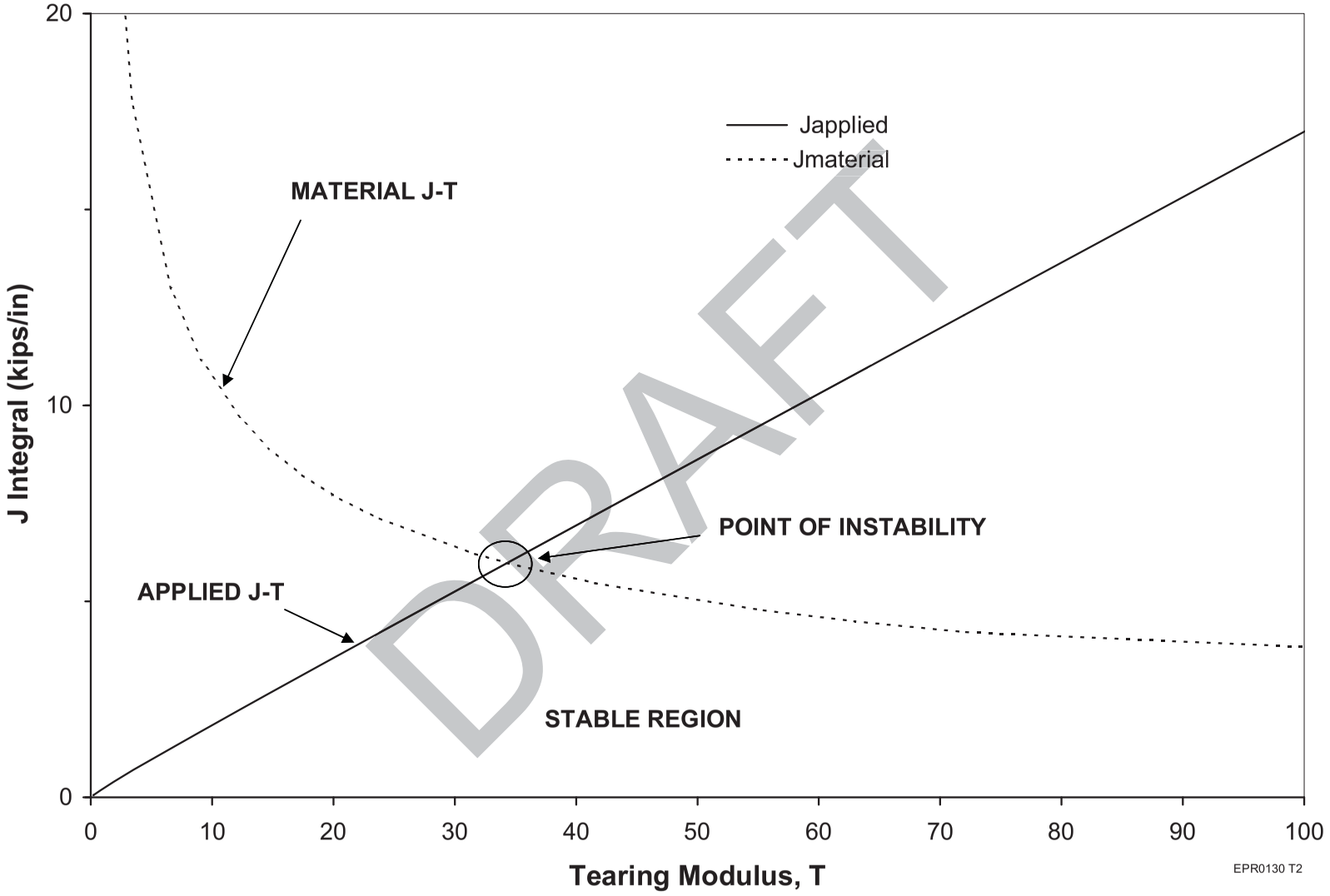

Figure 3.6.3-11—Typical Allowable Load Limit (ALL) Diagram Considering Various Axial Loadings

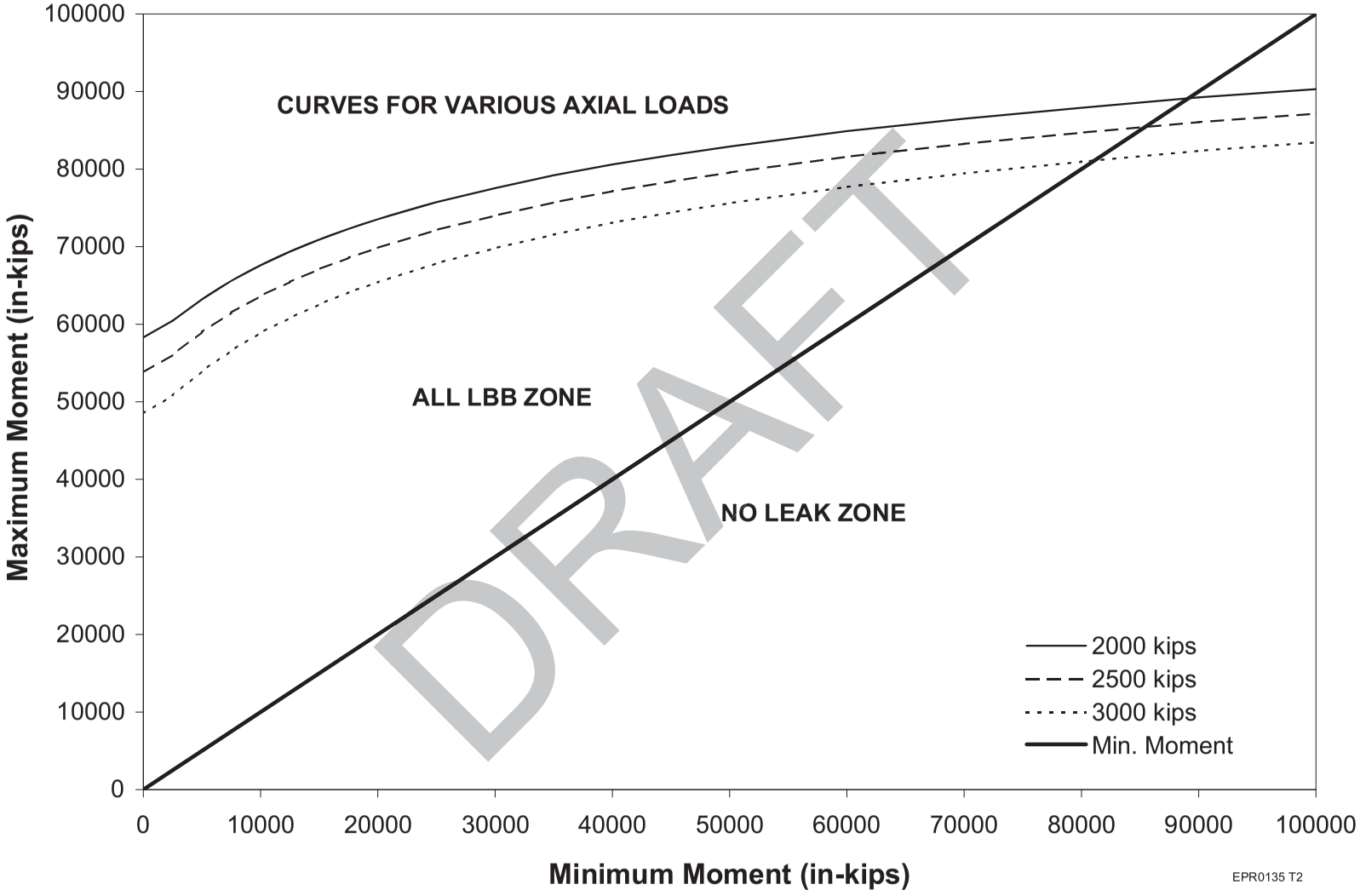

Figure 3.6.3-12—ALL for Reactor Vessel Outlet Nozzle Region at Hot Leg (Location 1)

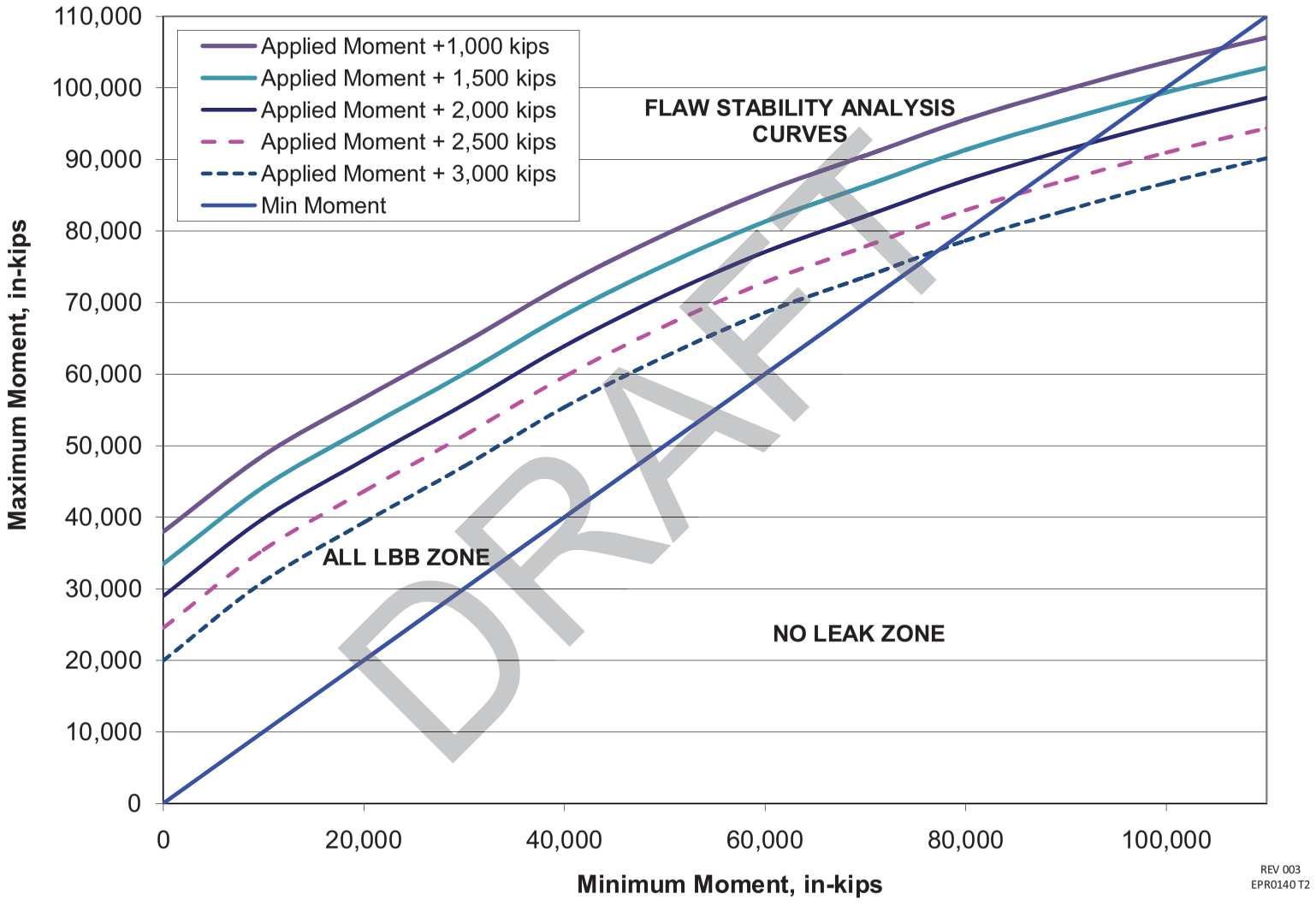

Figure 3.6.3-13—ALL for Hot Leg Pipe (Location 2)

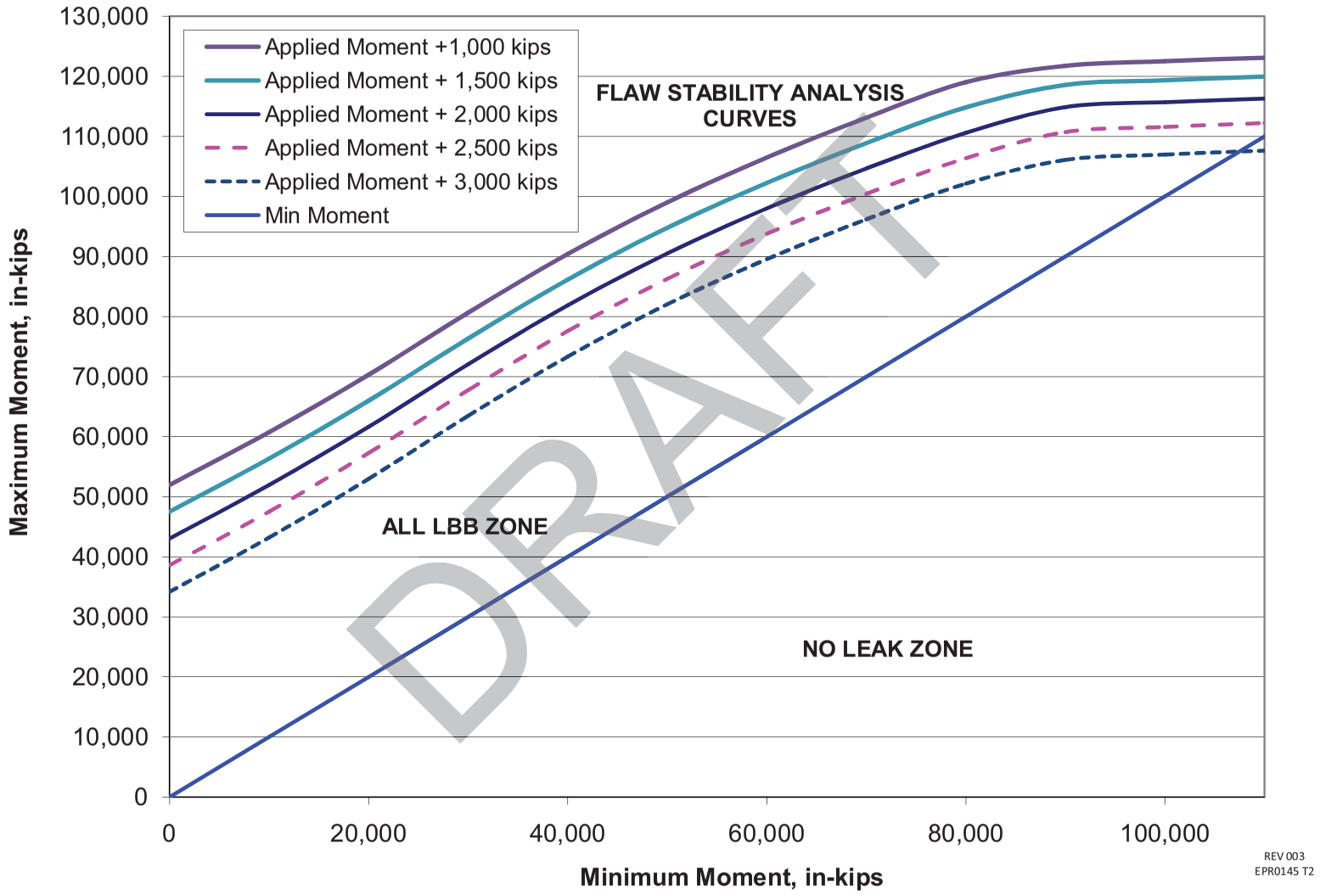

Figure 3.6.3-14—ALL for Steam Generator Inlet Nozzle at Hot Leg (Location 3)

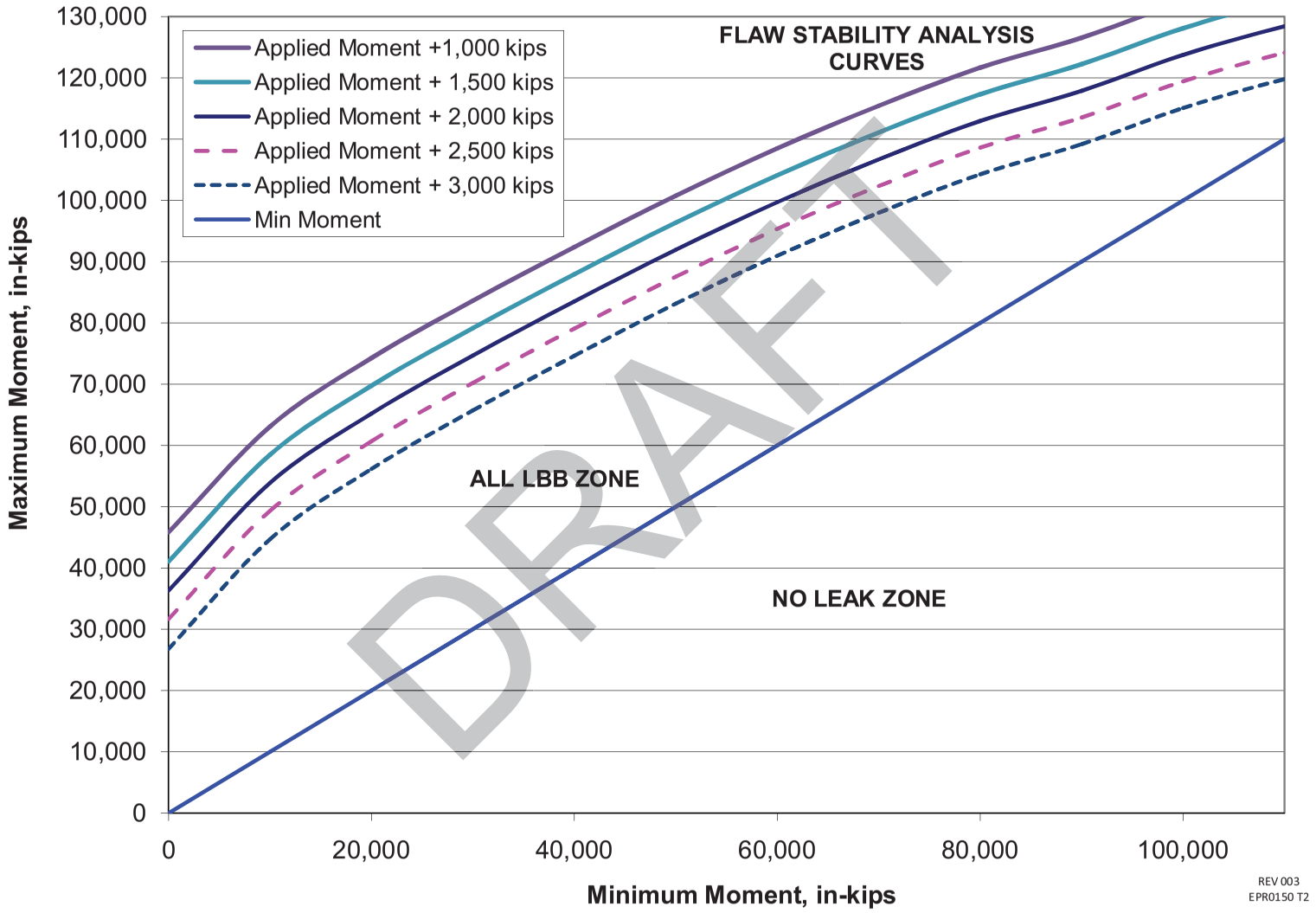

Figure 3.6.3-15—ALL for Steam Generator Outlet Nozzle (Location 4)

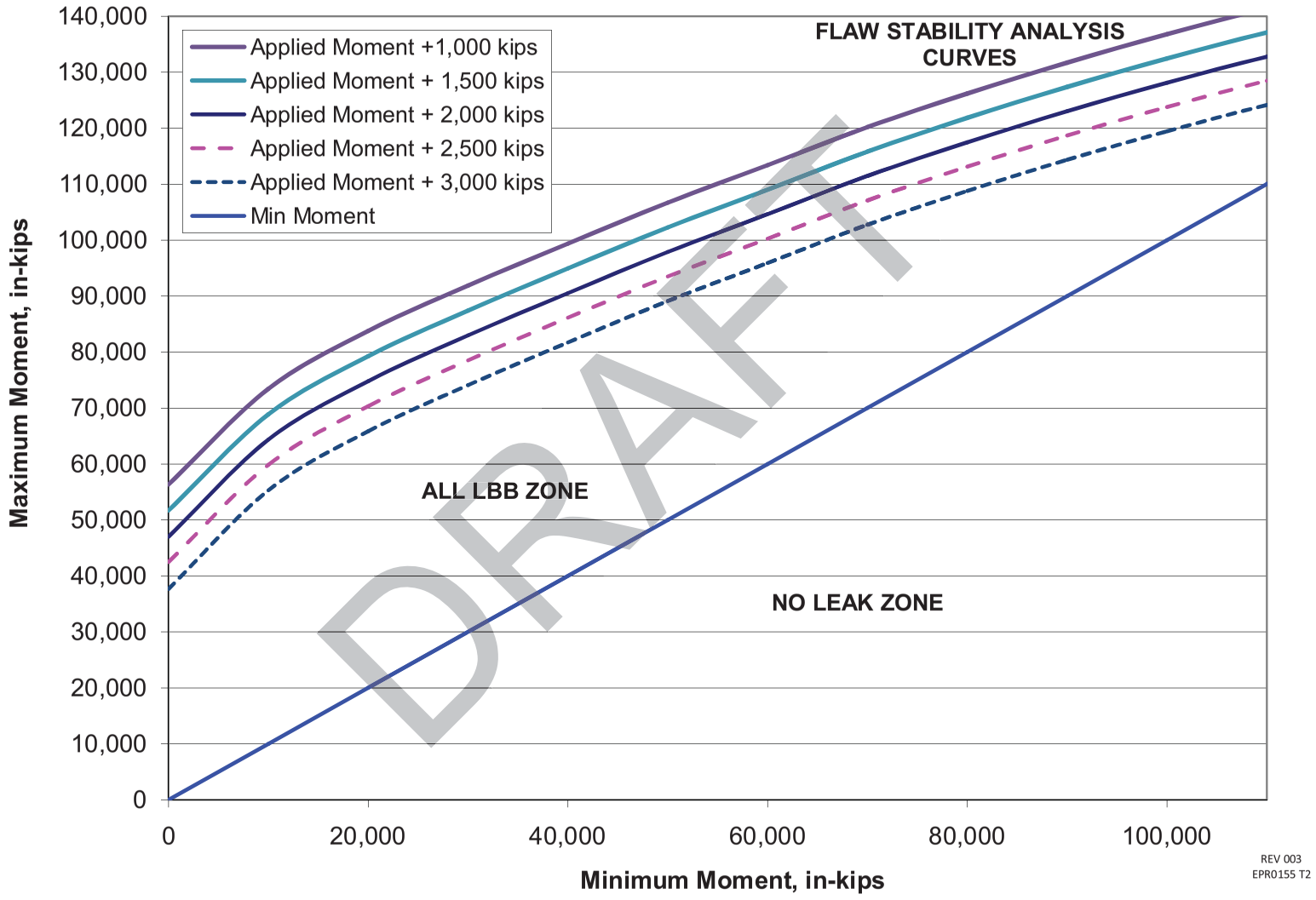

Figure 3.6.3-16—ALL for Crossover & Cold Leg Pipe (Locations 5 & 8)

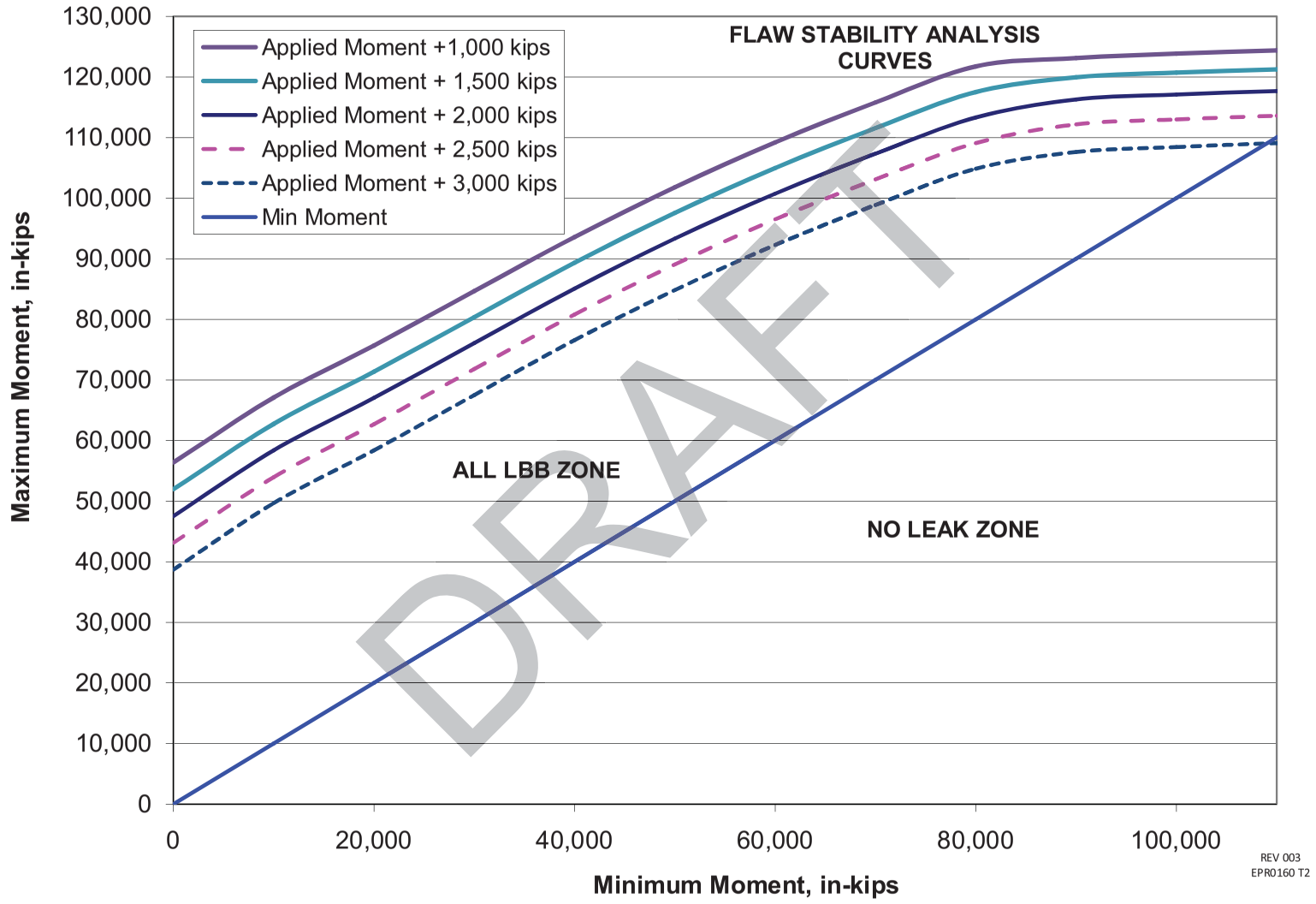

Figure 3.6.3-17—ALL for RCP Inlet Nozzle (Location 6)

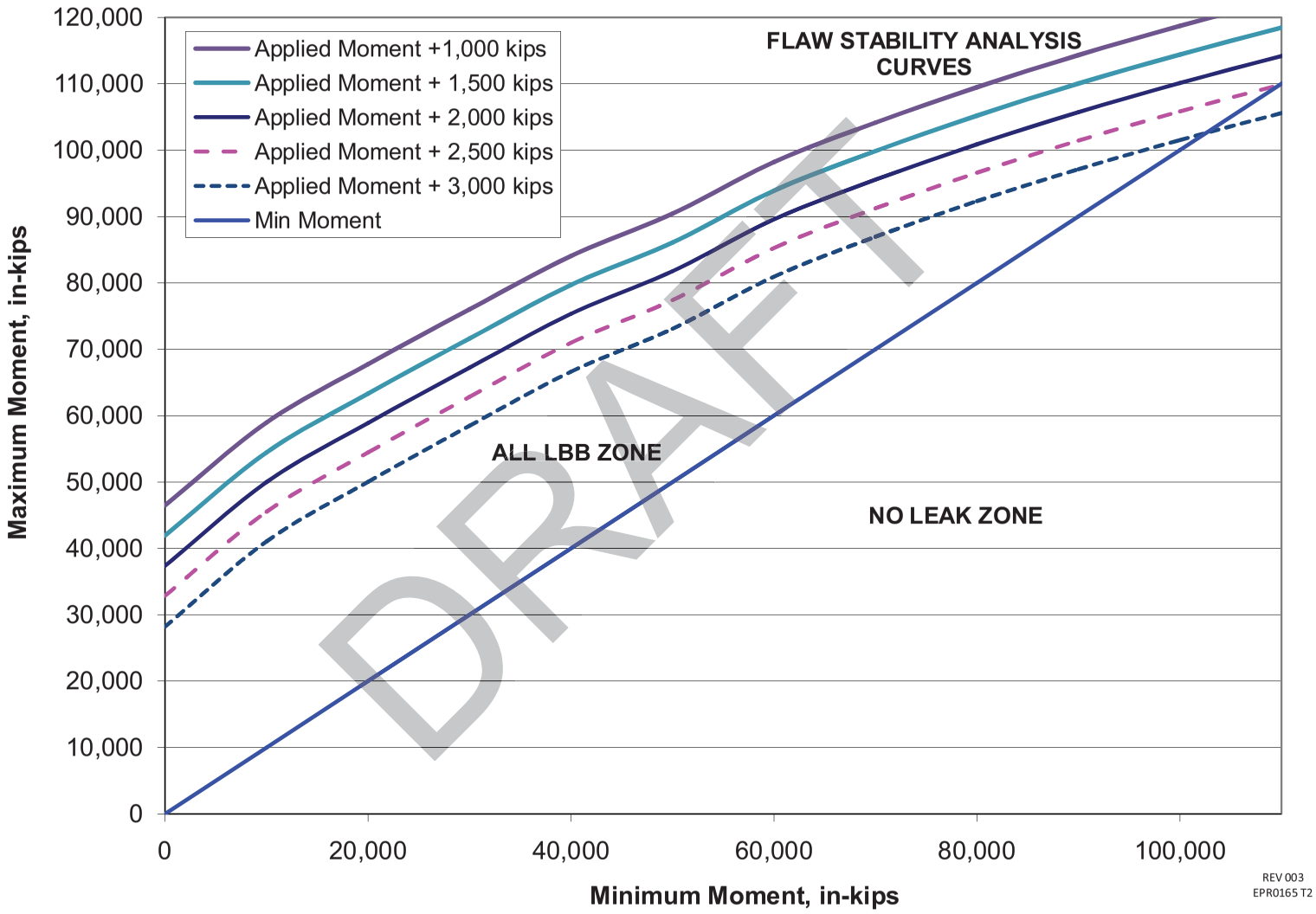

Figure 3.6.3-18—ALL for Pressurizer Surge Nozzle at Alloy 52 Weld

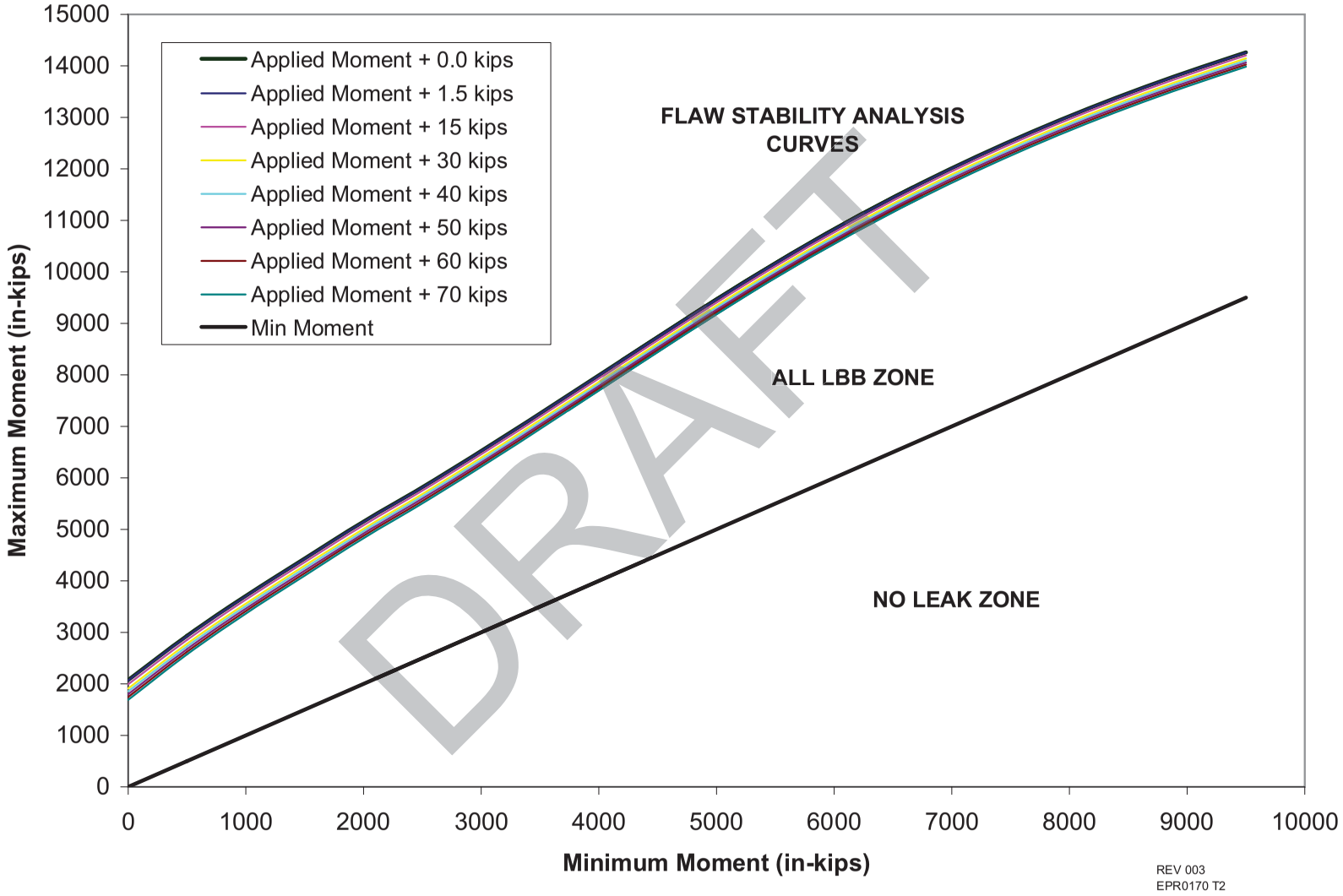

Figure 3.6.3-19—ALL for Surge Line Piping

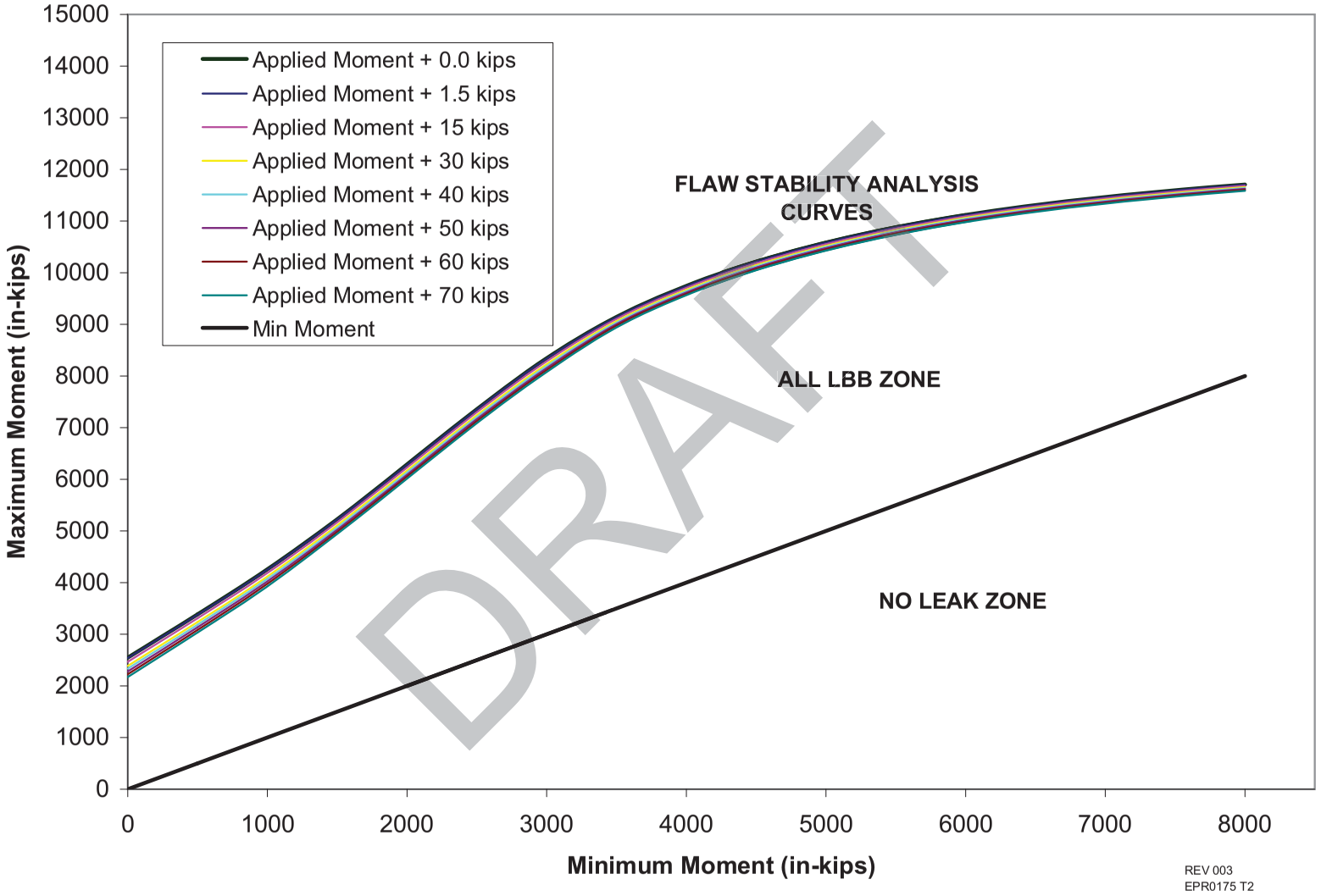

Figure 3.6.3-20—ALL for Hot Leg Nozzle

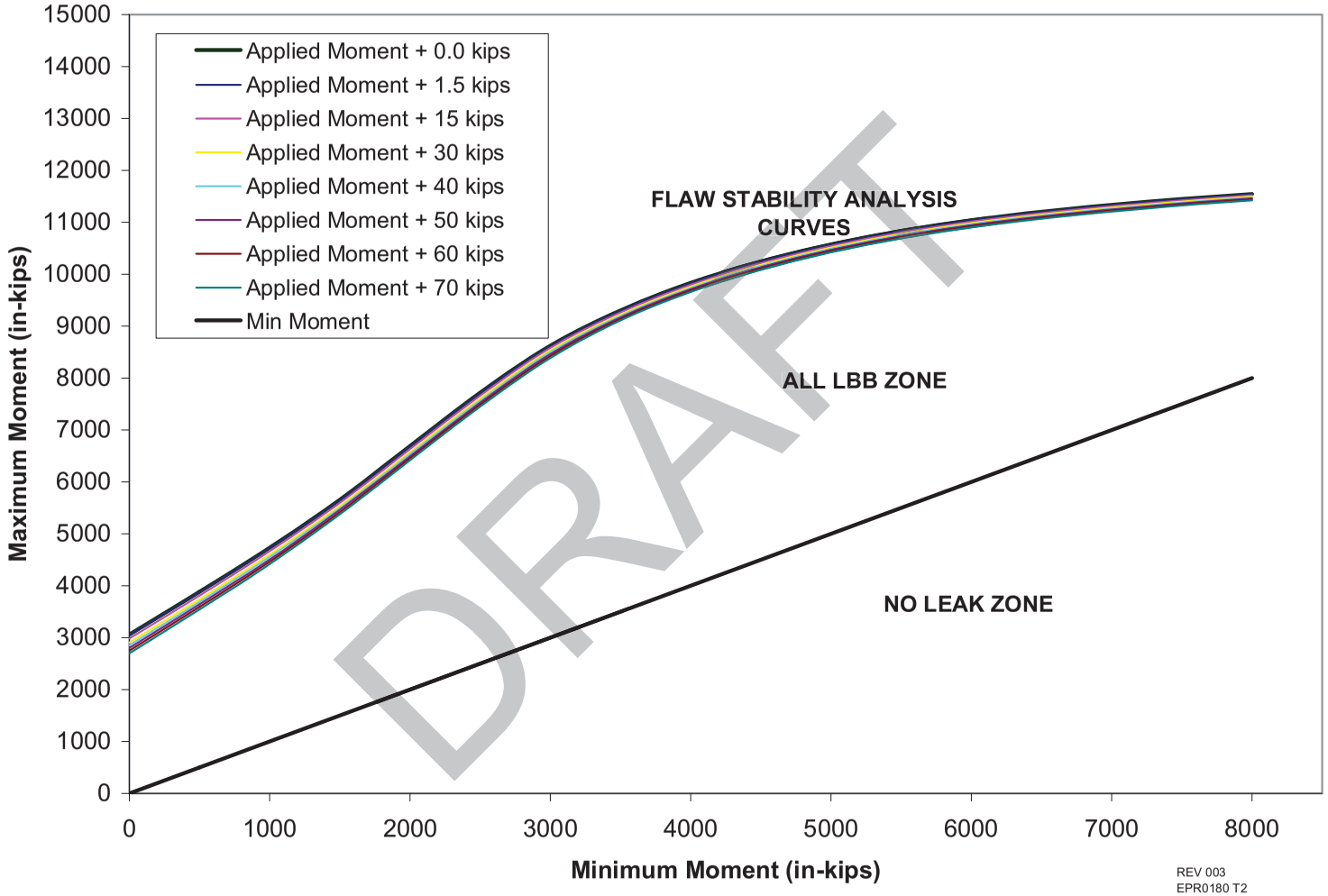

Figure 3.6.3-21—Comparison of Base and Weld Metal ALL in Main Steam Line Piping

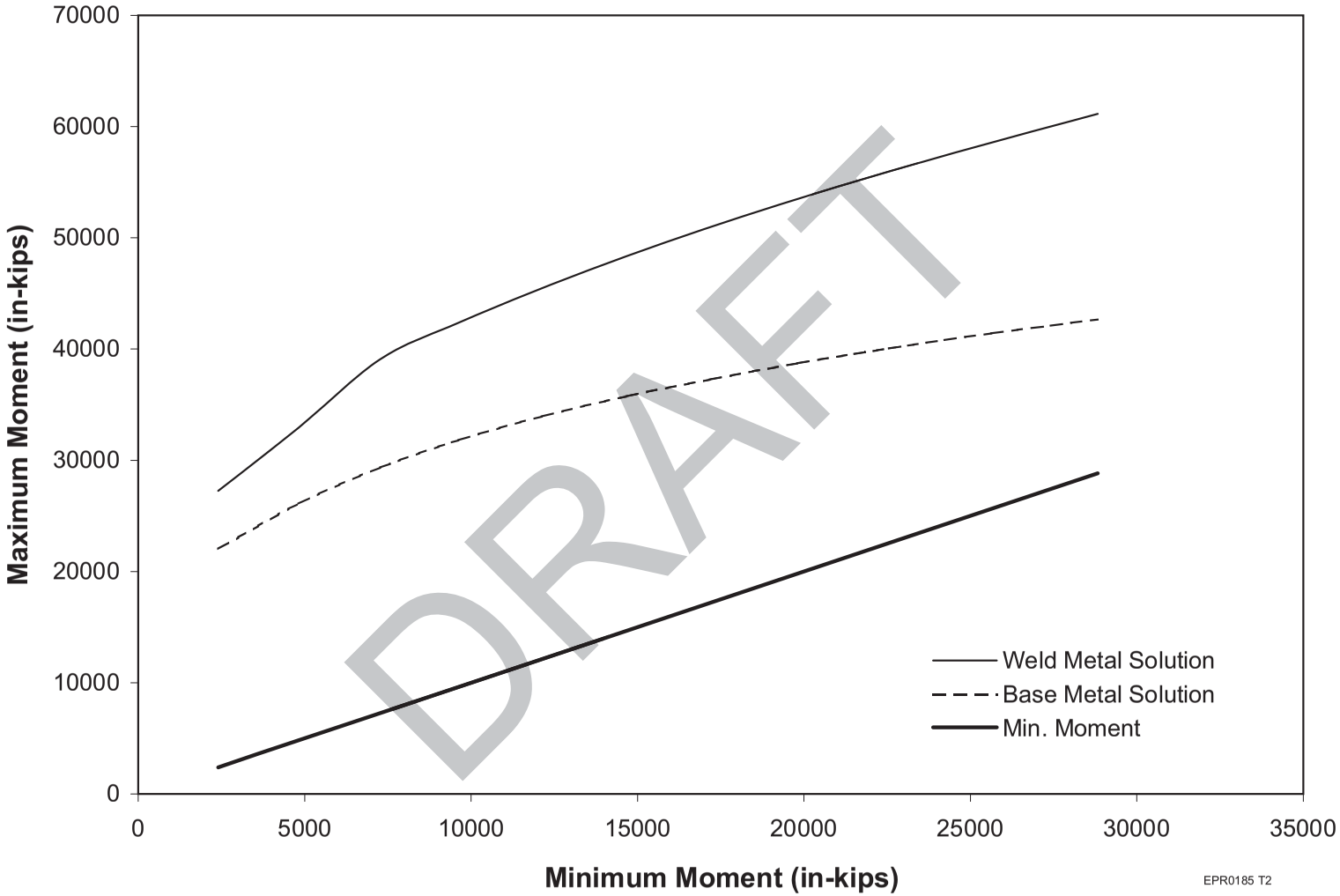

Figure 3.6.3-22—ALL for Main Steam Line Piping with Safety Factor of 2 on Flaw Size (Base Metal)

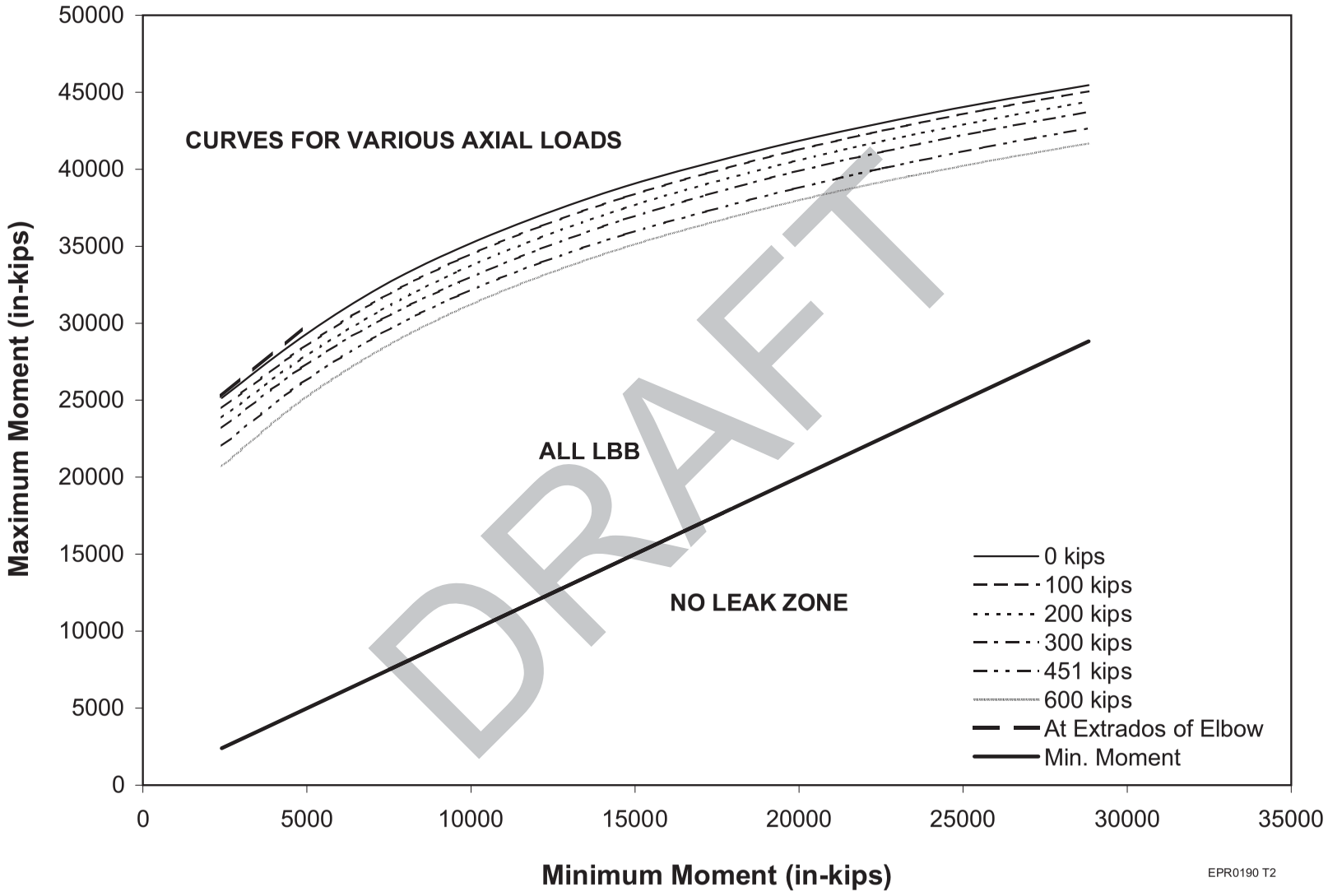

Figure 3.6.3-23—Deleted

Figure 3.6.3-24—ALL for RCP Outlet Nozzle (Location 7)

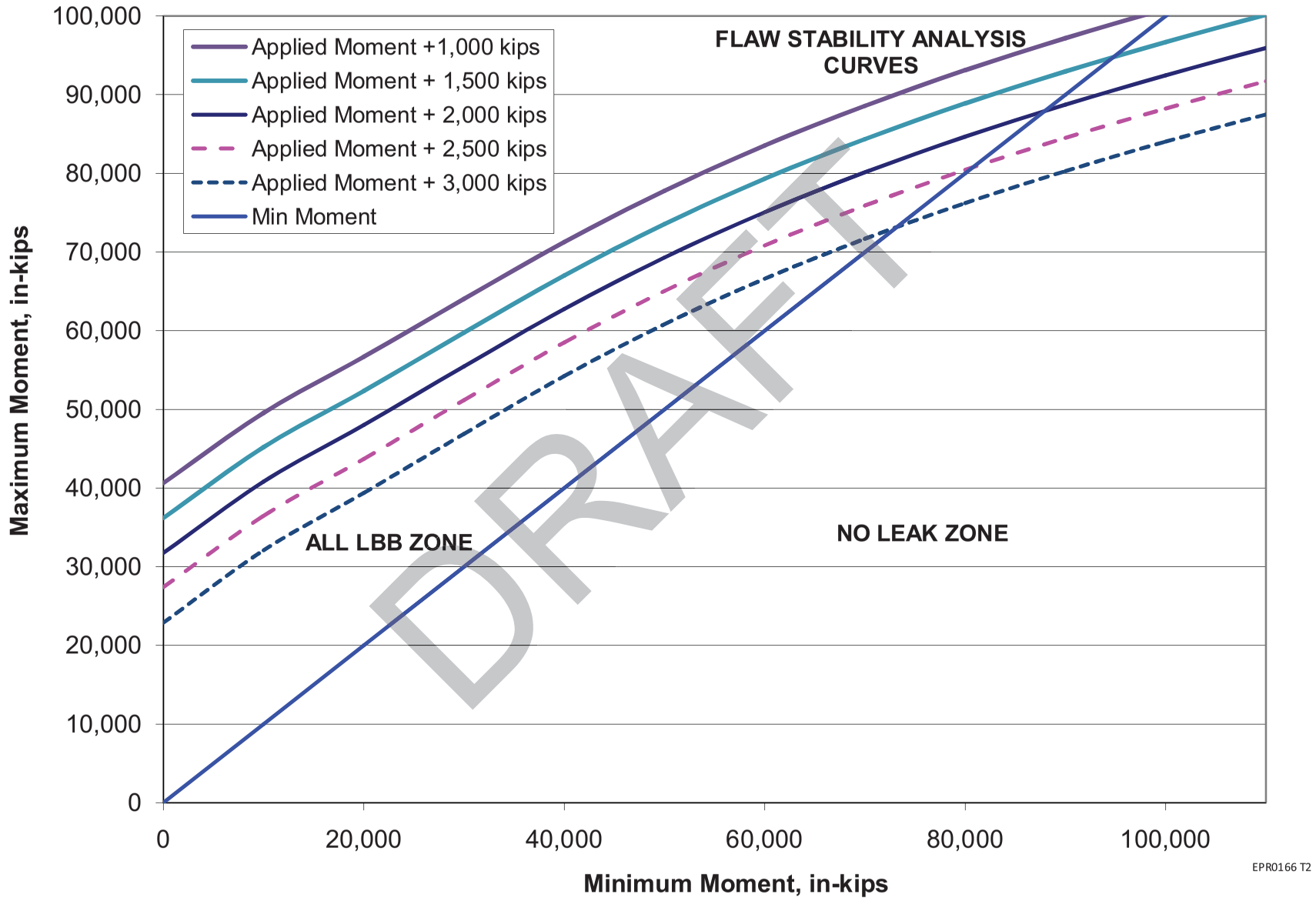

Figure 3.6.3-25—ALL for RV Inlet Nozzle (Location 9)

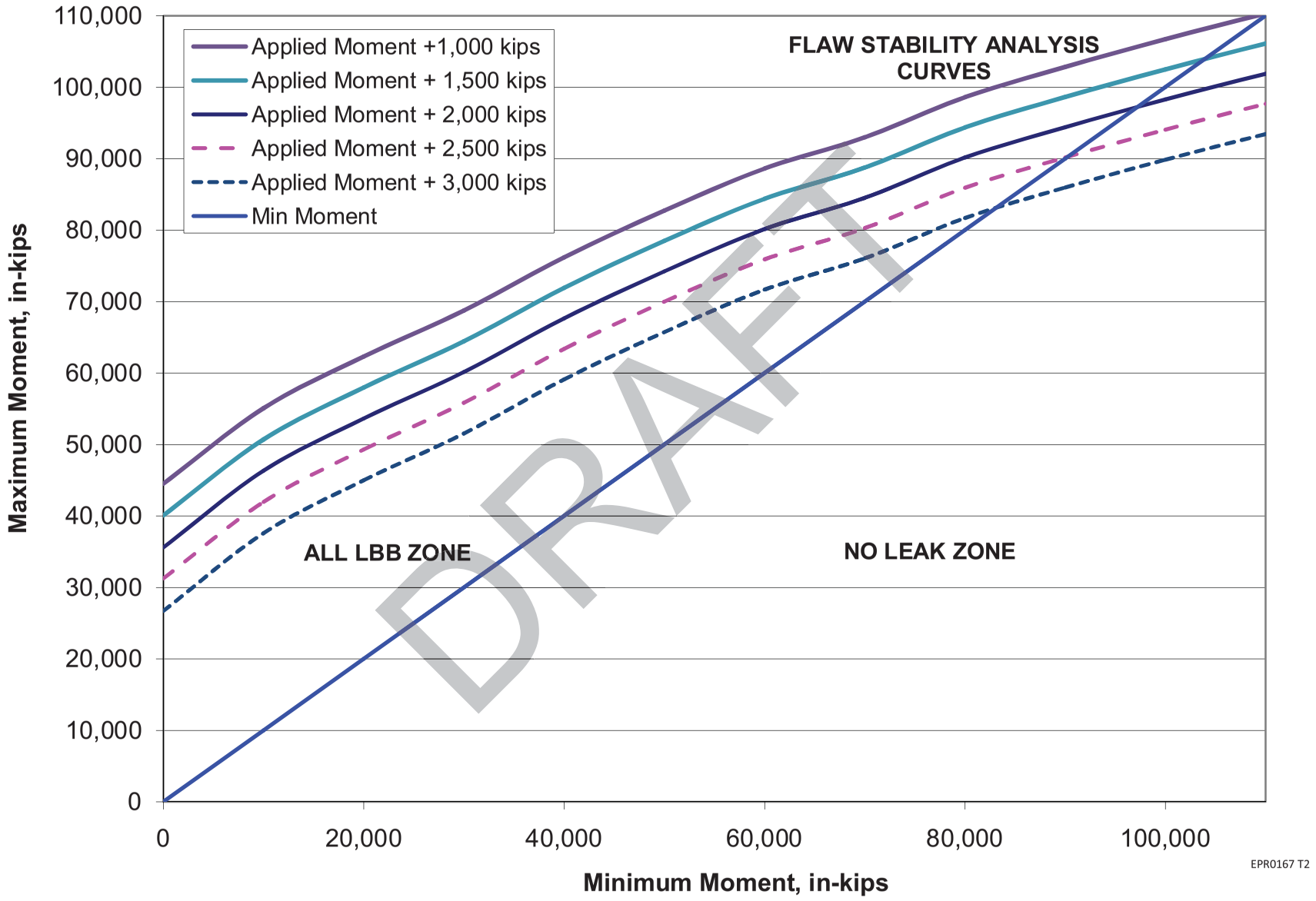

Next File